Reversed electron transport in syntrophic degradation of glucose, butyrate and ethanol

Dissertation

zur Erlangung des Grades eines Doktors der Naturwissenschaften (Dr. rer. nat.) im Fachbereich Biologie der Mathematisch-Naturwissenschaftlichen Sektion der Universität Konstanz

vorgelegt von

Nicolai Müller

Konstanz

Februar 2010

Tag der mündlichen Prüfung : 09. April 2010

1. Referent : Prof. Dr. Bernhard Schink

2. Referent : Prof. Dr. Alasdair Cook

3. Referent : Prof. Dr. Wolfgang Buckel (Universität Marburg)

Danksagung

Die vorliegende Arbeit wurde im Zeitraum von Juni 2006 bis Januar 2010 am Lehrstuhl für Mikrobielle Ökologie von Prof. Dr. Bernhard Schink angefertigt.

Mein besonderer Dank gilt Herrn Prof. Dr. Bernhard Schink für die Überlassung des Themas sowie sein stetes Interesse und seine ständige Diskussionsbereitschaft zu dieser Arbeit.

Herrn Prof. Dr. Alasdair Cook danke ich für die Übernahme des Koreferates.

PD Dr. Bodo Philipp danke ich für die zahlreichen methodischen Ratschläge und Diskussionen zu meiner Arbeit, insbesondere zu Beginn meiner Zeit als Doktorand.

Mein Dank gilt ebenfalls Dr. David Schleheck, insbesondere für seine Kooperation und seinen Beitrag zum Manuskript über die syntrophe Oxidation von Butyrat nach der ersten Revision, aber auch für viele experimentelle Ratschläge und Diskussionsbereitschaft zum Butyratprojekt.

Für ihre Hilfe, nicht nur bei der Optimierung der Proteinreinigung und SDS-PAGE, danke ich Karin Denger und Diliana Simeonova.

Bei Antje Wiese bedanke ich mich insbesondere für ihre Unterstützung im Labor und die Herstellung der Kultivierungsmedien.

Allen Mitgliedern der AG Schink und AG Cook, denen ich während meiner Zeit als Doktorand begegnet bin, danke ich für ihre Hilfsbereitschaft sowie eine sehr angenehme Arbeitsatmosphäre.

Meinen Eltern danke ich herzlich für ihr Verständnis und ihre Unterstützung in all den Jahren meiner akademischen Ausbildung.

Table of Contents

Chapter 1

General Introduction

Fermentation of monomeric organic substrates by bacteria provides only a small amount of ATP for bacterial growth compared to the high ATP yields of respiratory oxidation processes. The amount of ATP conserved by fermentation varies greatly depending on the degradability of the substrate. Hence, one would expect that there are fermenting bacteria existing that can gain only a minimum of ATP and therefore live at the margin of subsistence. The irreversible formation of ATP generally requires a minimum of 60-70 kJ per mol of Gibbs free energy change from an oxidation reaction (Schink, 1997). Energy conserving reactions therefore should release at least this amount of energy for ATP production (Schink, 1990). However, it is known that through electron transport phosphorylation also reactions with a lower free energy change can provide enough energy for the formation of ATP by proton translocation across the membrane (Mitchell, 1966). The energy needed for proton translocation across the cytoplasmic membrane amounts to one third of the energy of ATP synthesis (approximately 20 kJ per mol) and has therefore been defined as the minimum amount of energy required for growth (Schink, 1990, Schink, 1997).

The amount of energy conserved in the form of ATP per total energy available through the oxidation of a substrate (S→P) is expressed as thermodynamic efficiency η with n being the amount of ATP formed (eq.1, Thauer et al., 1977).

$$\eta = \frac{n \times \Delta G(ATP \rightarrow ADP + Pi)}{\Delta G(S \rightarrow P)} \times 100 \qquad \text{(eq. 1)}$$

Values for η were designated between 25 % - 50 % for the majority of anaerobes and even 80 % in exceptional cases, depending on the biological degradability of the substrate and the biochemical prerequisites in the fermenting bacteria (Thauer et al., 1977). The reason for this low thermodynamic efficiency of most anaerobes is that part of the substrate has to be sacrificed as electron accepting system in disproportionating reactions or that reducing equivalents have to be regenerated by reduction of protons to form hydrogen. This process becomes endergonic with increasing partial pressure of hydrogen depending on the headspace volume of the culture. Moreover, some reactions like for example the reduction of acetaldehyde with NADH to ethanol and NAD^+ carried out by alcohol dehydrogenases in

many fermenting bacteria are not coupled to an energy-conserving reaction and therefore a great proportion of the free enthalpy of the reaction is dissipated as reaction heat (Thauer et al., 1977). This suggests that one possible point for optimization of metabolic pathways for energy conservation could be the enzyme reactions of the reductive branch of substrate degradation by minimizing energy loss through heat.

Although most fermentative pathways known provide enough energy for the formation of at least 1 ATP, in some exceptional cases of organic substrates, fermentation does not release the required energy amount from a thermodynamic point of view, as the reaction yields less than 60-70 kJ per mol of substrate, or is even endergonic (Schink, 1997). In an attempt to explain the fact that some bacterial enrichment cultures have been found that are able to grow with these substrates led to the discovery that the latter are degraded in cooperation of fermenting bacteria with either hydrogenotrophic sulfate reducers or methanogenic archaea. The ethanol-fermenting coculture *Methanobacillus omelianskii* was the first described co-culture of this kind (Barker, 1940). The obligate dependence of the fermenting bacteria in those consortia on hydrogenotrophic partner organisms has been termed „syntrophy“, where electrons derived from oxidation of the substrate are transferred to the respective partner organisms via so-called interspecies electron transfer (McInerney et al., 1979, Schink, 1997).

Interspecies electron transfer

Besides hydrogen, formate and acetate can serve as metabolite for interspecies transfer of reducing equivalents (Schink, 1997). However, hydrogen has been regarded as the major electron shuttle (Schink, 1997). The importance of formate has been accentuated by other sources later as most syntrophic bacteria investigated so far had activities of both hydrogenase and formate dehydrogenase (Stams and Plugge, 2009). As mentioned above, formation of hydrogen in the release of reducing equivalents plays a crucial role in the absence of external electron acceptors, also in syntrophic degradations. Hydrogen produced in these reactions is transferred to the syntrophic partner and the latter has to keep the hydrogen partial pressure constantly low to pull the endergonic reaction. The extent of lowering the hydrogen partial pressure is limited as the formation of methane from hydrogen and CO_2 becomes endergonic at a hydrogen partial pressure of 10^{-6} bar; at a partial pressure of 10^{-5} bar the free energy change is barely sufficient to provide formation of roughly one third of ATP per mol of methane formed (Schink, 1997). However in some cases (e.g. syntrophic oxidation of butyrate), the hydrogen partial pressure required for the reaction is 10^{-10} bar which means the hydrogen partial pressure maintained by methanogens is not sufficient to pull the reaction

(Thauer and Morris, 1984, Schink, 1997). Therefore, it was postulated for these reactions that the fermenting bacterium has to invest part of the gained energy into a so-called reversed electron transport in order to reoxidize cell-internal electron carriers with protons to form hydrogen (Thauer and Morris, 1984, Schink, 1997).

Although the biochemistry of syntrophic bacteria has been investigated for four decades and the reactions of the central energy metabolism have been analysed it still remains unclear in most bacteria how reducing equivalents are transferred to protons to form hydrogen or formate (Schink, 1997).

Reversed electron transport

Most of the reactions presented in this work release electrons at redox potentials higher than -320 mV. This means that reducing equivalents arise in the form of NADH or an electron-accepting system of a higher redox potential. The redox potentials of hydrogen or formate formation under standard conditions at pH 7.0 are -414 mV and -432 mV, respectively (Thauer et al., 1977). Therefore, electrons derived from the oxidation reactions described in this work have to be endergonically shifted to the level of hydrogen or formate formation, and this process is defined as reversed electron transport (Thauer and Morris, 1984, Schink, 1997). The exact biochemical mechanisms of reversed electron transport in syntrophic cooperations are not known to date but several theories have been developed during the last decade. For example in *Syntrophus aciditrophicus*, a syntrophic butyrate fermenting bacterium, rnf-proteins have been found which could perform the reversed electron transport (McInerney et al., 2007). In detail, NADH from the central pathway of butyrate degradation is reoxidized by these membrane-bound rnf-proteins with ferredoxin, a small iron sulfur protein that transfers electrons to accepting systems in the cell. This reaction is endergonic as the redox potential of ferredoxin lies around -400 mV depending on the organism, and the redox potential of NADH is -320 mV under standard conditions at pH 7.0 (Thauer et al., 1977). The reaction can occur only with the help of sodium or proton influx into the cytoplasm through the ion channel of the rnf-protein (McInerney et al., 2007). This means that ATP is hydrolyzed in *S. aciditrophicus* by ATPase to produce a proton or sodium gradient which drives the endergonic oxidation of NADH (McInerney et al., 2007). However, the main endergonic reaction in syntrophic butyrate oxidation is the transfer of electrons from butyryl-CoA oxidation to the level of protons (Schink, 1997). Therefore, those electrons first have to be transferred to NAD^+ and then from NADH to ferredoxin and protons (Schink, 1997). In *S. aciditrophicus* this is accomplished by electron-transferring flavoproteins (ETF) which

transfer electrons from butyryl-CoA oxidation to components of the membrane and finally to NAD^+ (McInerney et al., 2007). A similar mechanism of reversed electron transport has been proposed for the butyrate-oxidizing *Syntrophomonas wolfei* which also involves electron transfer to membrane components and energetization by a proton gradient (Wallrabenstein and Schink, 1994).

In contrast, the hypothesis recently postulated for syntrophic oxidation of butyrate does not involve redox-active components of the membrane (Herrmann et al., 2008). This hypothesis is based on the discovery of a bifurcating butyryl-CoA dehydrogenase in *Clostridium kluyveri* (Li et al., 2008). This enzyme catalyzes the endergonic oxidation of NADH with ferredoxin driven by the exergonic oxidation of another molecule of NADH with crotonyl-CoA in one enzyme reaction (Li et al., 2008). Herrmann et al. (2008) postulated that such an enzyme system which is also present in the genome sequences of *S. aciditrophicus* and *S. wolfei* could work in the opposite direction, i.e., endergonic butyryl-CoA oxidation with NAD^+ driven by exergonic ferredoxin oxidation.

Another bifurcating reaction has been described recently for the hydrogenase of *Thermotoga maritima* (Schut and Adams, 2009). Here, electrons from NADH oxidation are transferred to protons driven by reduced ferredoxin which has an unusually low redox potential of -453 mV and can therefore provide enough energy change with proton reduction to hydrogen to fuel the oxidation of NADH with protons (Schut and Adams, 2009).

However, all these theories have not been tested until now for the syntrophic bacteria described in this thesis and are largely based on genome data with only little biochemical proof available for these reactions in syntrophic degraders.

Aim of this thesis

In this study, several different kinds of syntrophic cooperations were investigated with the focus on the biochemical mechanisms that enable syntrophic fermenters to perform a reversed electron transport.

In the exceptional case of *Bacillus* sp. BoGlc83 growing with glucose as an easily fermentable substrate, we wanted to understand the reasons for the obligate dependence of this bacterium on methanogenic partner organisms.

Syntrophic oxidation of butyrate and ethanol were investigated with the objective to reveal the enzyme mechanisms responsible for the reversed electron transport. This was accomplished mainly by identifying the proteins potentially involved in syntrophic butyrate

oxidation based on earlier investigations as well as the genome sequence of the organism investigated. Syntrophic oxidation of ethanol was investigated in two different cocultures by classical enzyme assay approaches and comparative growth yield determination.

Chapter 2: Syntrophic Oxidation of Glucose

Dominant sugar utilizers in sediment of Lake Constance depend on syntrophic cooperation with methanogenic partner organisms

Nicolai Müller, Benjamin M. Griffin, Ulrich Stingl, and Bernhard Schink

Published in Environmental Microbiology (2008) **10**(6), 1501-1511

Summary

Six strains of novel bacteria were isolated from profundal sediment of Lake Constance, a deep freshwater lake in Germany, by direct dilution of the sediment in mineral agar medium containing a background lawn of the hydrogen-scavenging *Methanospirillum hungatei* as a syntrophic partner. The numbers of colony-forming units obtained after incubation for more than two months were in the same range as those of total bacterial counts determined by DAPI staining (up to 10^8 cells per ml) suggesting that these organisms were dominant members of the community. Identical dilution series in the absence of methanogenic partners yielded numbers that were lower by two to three orders of magnitude. The dominant bacteria were isolated in defined coculture with *M. hungatei,* and were further characterized. Growth was slow, with doubling times of 22-28 h at 28°C. Cells were small, 0.5 × 5 μm in size, Gram-positive, and formed terminal oval spores. At 20°C, glucose was fermented by the coculture strain BoGlc83 nearly stoichiometrically to two mol of acetate and one mol of methane plus CO_2. At higher temperatures, also lactate and traces of succinate were formed. Anaerobic growth depended strictly on the presence of a hydrogen-scavenging partner organism and was inhibited by bromoethane sulfonate, which together indicate the need for a syntrophic partnership for this process. Strain BoGlc83 grew also aerobically in the absence of a partner organism. All enzymes involved in ATP formation via glycolysis and acetyl CoA were found, most of them at activities equivalent to the physiological substrate turnover rate. This new type of sugar-fermenting bacterium appears be the predominant sugar utilizer in this environment. The results show that syntrophic relationships can play an important role also for the utilization of substrates which otherwise can be degraded in pure culture.

Introduction

Only a small fraction, in the range of 0.1–1%, of the total microbial community present in natural environments has been cultivated by conventional techniques (Staley and Konopka, 1985, Amann et al., 1995, Fry, 2000). In some cases, the cultivation efficiency could be improved substantially after design of better adapted cultivation media and supply of specific growth factors such as signal molecules (Schut et al., 1993, Bussmann et al., 2001, Bruns et al., 2002). Cultivation-independent techniques for identification of microbes *in situ*, e.g. by hybridization with specific 16S rRNA-targeted probes, have helped to identify at least part of the non-cultivated microbial community (Giovannoni et al., 1990, Amann et al., 2001, Ramakrishnan et al., 2001). However, only in exceptional cases these techniques provide sufficient information on the metabolic capacities and the possible ecological function of the respective organisms (Wagner et al., 2002), and the cultivation and physiological characterization of the majority of microbes in natural habitats is still the most demanding challenge in microbial ecology.

In anoxic, sulfate-poor environments, biomass is converted mainly to methane and CO_2 by a complex community of fermenting bacteria in cooperation with methanogens and homoacetogens which keep the hydrogen partial pressure in the range of 10^{-4} - 10^{-5} atm (Schink, 1997, Schink and Stams, 2001). Under such conditions, the fermentation of sugars by fermenting bacteria such as *Clostridium* spp. or *Ruminococcus albus* is shifted from the production of reduced side products such as butyrate or ethanol to nearly exclusive formation of acetate, CO_2 and H_2 (Ianotti et al., 1973, Zeikus, 1977, Zeikus, 1983, Tewes and Thauer, 1980), according to the equation

$$C_6H_{12}O_6 + 2\ H_2O \rightarrow 2\ CH_3COO^- + 2\ H^+ + 2\ CO_2 + 4\ H_2\ ;\ \Delta G^{0\prime} = -216\ \text{kJ per mol.}$$

Alternatively, formate could be formed instead of H_2 with a similar energy yield (-202 kJ/mol). Fermentation according to this equation does not provide sufficient energy for concomitant formation of 4 ATP which is linked directly to glycolytic sugar fermentation through substrate-level phosphorylation steps, which would require a minimum of 4 × 60-70 kJ per ATP (Thauer et al., 1977, Schink, 1997). At 10^{-4} atm hydrogen pressure, the reaction yields 317 kJ per mol, sufficient to allow synthesis of 4 ATP per mol glucose. In pure culture, therefore, known sugar-fermenting anaerobes produce butyrate, ethanol, or lactate as side products, leading to lower ATP yields.

In the present study, we tested the hypothesis that not all sugar-utilizing anaerobes fermenting hexoses according to the equation above would be able to shift to production of reduced side

products, and would therefore depend on syntrophic cooperation with hydrogen- or formate-oxidizing partners.

Materials and Methods

Sources of microorganisms

Strain BoGlc83 was enriched from profundal sediments of Lake Constance, Constance, Germany and deposited at the german strain collection (DSM 19598). *Methanospirillum hungatei* strain Mh1 was isolated in our lab from the same source and *Methanobrevibacter arboriphilus* strain DH1 was purchased from the DSM (No. 1125).

Sampling sites

Sediment samples were taken from cores of Lake Constance sediment at about 80 m water depth, about 1 - 2 cm below the sediment surface, at the transition from a grey surface layer to a blackish, sulfidic sediment below. Oxygen penetrates into this sediment only to 5 mm depth at maximum (Hauck et al., 2001). Sediment material was homogenized with sterile, anoxic mineral medium by vigorous shaking, and subsequently diluted in 1:10 steps in agar shake cultures in the same medium. Glucose, sucrose (both 2 mM) or soluble starch (0.5 g per l) was used as substrate, with 2 mM acetate as background co-substrate, with and without a background lawn of *Methanospirillum hungatei* strain M1h (about 10^7 cells per ml).

Medium and growth conditions

Bacteria were cultivated in a bicarbonate-buffered, sulfide-reduced anoxic freshwater mineral medium (Widdel and Bak, 1992). Trace elements, selenate and tungstate and a seven-vitamins solution were added from 1000 times concentrated stock solutions (Widdel et al., 1983). In order to minimize iron sulfide precipitation, a new trace element stock solution SL 13 was developed containing the same components as the original solution SL 10, but the $FeCl_2$ concentration was adjusted to 5 mM, with 14 mM EDTA. Resazurin was added as redox indicator at a concentration of 0.4 mg per liter.

The medium was prepared in 4-l flasks, autoclaved at 121°C and 1 bar overpressure for 40 min and distributed to 1-l infusion bottles or 120-ml serum bottles (70 ml headspace) which were sealed with rubber septa under a headspace of N_2/CO_2 (80:20). Substrates and other

additions were added from filter-sterilized stock solutions. Cultures were incubated at 28 to 30°C in the dark and optical densities were measured at 578 nm in a Uvikon 860 double-beam photometer (Kontron, Zürich, CH) against oxic medium to correct for the absorption of oxidized resazurin.

Pure cultures were obtained by repeated serial dilution in agar medium (Widdel and Bak, 1992). Additionally, cultures were pasteurized at 80°C for 30 min after growth and spore formation, and afterwards transferred to fresh medium with a background lawn of *Methanospirillum hungatei* (5 ml of an outgrown *M. hungatei* culture added to 50 ml medium). Purity was checked microscopically in cultures grown in mineral media with 2 – 10 mM glucose, 2 -10 mM fumarate, or in media containing 0.05% (w/v) yeast extract or 0.05% (w/v) Nutrient Broth plus 2 mM glucose.

For aerobic cultivation, SOC-medium was used (Sambrook, 1989) in sterile cotton-stoppered Erlenmeyer flasks or tubes on a rotary shaker at 200 rpm.

Spent media were prepared by filter sterilization of cultures of *Methanospirillum hungatei* or the coculture (BoGlc83 plus *M. hungatei*) through 0.2 µm cellulose acetate filters FP 30/0.2 CA-S (Whatman, Dassel, Germany). Filtrates were used undiluted or mixed with fresh medium in various amounts. Finally, 2 mM glucose and 5 mM BES were added.

DNA extraction

Aliquots of 2 ml from co-cultures of *Methanospirillum hungatei* with strains BoGlc81, BoGlc83 and BoGlc85, respectively, were centrifuged (10,000 × *g*, 15 min) and the supernatant was discarded. DNA from the pellets was extracted using a bead-beating method (Henckel et al., 1999), purified with the EZNA cycle pure kit (peqlab, Erlangen, Germany) and eluted with 50 µl sterile water.

PCR of bacterial 16S rRNA genes and phylogenetic analysis

Bacterial 16S rRNA genes were amplified using primers 27F (5'-AGA GTT TGA TCC TGG CTC AG-3'; *Escherichia coli* position 8–27) (Edwards et al., 1989) and 1492R (5'-TAC GGY TAC CTT GTT ACG ACT T-3'; *E. coli* position 1492–1512) (Weisburg et al., 1991) using 1 µl of the extracted DNA as template. PCR (30 cycles) was carried out as described previously (Henckel et al., 1999), except that the annealing temperature was 55°C. PCR products were purified with the QIAquick PCR purification kit (Qiagen, Hilden, Germany)

and partially sequenced using the 27F primer (GATC, Konstanz, Germany). Since nearly identical sequences (sequence similarity >99.5%) were obtained with the three isolates, only the 16SrRNA gene of strain BoGlc83 was further sequenced with primers 533F, 907F and 1492R (Stingl et al., 2004).

Sequences were assembled using DNAStar (www.dnastar.com). Sequence data were analyzed using the ARB software package (version 2.5b; http://www.arb-home.de; Ludwig et al., 1997). The new sequences were added to the ARB database and aligned using the Fast Aligner tool implemented in ARB. Alignments were checked and manually corrected where necessary. Sequences were compared to 16S rRNA gene sequences in public databases using BLAST (Altschul et al., 1990); sequences with high similarities to those determined in this study were retrieved and added to the alignment. Highly variable regions of the 16S rRNA gene sequences and sequence positions with possible alignment errors were excluded by using only those positions of the alignment that were identical in at least 50% of all sequences. The phylogenetic tree was calculated using fastDNAmL (Olsen et al., 1994), a maximum-likelihood method implemented in ARB, using only almost-full-length sequences (>1300 bases). The stability of the branching pattern was verified using the neighbor-joining and maximum-parsimony (DNAPARS) methods included in the PHYLIP package (Felsenstein, 1989) implemented in ARB.

16S rDNA sequences of strain BoGlc83 obtained in this study were deposited with Genbank under the accession number AY 189804.

Growth experiments

Sterile 60 ml serum bottles containing 30 ml medium with 2 mM glucose were inoculated with 3 ml of an exponentially-growing preculture. Controls contained either inoculum, 2 mM glucose, and 5 mM bromoethane sulfonate (BES), or 2 mM glucose and no inoculum. Samples were withdrawn with syringes from the cultures as well as from the headspace for product determination. Cultures were incubated at 20°C, 30°C and 40°C, respectively, in thermoconstant rooms or incubators. For determination of electron balances and fermentation stoichiometries, 120 ml serum bottles with 50 ml medium and 70 ml headspace were used.

Quantification of cell dry mass

Bacteria were cultivated in three 1 l infusion bottles containing growth medium with 2 mM glucose from the same 4-l batch. Trace element solution SL 13 was used to avoid FeS precipitates in the medium. Cells were harvested exactly at the time point when glucose was totally consumed and before spore formation started. The OD_{578} was recorded and the cultures were centrifuged at 13,500 × *g* for 5 min at 4°C in 20 steps using 50 ml polypropylene tubes (Deltalab, Barcelona, Spain) which were dried to constant weight before use in a lyophilizer Alpha 1-4 /LDC-1M (Christ, Osterode, Germany). Cells of three 1-l cultures were sedimented, the pellets frozen in liquid nitrogen, and lyophilized to constant weight. Cell dry mass was calculated from the mass differences of the tubes.

Preparation of cell-free extracts

Cultures grown in 1 l medium were harvested at the end of the exponential phase in an anoxic chamber (Coy, Ann Arbor, Mich., USA) by centrifuging the culture in anoxic polypropylene centrifuge bottles at 16,270 × *g* for 10 min at 4°C in a Sorvall RC-5B centrifuge (Du Pont de Nemours, Bad Homburg, Germany) . Cells were washed once by resuspending the pellet in the same volume of anoxic 0.1 M Tris-HCl buffer, pH 7.6, followed by centrifugation as described above. The pellet was resuspended in 4-6 ml washing buffer and cells were broken by repeated passage through a cooled French-Pressure cell at 137 MPa pressure under anoxic conditions. Alternatively, eubacterial cells were opened selectively by treatment with mutanolysin as described before (Wallrabenstein and Schink, 1994). Cell debris was removed anoxically by centrifugation (Optima TL-ultracentrifuge, TLA-100.4-rotor; Beckman, München, Germany) at 30,373 × *g* for 20 min and the supernatant (cell-free extract) was stored under N_2 on ice. Cultures grown in larger volumes were harvested by centrifugation in anoxic 120-ml infusion bottles gassed with N_2 as described before, with the same washing buffer as mentioned above (Brune and Schink, 1990).

Enzyme assays

Enzyme activities were measured continuously by following absorption changes with a spectrophotometer 100-40 (Hitachi, Tokyo, Japan) connected to an analogous recorder (SE 120 Metrawatt, BBC Goerz, Vienna, Austria). Assays were performed anoxically in a volume

of 1 ml in rubber-stoppered cuvettes at 25°C. Additions were made with microliter syringes from anoxic stock solutions. One unit of specific enzyme activity was defined as one µmol of substrate or product per min at 25°C, and normalized to mg of protein unless specified otherwise.

Hexokinase (EC 2.7.1.1) was measured with a method modified after Wood (1971). The assay mixture contained 66 mM triethanolamine-HCl (TEA-HCl) buffer, pH 7.6, 2.5 mM ATP, 1.3 mM $MgCl_2$, 0.33 mM $NADP^+$, 0.1 units of glucose-6-phosphate dehydrogenase (yeast) per ml, and 50 µl of cell-free extract. The reaction was started by addition of 1 mM glucose and was measured as NADPH absorption increase at 340 nm ($\varepsilon = 6.22\ mM^{-1}\ cm^{-1}$).

Phosphofructokinase (EC 2.7.1.11) was measured as NADH decrease coupled to aldolase, triosephosphate isomerase and glycerophosphate dehydrogenase (modified after Kemerer et al., 1975). The assay consisted of 75 mM Tris-HCl, pH 7.6, 0.43 mM NADH, 1.3 mM $MgCl_2$, 1.7 mM ATP, 0.7 U/ml of aldolase (rabbit muscle), 25 U/ml triosephosphate isomerase, 2.5 U/ml glycerophosphate dehydrogenase (rabbit muscle), and 10-50 µl cell-free extract. The reaction was initiated by addition of 6.7 mM fructose-6-phosphate.

The reaction mixture for fructose-bisphosphate aldolase (EC 4.1.2.13) contained 78 mM TEA-HCl, pH 7.6, with 3 mM dithioerythritol (DTE), 0.26 mM NADH, 10 U/ml triosephosphate isomerase, 1 U/ml glycerophosphate dehydrogenase and 50 µl of cell-free extract. The reaction was started by addition of 0.3 mM fructose-1,6-bisphosphate (modified after Wood, 1971).

For measurement of triosephosphate isomerase activity (EC 5.3.1.1), 85 mM Tris-HCl, pH 7.6, 0.26 mM NADH, 2 U/ml glycerophosphate dehydrogenase (rabbit muscle) and 50 µl cell-free extract were provided in the cuvette. Addition of 2 mM of glyceraldehyde-3-phosphate started the reaction (modified after Takahashi et al., 1995).

Glyceraldehyde-3-phosphate dehydrogenase (EC 1.2.1.12) was measured following the increase in NADH-concentration in 85 mM potassium-phosphate buffer (PPB), pH 7.6, with 3 mM DTE, 0.7 mM NAD^+, and 10-50 µl cell free extract. The reaction was started with 1.5 mM glyceraldehyde-3-phosphate.

Phosphoglycerate kinase activity (EC 2.7.2.3) was measured in 84 mM TEA-HCl,pH 7.6, 1.3 mM $MgCl_2$, 0.26 mM NADH, 1.6 U/ml glyceraldehyde-3-phosphate dehydrogenase, 2.5 mM ATP, and 10-50 µl cell free extract. The reaction was started with 10-20 mM 3-phosphoglycerate.

Pyruvate kinase activity (EC 2.7.1.40) was measured in 69 mM Tris-HCl, pH 7.6, with 3 mM DTE, 0.33 mM NADH, 1.6 mM phosphoenolpyruvate, 1.3 mM $MgCl_2$, 0.5 U/ml of lactate dehydrogenase, 5 mM NH_4Cl, and 10-100 µl cell-free extract. The reaction was started with 1 mM ADP.

The reaction mixture for pyruvate: acceptor oxidoreductase (pyruvate synthase; EC 1.2.7.1) contained 88 mM Tris-HCl, pH 7.6, 0.1 mM coenzyme A, 2 mM benzyl viologen (1,1'-dibenzyl-4,4'-bipyridinium-dichloride, $\varepsilon_{578\ nm}$ = 8.65 mM^{-1} cm^{-1}) prereduced with ~ 10 µM sodium-dithionite, and 10-50 µl cell free extract. The reaction was started with 20 mM sodium pyruvate (modified after Williams et al., 1987, Uyeda and Rabinowitz, 1971).

Hydrogen: acceptor oxidoreductase (hydrogenase; EC 1.18.99.1) was measured in the same way as pyruvate:acceptor oxidoreductase except that pyruvate and coenzyme A were omitted and that headspace and buffer were saturated with H_2. The reaction was started with 10-50 µl cell-free extract (modified after Diekert and Thauer, 1978).

Formate dehydrogenase (1.2.1.2) was measured in the direction of CO_2 and H_2 formation with benzylviologen, methylviologen, NAD^+ or $NADP^+$ as electron acceptors. One assay mixture contained 90 mM Tris-HCl, pH 7.6, 2-50 µl of cell-free extract, 1 mM methyl- or benzylviologen or 0.3 mM NAD^+ or $NADP^+$. The reaction was initiated by adding 25 mM of sodium formate. Addition of dithionite for prereduction of viologens was not necessary.

Pyruvate formate lyase was assayed as electron-acceptor-independent formation of acetyl CoA (A_{233}) from pyruvate.

The assay method for phosphotransacetylase (EC 2.3.1.8) was that of Bergmeyer (1974) , following acetyl-coenzyme A formation at 233 nm (ε = 4.44mM^{-1} cm^{-1}) from 0.33 mM coenzyme A and 3.58 mM acetyl-phosphate in 90 mM Tris-HCl, pH 7.6, with 17-34 µl cell-free extract.

Acetate kinase (EC 2.7.2.1) was measured discontinuously by colorimetric determination of acetyl-phosphate decrease (modified after Nishimura and Griffith, 1981). An assay mixture of 3 ml contained 80 mM Tris-HCl, pH 7.6, 3 mM acetyl phosphate, 5 mM ADP, 5 mM $MgCl_2$, and 150 µl ml cell-free extract in rubber-stoppered, N_2-gassed 4 ml glass vials. Samples of 400 µl volume were taken at regular intervals with microliter syringes and mixed with 300 µl of a 1.6 M hydroxylamine solution adjusted to pH 7.0. After 5 min, 300 µl of a 10% $FeCl_3$ solution in 1.36 M HCl / 0.4 M trichloroacetic acid was added, and the absorption at 535 nm was recorded after an additional incubation for 5 min. Calibration curves were prepared with 0-3 mM acetyl phosphate.

Analytical methods

Glucose, fatty acids and alcohols were analyzed by gas chromatography (Platen and Schink, 1987) or by HPLC (Klebensberger et al., 2006) using an Aminex HPX-87H ion-exchange column (BioRad) and an LC-10AT vp pump (Shimadzu).

Methane and molecular hydrogen were quantified by gas chromatography (Platen and Schink 1987, Friedrich and Schink, 1993).

Protein concentrations were determined by the microprotein assay (Bradford, 1976) with bovine serum albumin as standard.

Chemicals

All chemicals were of analytical or reagent grade quality and were obtained from Boehringer (Mannheim, Germany), Eastman Kodak (Rochester, NY, USA), Fluka (Neu-Ulm, Germany), Merck (Darmstadt, Germany), Pharmacia (Freiburg, Germany), Serva (Heidelberg, Germany), and Sigma (Deisenhofen, Germany). Gases were purchased from Messer-Griesheim (Darmstadt, Germany), and Sauerstoffwerke Friedrichshafen (Friedrichshafen, Germany).

Results

Enrichment and isolation of anaerobic sugar oxidizers

Syntrophic sugar oxidizers were isolated in agar shake dilution series in sulfide-reduced mineral medium with *Methanospirillum hungatei* in the background. After three weeks of incubation at 28 °C, colonies were found in all dilution series to a maximum of 10^5 colony-forming units per ml inoculum. Direct counting of the inoculum material after diamidino phenylindol (DAPI) staining revealed a total of $8.7 \pm 0.5 \cdot 10^7$ cells per ml (n = 3). After further incubation for another six to eight weeks, further small colonies became visible in the dilution series with the methanogenic partner, corresponding to $1.4 \cdot 10^8$ colony-forming units per ml sediment with glucose, and $4.2 \cdot 10^7$ or $1.6 \cdot 10^7$ with starch and sucrose, respectively (Table 1). These colonies were small, only about 0.1 to 0.5 mm in diameter, and were surrounded by satellite colonies of the methanogenic partner (Fig.1A).

Table 1: Enumeration of sugar-fermenting bacteria in sediment of Lake Constance in the presence or absence of a methanogenic partner bacterium. Tubes were incubated at 28°C for 2 months. The total count (DAPI) was $8.7 \pm 0.5 \times 10^7$ cells per ml sediment (n=3).

Substrate	Cultivation conditions	CFU per ml
Glucose	- *M. hungatei*	$1.2 \cdot 10^5$
	+ *M. hungatei*	$1.4 \cdot 10^8$
Starch	- *M. hungatei*	$2.0 \cdot 10^5$
	+ *M. hungatei*	$4.2 \cdot 10^7$
Sucrose	- *M. hungatei*	$8.0 \cdot 10^4$
	+ *M. hungatei*	$1.6 \cdot 10^7$

No such colonies were found in dilution series without methanogenic partners. Finally, six strains of defined cocultures were isolated in liquid medium from the tubes with glucose as substrate. These cultures contained, beyond *M. hungatei,* motile, short rod-shaped bacteria, 0.5 - 5 µm in size, which stained Gram-positive and formed subterminal spores in the stationary phase (Fig. 1B and C). Growth with glucose with all these strains was slow, with doubling times of 22-28 h. Addition of 5 mM bromoethane sulfonate, a specific inhibitor of methanogens (Gunsalus et al., 1978), inhibited growth and substrate utilization in all these cultures.

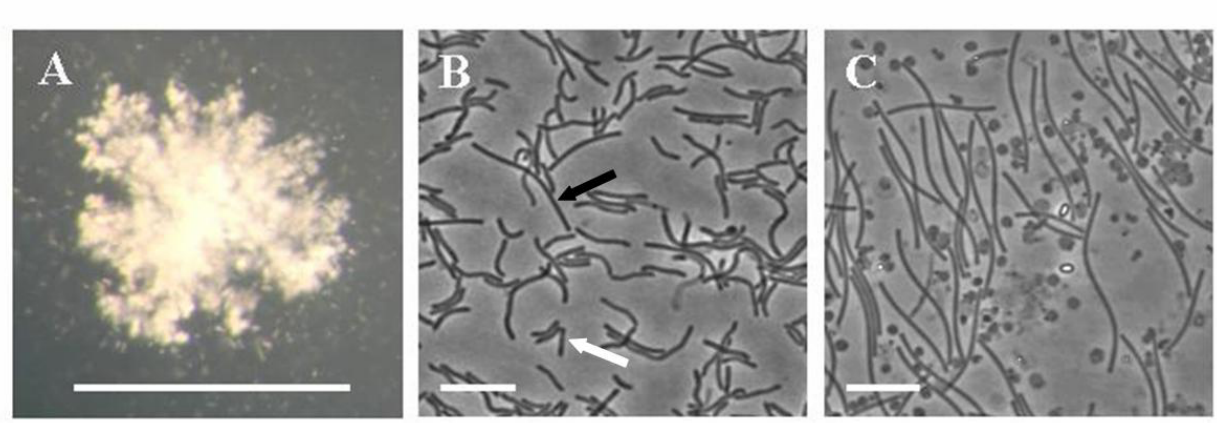

Figure 1 Micrographs of strain BoGlc83. A: Colony of strain BoGlc83 in agar medium surrounded by satellite colonies of *Methanospirillum hungatei*. Bar corresponds to 1 mm. B, C: Phase contrast photomicrographs of cells of the coculture. Bar corresponds to 10 µm. B. Exponential growth phase cells. White arrow: strain BoGlc83, black arrow: *Methanospirillum hungatei*. C: Outgrown culture showing cells of *Methanospirillum hungatei,* debris of lysed cells, and spores of strain BoGlc83.

No growth was observed in spent medium. All isolates grew optimally with 2–3 mM glucose; higher substrate concentrations were inhibitory. Three strains were analysed with respect to their 16S-rDNA sequences (see below).

Because they exhibited identical sequences, only one of them, strain BoGlc83, was used for further investigation after repeated isolation of single colonies and pasteurisation of liquid cultures for selective elimination of contaminants. No growth was observed if the coculture was incubated with 0.05% (w/v) yeast extract or 0.05% (w/v) nutrient broth. Yeast extract provided with glucose did not enhance growth. A wide range of substrates including diverse sugars, organic acids and alcohols was checked for utilization by strain BoGlc83. Reproducible growth was observed only with glucose, fructose, and maltose. Addition of alternative electron acceptors such as sulfate, nitrate, or fumarate did not increase maximal optical densities reached. Aerobic growth of strain BoGlc83 was observed with glucose, fumarate or lactate, preferentially on complex media (e.g. SOC-medium). With the coculture of strain BoGlc83 and *M. hungatei*, OD_{578} of 0.1 corresponded to 26.4 (±3) mg cell dry mass per liter.

Similar dilution experiments with pasteurised sediment samples after incubation for 2.5 months yielded numbers of colony-forming units that were by 3 orders of magnitude lower than the maximum numbers documented in Tab. 1, indicating that the predominant fraction of these bacteria was present in the sediment as metabolically active cells, not as spores.

In order to find alternative anaerobic cultivation conditions for strain BoGlc83, pasteurized samples of aerobically grown cells were inoculated in media with *Methanobrevibacter arboriphilus* in the background which can only use molecular hydrogen as energy source. Parallel incubation of the spores with *M. hungatei* helped to insure that restorage of anaerobic growth is possible after cultivation in oxic medium. Although a small increase of optical density was observed (ΔOD_{578} maximally 0.064 after seven days of incubation), no significant accumulation of fermentation products was detected. Anaerobic growth was fully restored in cultures with the formate plus hydrogen utilizing *M. hungatei* as syntrophic partner.

Phylogenetic characterization

For classification of the isolated strains, the 16S-rRNA-gene of three strains was amplified with primers targeting the Bacterial Domain, sequenced, and compared with the NCBI database.

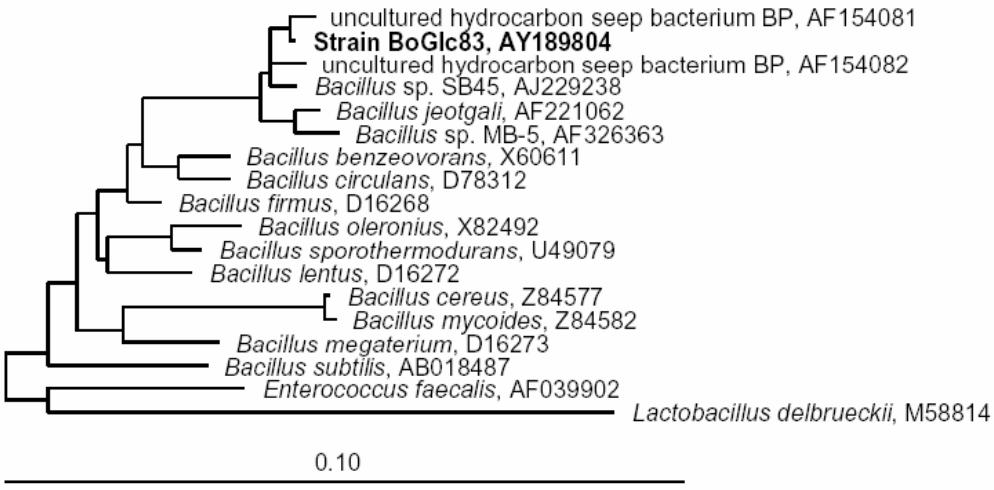

Figure 2: 16S rRNA gene-based phylogenetic tree showing the relation of strain BoGlc83 to other members of the *Bacillales*. The phylogenetic tree was constructed by utilising a maximum likelihood method implemented in ARB. *Enterococcus faecalis* and *Lactobacillus delbrueckii* were used as outgroup references. The scale bar represents 10 substitutions per 100 nt.

The sequences of all three strains were identical and showed highest sequence similarities with representatives of the low GC Gram-positive bacteria, with *Bacillus jeotgali* (Yoon et al., 2001) as the only described species (Fig. 2).

Another strain in the same cluster has been described as an iron-reducing bacterium dominant in rice paddies (Chin et al., 1999); other sequences from this cluster refer to uncultivated strains.

Fermentation pattern

Growth experiments and chromatographic analysis of the culture supernatant revealed that glucose was fermented to acetate, minor amounts of lactate, and a very small amount of succinate which was detected only with glucose concentrations higher than 2 mM (Tables 2 and 3). The peaks of standards of other possible fermentation products (formate, propionate, butyrate, acetoin, 2,3-butanediol or ethanol) were clearly separated from those of the detected substances. After addition of 1 mM of the respective substances as internal standards to the samples prior to analysis, no additional peaks or split peaks could be detected in the chromatograms.

Table 2. Fermentation products after growth at different temperatures on 2 mM glucose.

	Endconcentrations after 230 h incubation (mM)[a]					
	Coculture			Coculture + 5 mM BES		
	20°C	30°C	40°C	20°C	30°C	40°C
Glucose	0	0	0	1.70	1.47	1.62
Acetate[b]	2.89	2.64	2.35	0.20	0.30	0.17
Lactate	0.15	0.41	0.90	0.18	0.51	0.36
Formate	0	0	0	0.17	0.31	0
Methane	1.21	1.24	0.94	0.02	0.02	0.04

[a]Volumes at the end of the experiment: headspace 35 ml; culture 25 ml
[b]Values corrected for initial acetate concentration resulting from inoculum

Increasing cultivation temperatures caused a metabolic shift towards enhanced lactate formation (Table 2). At 20°C, the cells converted glucose almost completely to acetate, CO_2 and methane. The final concentrations of all metabolites were stable for at least 375 h at all temperatures. Cultures grown at 30°C or 40°C produced significantly more lactate and less acetate and methane than cultures incubated at 20°C (Fig. 3).

Cultures inhibited by 5 mM BES produced only small amounts of acetate, lactate, and formate, with no significant increase in $OD_{578\ nm}$ (Table 2). No accumulation of hydrogen was detected in BES-inhibited cultures (detection limit 10^{-3} bar).

Table 3: Stoichiometry of fermentation of strain BoGlc83

Glucose provided[a]	maximum OD_{578}[a]	Cell dry mass formed (mg)[b]	Substrate assimilated (µmol)[c]	Substrate dissimilated (µmol)	Products formed (µmol)[a]				Electron recovery (%)
					Acetate	Lactate	Succinate	Methane	
2.02 mM	0.112	1.47	10.11	90.89	145.5	18.5	2.5	92.4	98.3
5.35 mM	0.16	2.108	14.5	253	367	78.5	18.5	218.4	95

[a] Mean values from eight 120 ml serum bottles with 50 ml culture and 70 ml headspace
[b] Calculated from the above determined correlation factor: OD_{578} 0.1 = 26.35 mg/l
[c] Assimilation equation: 17 $C_6H_{12}O_6$ → 24 <$C_4O_3H_7$> + 6 HCO_3^- + 12 H_2O + 6 H^+

In another experiment, stoichiometries of glucose oxidation were calculated. Fermentation product analysis in eight parallel assays proved equilibrated electron balances. The amount of produced lactate increased significantly at higher initial glucose concentrations (Table 3).

Accumulation of the above mentioned fermentation products was occasionally observed also in aerobic cultures.

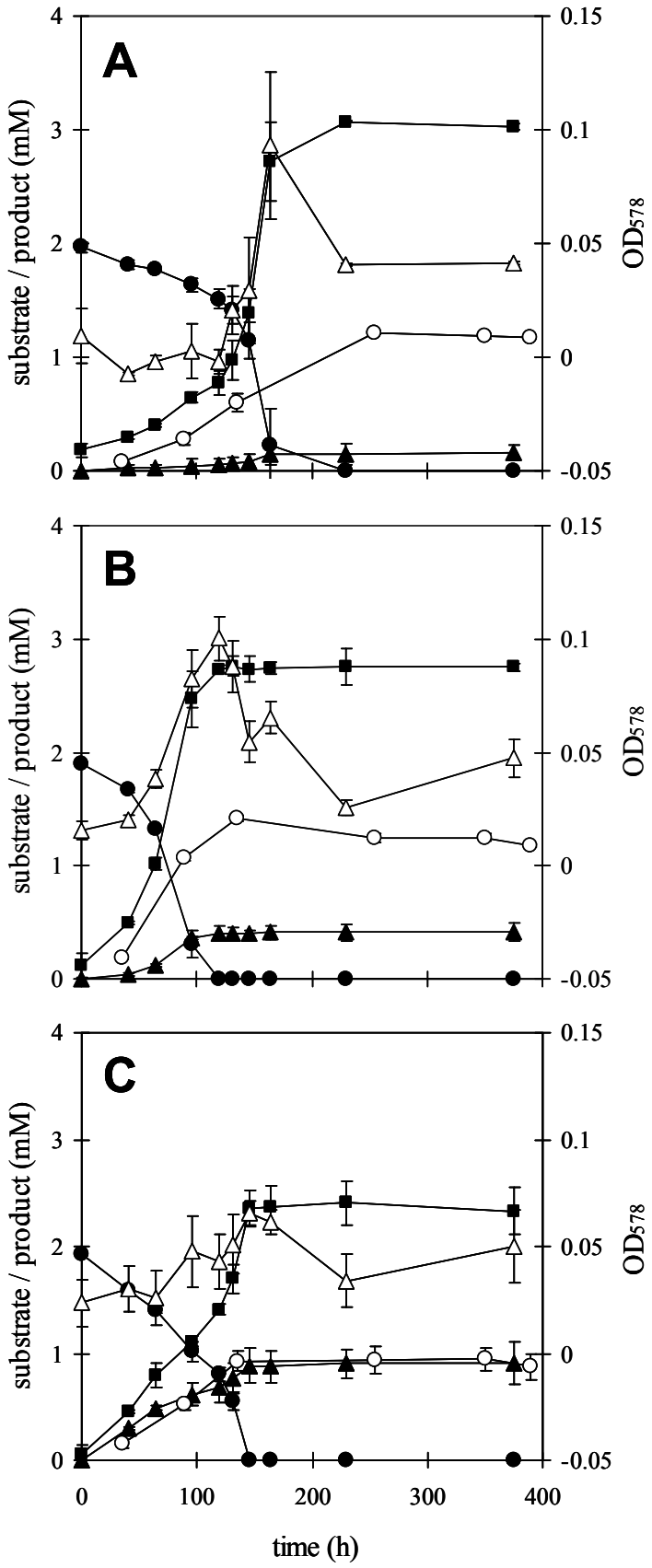

Figure 3: Time course of glucose fermentation by strain BoGlc83. Incubation temperatures: A: 20°C, n=2; B: 30°C, n=3; C: 40°C, n=3. Shown are mean values ± standard deviations of OD_{578} (open triangles) and concentrations of glucose (filled circles), acetate (filled squares), lactate (filled triangles) and methane (open circles). Some error bars are smaller than symbol size.

Enzyme activities

In order to investigate the metabolic pathways of syntrophic glucose oxidation in strain BoGlc83, enzyme assays were carried out with cell-free extracts. Activities of all key enzymes of the classical Embden-Meyerhof-Parnas pathway were detected (Table 4). Pyruvate is oxidized most likely via the *Clostridium*-type fermentation enzymes pyruvate: ferredoxin oxidoreductase, phosphotransacetylase, and acetate kinase (Table 4).

Table 4. Enzyme activities in cell-free extracts

Enzyme	Specific activity (U/mg protein)
Hexokinase[a]	0.127 – 0.242
Phosphofructokinase[a]	0.145 – 0.291
Aldolase[a]	0.028 – 0.121
Triosephosphate isomerase[a]	0.242 – 1.04
Glyceraldehyde-3-P-dehydrogenase (NAD – reducing)[a]	0.129 – 0.659
Phosphoglycerate kinase[c]	0.571
Pyruvate kinase[a]	0.039 – 0.274
Pyruvate:acceptor-oxidoreductase (benzylviologen)[b]	0.188
Formate dehydrogenase (benzylviologen)[d]	3.20
Formate dehydrogenase (methylviologen)[d]	1.72
Hydrogenase (benzylviologen)[b,c]	0.436
Phosphotransacetylase[a]	1.53 – 2.67
Acetate kinase[b]	0.290

[a]Minimal and maximal activities from at least three independent cell-free extracts of different growth stages
[b]Mean values from at least three measurements in one cell free extract
[c]Hydrogenase activity was not measured in extracts selectively prepared with mutanolysin
[d]Measured in mutanolysin-extracts. Activities comparable to those observed in French-Press extracts

No activity of lactate dehydrogenase (LDH) was found, neither with NAD^+ nor with dichlorophenol-indophenol (DCPIP) as electron acceptor. Addition of known allosteric

activators of LDH like fructose-1,6-bisphosphate did not help to initiate the reaction. Fructose-1,6-bisphosphate aldolase, glyceraldehyde-3-phosphate dehydrogenase, and pyruvate kinase required reduced assay conditions which were obtained by addition of DTE. Pyruvate kinase activity was enhanced by addition of NH_4Cl. Pyruvate was oxidized to acetyl coenzyme A by pyruvate: ferredoxin oxidoreductase, as indicated by the coenzyme A- and pyruvate-dependent reduction of benzyl viologen. No indication of pyruvate: formate lyase or formate: H_2 lyase was obtained. The presence of formate dehydrogenase (FDH) and hydrogenase (H_2: benzyl viologen oxidoreductase) in French-Press extracts shows that formate or hydrogen could be released from reduced ferredoxin. High FDH- and no hydrogenase activity was detected in cell free extracts produced by selective cell lysis with mutanolysin. FDH activities were detected only with benzylviologen or methylviologen as electron acceptors and no activity was observed with NAD^+ or $NADP^+$. Most enzyme activities varied with the growth state of the cells (Table 4). In contrast, triosephosphate isomerase and phosphotransacetylase were present always at comparably high activities (>1 U/mg). It was not possible to measure acetate kinase in the direction of acetyl phosphate and ADP formation from acetate and ATP. Therefore, a discontinuous assay was adapted to measure acetylphosphate decrease.

Discussion

The novel bacteria described in the present study differ from known fermenting bacteria in a series of unusual properties. They depend for fermentative degradation of hexoses on a syntrophic cooperation with a putatively hydrogen-utilizing methanogenic partner bacterium. Moreover, they appear to be the dominant sugar utilizers in a deep lake sediment, with total numbers ranging in the same order of magnitude as that of the total DAPI counts. Finally, they are spore-forming, facultatively anaerobic bacteria which have to be associated on the basis of 16S rRNA sequence comparisons with aerobic *Bacillus* representatives.

Physiology

Degradation of glucose by strain BoGlc83 depends on the cooperation with a formate- or hydrogen-scavenging methanogenic partner. Dependence of sugar degradation on a syntrophic partner bacterium has so far been described only for *Syntrophococcus sucromutans* (Krumholz and Bryant, 1986), a homoacetogenic bacterium which lacks formate dehydro-

genase and depends for that reason on cooperation with partners (Dore and Bryant, 1990). Another case of a fermenting bacterium which catalyzes an exergonic reaction but needs cooperation with a syntrophic partner is *Gelria glutamica*, a thermophilic, glutamate-degrading anaerobe which requires a hydrogen-scavenging partner for glutamate degradation but can grow in pure culture with pyruvate, lactate, glycerol or several sugars (Plugge et al. 2002). Otherwise, hydrogen-, formate-, or acetate-scavenging partners are required mainly in fermentative degradation of alcohols, fatty acids, certain amino acids and some other cases because these reactions can provide energy for growth only if electrons are removed, e.g., as hydrogen at low partial pressures (10^{-4} - 10^{-5} atm., Schink, 1997, Schink and Stams, 2001).

Strain BoGlc83 ferments glucose in cooperation with *Methanospirillum hungatei* roughly according to the equation

$$C_6H_{12}O_6 \rightarrow 2\ CH_3COO^- + 2\ H^+ + CO_2 + CH_4$$

Traces of lactate and succinate were formed mainly at enhanced temperatures. Formation of formate as a fermentation side product, lack of hydrogenase activity in selectively prepared cell free extracts, and preferential syntrophic growth with *Methanospirillum hungatei* rather than with *Methanobrevibacter arboriphilus* indicate that strain BoGlc83 catalyzes the reaction

$$C_6H_{12}O_6 + 2\ H_2O + 2\ CO_2 \rightarrow 2\ CH_3COO^- + 4\ HCOO^- + 6\ H^+$$

although we cannot rule out that some electrons may be released also in the form of hydrogen. This reaction yields -202 kJ per mol glucose under standard conditions, which is not sufficient to synthesize 4 mol ATP per mol glucose. Fermentation of hexoses to exclusively acetate and formate or H_2/CO_2 becomes more exergonic at enhanced temperatures (-275 kJ per mol glucose at 80°C), and some thermophilic bacteria have been described that ferment sugars accordingly (e.g., Soutschek et al., 1984, Rainey et al., 1991). However, re-examination of the fermentation patterns of these bacteria in our laboratory could not reproduce these fermentation balances. Either the substrate conversion was incomplete, and only a small fraction of the substrate was converted, or side products were formed by simultaneous fermentation of complex medium additions such as yeast extract etc., thus rendering an exact analysis of the fermentation balance difficult (H. Miller and B. Schink, unpublished results). The energetic situation can be substantially improved if the hydrogen- or formate concentration is lowered to 10^{-4} atm. or 10^{-4} M respecively, e.g., by the activity of a methanogenic partner, changing the overall free energy change to -290 kJ, and thus allowing the synthesis of 4 ATP per mol glucose. Our enzyme measurements confirm that glucose is degraded in our strain through the Embden-Meyerhof pathway, and in particular the enzymes

responsible for ATP synthesis, i.e., 3-phosphoglycerate kinase and pyruvate kinase, as well as phosphotransacetylase and acetate kinase are present at sufficient activity to support our concept of this metabolism. With this, strain BoGlc83 represents an extreme case of the known behaviour of *Clostridium butyricum, Ruminococcus albus* and others which carry out the same fermentation at low hydrogen pressure but can shift to formation of other, reduced fermentation products in pure culture if needed (Tewes and Thauer, 1980, Schink and Zeikus, 1982). Unlike those, strain BoGlc83 is unable to use alternative fermentations to optimize its energy metabolism in the absence of a suited partner. It is also surprising how specialized this organism is on the utilization of only three sugars which all are degraded anaerobically only in the presence of a partner organism. No growth was found with any substrate in the absence of a partner, and no growth was found either in mixed culture if the methanogenic partner was inhibited by bromoethane sulfonate. Strain BoGlc83 also represents the first case of a facultatively aerobic bacterium which can shift under anoxic conditions to a syntrophic mode of metabolism. This is especially surprising because obligately syntrophic fermenting bacteria require a specific set of reversed electron transport systems (McInerney et al., 2007) which differ substantially from aerobic electron transport.

Ecology

Fermenting bacteria similar to strain Glc83 were found to outnumber classical sugar-fermenting bacteria by 2 - 3 orders of magnitude. Obviously, this new type of syntrophic sugar fermentation is the dominant type of sugar fermentation in such an anoxic environment of long-term stability, with slow but continuous input of organic matter and lack of significant environmental challenges such as bioturbation, temperature shifts, or other changes. Under these conditions, this new type of sugar fermentation yields optimal energy, and there is very little chance that the bacterium has to adapt to varying life conditions over time. As well, our strains are slow compared to classical sugar fermenters, with doubling times of more than one day under optimal conditions at 28°C. Thus, isolation of these organisms in visible colonies in the presence of the partner organism needed incubation times of 2 - 3 months whereas the usual, fast-growing fermenters showed visible colonies already after 2 - 3 weeks. Our new strains, therefore, appear to constitute the "autochthonous" sugar-degrading community in this environment, whereas the fast-growing competitors are the "zymogenous" representatives *sensu* Winogradsky (1949). Attribution of these new bacteria to this ecophysiological group is further supported by the fact that they are obviously adapted only to low substrate

concentrations, and that glucose at concentrations higher than 2 mM inhibited growth significantly. Although they are able to form spores, our counting experiments with pasteurized sediment material indicate that these cells were not at a dormant state in the sediment but physiologically active, probably at very low substrate turnover rates.

The growth yields we obtained in our cultures were far lower than one would expect from a metabolism yielding 4 ATP per mol glucose. With bacteria growing with glucose, a Y_{ATP} of roughly 10 - 12 g per mol ATP would be expected, i.e., 40 - 50 g per mol glucose. The yields we observed were far less than that, roughly one quarter of the expected value. This low value may be due to the comparably slow growth and the concomitant high expenditures into maintenance energy. Moreover, we observed that the growth yield is obviously not an easy, linear function of the amount of substrate provided, and that the highest growth yields were observed with the lowest substrate concentrations used. This effect could only partly be compensated by addition of a further buffering system, indicating that either the small accumulations of acetate inhibited growth, e.g., by partial depolarization of the cytoplasmic membrane, or that the bacteria have a basic problem dealing with enhanced substrate concentrations in general. The non-linear dependence of growth yields on substrate supply may also be due to the observed enhanced formation of lactate, concomitant with lower energy yields and decreased support of the methanogenic partner. Thus, the growth yield data documented here are only of preliminary value and might have to be challenged again, e.g., by growth studies in chemostats.

Taxonomy

According to classical taxonomy, a facultatively anaerobic, spore-forming, fermenting bacterium should be attributed to the genus *Bacillus* (Sneath, 1986). Sequence similarity analysis of the 16S rRNA and comparison with related strains suggests attributing these new strains among several bacteria that are known so far only through sequence comparison from environmental samples, and have not been cultivated yet. The only relatives which have been described so far in defined cultures appear to be aerobic bacteria belonging to the genus *Bacillus*; the closest physiologically characterized representative is *Bacillus jeotgali* (Yoon et al., 2001). Also other *Bacillus* species have been described to change to a fermenting type of metabolism (Sneath, 1986), however, syntrophic cooperation with methanogens has not been documented so far.

Acknowledgements

The authors want to thank Prof. Dr. Werner Hofer, Konstanz, for numerous helpful suggestions to improve our enzyme analysis techniques, and Elisabeth Kayser for technical help with growth experiments. This study was supported by a research grant of the National Science Foundation, Washington, USA, to B. M. G., and by research funds provided by the University of Konstanz, Germany.

Dedicated to Prof. Dr. Norbert Pfennig on the occasion of his 82nd birthday.

Chapter 3: Syntrophic Oxidation of Butyrate

Involvement of NADH: acceptor oxidoreductase and butyryl-CoA dehydrogenase in reversed electron transport during syntrophic butyrate oxidation by *Syntrophomonas wolfei*

Nicolai Müller, David Schleheck and Bernhard Schink

Published in Journal of Bacteriology (2009) **191**(19):6167-6177

Summary

Methanogenic oxidation of butyrate to acetate requires a tight cooperation between the syntrophically fermenting *Syntrophomonas wolfei* and the methanogen *Methanospirillum hungatei*, and a reversed electron transport system in *S. wolfei* was postulated to shift electrons from butyryl-CoA oxidation to the redox potential of NADH for H_2 generation. The metabolic activity of butyrate-oxidizing *S. wolfei* cells was measured via production of formazan and acetate from butyrate, with 2,3,5-triphenyltetrazolium chloride as electron acceptor. This activity was inhibited by trifluoperazine (TPZ), an antitubercular agent known to inhibit NADH:menaquinone oxidoreductase. In cell-free extracts of *S. wolfei*, the oxidation of NADH could be measured with quinones, viologens, and tetrazolium dyes as electron acceptors, and also this activity was inhibited by TPZ. The TPZ-sensitive NADH:acceptor oxidoreductase activity appeared to be membrane-associated, but could be dissociated from the membrane as a soluble protein, and was semi-purified by anion-exchange chromatography. Recovered proteins were identified by peptide-mass fingerprinting which indicated the presence of a NADH:acceptor oxidoreductase as part of a three-component [FeFe] hydrogenase complex, and a selenocysteine-containing formate dehydrogenase. Furthermore, purification of butyryl-CoA dehydrogenase (Bcd) activity and peptide mass fingerprinting revealed two Bcd proteins different from the Bcd subunit of the Bcd/electron-transfer flavoprotein complex (Bcd/EtfAB) predicted from the genome sequence of *S. wolfei*. The results suggest that syntrophic oxidation of butyrate in *S. wolfei* involves a membrane-associated TPZ-sensitive NADH:acceptor oxidoreductase as part of a hydrogenase complex

similar to the recently discovered 'bifurcating' hydrogenase in *Thermotoga maritima*, and butyryl-CoA dehydrogenases that are different from Bcd of the Bcd/EtfAB complex**.**

Introduction

Butyrate is fermented to methane and CO_2 by syntrophic communities in which a methanogenic partner organism maintains a low hydrogen partial pressure to allow the oxidation of butyrate to acetate (McInerney et al., 1986, McInerney, 1988, Schink, 1997). Only under such conditions, butyrate-oxidizing bacteria such as *Syntrophomonas wolfei* can gain energy from the latter reaction in a range of approximately -20 kJ per mol butyrate, which is just sufficient to support microbial growth (Schink, 1997). It was postulated that *S. wolfei* has to invest some of the ATP that is formed in the acetate kinase reaction during β-oxidation of butyrate into an ATP-driven reversed electron transport, in order to shift electrons from butyryl-CoA oxidation to the redox potential of NADH (Thauer and Morris, 1984).

Experimental evidence for the involvement of a proton gradient and of ATPase activity in this process was obtained with intact cell suspensions (Wallrabenstein and Schink, 1994), and it was hypothesized that menaquinone-7 could play an essential role in this reaction (Wallrabenstein and Schink, 1994). This would imply that membrane-bound enzymes similar to complex I of the aerobic respiratory chain, i.e. NADH dehydrogenase (NDH), operate in reverse to reduce NAD^+ with butyrate electrons.

Another option for a reversed electron transport during butyrate oxidation and hydrogen formation in *S. wolfei* could be a reversal of the so-called Buckel-Thauer reaction. In this reaction that was described for ethanol/acetate fermentation by *Clostridium kluyveri*, electrons from NADH are disproportionated to reduce both crotonyl-CoA and ferredoxin simultaneously. The reaction is catalyzed by the cytoplasmic butyryl-CoA dehydrogenase/electron-transfer flavoprotein (Bcd/EtfAB) complex (Herrmann et al., 2008, Li et al., 2008). Very recently, another 'bifurcating' electron pathway has been described for an NADH- and ferredoxin- co-accepting di-iron hydrogenase complex in *Thermotoga maritima* (Schut and Adams, 2009). Here, electrons from NADH and from ferredoxin are combined to produce hydrogen, and the genome sequence of *S. wolfei* has been shown to contain candidate genes for such a three-component hydrogenase complex (Schut and Adams, 2009). Nonetheless, the energetic situation of syntrophic butyrate oxidation is basically different from that of ethanol or glucose degradation: Electrons arise at comparably positive

redox potentials, i. e., at -125mV/-10 mV (Gustafson et al., 1986, Sato et al., 1999) and -250 mV, and there is no oxidation step involved that could be coupled directly with ferredoxin reduction.

In the present communication, we report that butyrate oxidation by *S. wolfei* cell suspensions can be inhibited by trifluoperazine (TPZ), an antitubercular agent which has been shown to inhibit Type II NADH:menaquinone oxidoreductase NDH-2 in *Mycobacterium tuberculosis* (Yano et al., 2006), and that a TPZ-sensitive NADH:acceptor oxidoreductase activity can be measured in cell-free extracts of *S. wolfei* cells. This enzyme system and a butyryl-CoA dehydrogenase were enriched by anion-exchange chromatograpy, and the obtained proteins were identified by peptide-mass fingerprinting.

Materials and Methods

Organisms and cultivation

Syntrophomonas wolfei subsp. *wolfei* (McInerney et al., 1979, McInerney et al., 1981) was purchased from the DSMZ, Braunschweig, Germany, as an actively growing coculture with *Methanospirillum hungatei* JF1 (DSM 2245B). For further growth experiments with cocultures, *Methanospirillum hungatei* M1h isolated in our lab was used.

Cocultures were grown in anoxic, bicarbonate-buffered and sulfide-reduced freshwater medium (Widdel and Bak, 1992, Widdel et al., 1983) containing 0.05 % yeast extract and 20 mM sodium butyrate. Axenic cultures of *S. wolfei* were grown with 20 mM sodium crotonate (Wallrabenstein and Schink, 1994). In addition, the medium contained resazurine (0.4 mg • l^{-1}) as redox indicator, EDTA, and a decreased amount of iron to minimize the precipitation of iron sulfide (Müller et al., 2008). The 7-vitamin solution of the original freshwater medium was supplemented with lipoic acid (200 µg • l^{-1}) and thiamine (400 µg • l^{-1}) to improve growth of *S. wolfei* as described earlier (Beaty and McInerney, 1990). The medium was prepared in 4 l jars and distributed to 1 l or 120 ml infusion bottles after autoclaving for 40 min as described earlier (Müller et al., 2008). Larger volumes of medium for protein purification were prepared directly in 10 l culture vessels. Cultures were incubated at 28-30°C in the dark under N_2/CO_2 (80:20) atmosphere. Growth was monitored *via* optical density against sterile medium. Prior to measurement, a few grains of sodium dithionite were added to the cuvettes to keep resazurine in its reduced state.

Anoxic buffers for cell harvest or cell suspension experiments were prepared at the concentration and pH value as stated below, transferred to infusion bottles, sealed with rubber stoppers, and evacuated via needles threaded through the stopper using a vacuum pump while stirring the buffer vigorously with a magnetic stirrer. After 30 min, an atmosphere of 100% N_2 with a slight overpressure (appr. 0.3 bar) was applied to the bottle for 10 min to saturate the buffer. This process was repeated three times.

Preparation of cell suspensions

Cocultures of *S. wolfei* and *M. hungatei* were harvested at the end of the exponential growth phase (OD_{578} = 0.1 – 0.18 after about 10 days) in an anoxic chamber (Coy, Ann Arbor, MI, USA) by centrifugation in polypropylene beakers at 16,300 × *g* for 10 min at 4°C in a Sorvall RC-5B centrifuge (Du Pont de Nemours, Bad Homburg, Germany) as described previously (Müller et al., 2008). Large culture volumes of 10 or 20 l were concentrated under air with a tangential filter device (MiniTan, Millipore, Bedford, Massachusetts, USA). All subsequent manipulations were done in an anoxic chamber. Cells were washed twice by repeated centrifugation under the conditions described above in anoxic 0.05 M potassium phosphate buffer, pH 7.5, and resuspended in 4-6 ml of the same buffer. Cells of *S. wolfei* and *M. hungatei* were separated in two or four centrifuge tubes containing 20 ml of a Percoll gradient from 55 to 70% (Beaty et al., 1987). After centrifugation at 2,200 x *g* for 1 h in SS-34 centrifuge tubes, the two cell types were separated and the upper, *S. wolfei*-containing layer was transferred to two 120 ml infusion bottles and washed twice by centrifugation at 2,600 × *g* for 20 min in 2 x 100 ml buffer. The pellet was suspended in 5 ml of 0.02 M Tris-HCl, pH 8.0, for cell lysis, or 0.05 mM potassium phosphate buffer, pH 7.5, for cell suspension experiments. The separated *S. wolfei* cell fractions contained almost no cells of *Methanospirillum hungatei*, as confirmed by microscopy.

Cell suspension experiments

Metabolic activity of butyrate-grown cells was tested with 2,3,5-triphenyltetrazolium chloride (TTC) as electron acceptor. Dense cell suspensions (OD_{578} = 2) of *S. wolfei* after separation on a Percoll density-gradient were prepared in 0.05 M potassium phosphate buffer, pH 7.5, containing 5 mM TTC and degassed to remove traces of hydrogen by repeatedly evacuating and regassing with 100% N_2. From this suspension, 2 ml aliquots were transferred to rubber-stoppered tubes containing an atmosphere of 100% N_2 gas. Experiments were started by

adding 20 mM sodium butyrate to each tube. The inhibited treatments received in addition 0.1 mM TPZ, whereas butyrate was omitted in the negative controls. Each treatment was started in triplicate, and the tubes were incubated at 30°C on a shaker at 150 rpm. Samples of 250 µl were taken with syringes at the start of the experiment, and at intervals thereafter. For HPLC analysis, 200 µl samples were stopped with 20 µl of 2 M H_2SO_4, and centrifuged at 15,700 × *g* for 5 min. The supernatant was transferred to HPLC vials and analyzed as described below. The remaining 50 µl of sample was mixed with 950 µl absolute ethanol to give a final concentration of 95%, incubated for 5 min at room temperature to extract formazan from the cells, and then centrifuged at 15,700 × *g* for 5 min. Finally, the absorbance of the supernatant was recorded at 483 nm wavelength against ethanol, and the formazan concentration was calculated (ε_{483}=21 mM^{-1} cm^{-1}; Altman, 1976).

Cell lysis and subcellular fractionation

Cells were opened by three passages through an anoxic, cold French Pressure cell operated at 137 MPa. The cell lysate was collected in an 8 ml serum vial and the cell debris and unbroken cells were removed by centrifugation in an SS-34 rotor at 3,000 × *g* for 20 min using rubber adaptors. The supernatant thus obtained (cell-free extract) was further fractionated in an Optima TL-ultracentrifuge using the TLA-100.4-rotor (Beckman, München, Germany) at 236,000 × g_{min} for 30 min which yielded the soluble fraction (supernatant) and the membrane fraction (pellet). The fractions were stored on ice under N_2 gas.

Solubilisation of membrane proteins

Cells were disrupted as described above, but with only one passage through the French Pressure cell (see results). Unbroken cells and debris were spun down at 3000 × g for 20 min, and the supernatant crude extract was removed and stored on ice. The pellet was resuspended in 4 ml potassium phosphate buffer, subjected to a second passage through the French Pressure cell, and centrifuged. The crude extracts were pooled and fractionated by ultracentrifugation as described above. Membrane particles were washed once in anoxic potassium phosphate buffer, centrifuged again at 236,000 × g_{min} for 30 min and finally suspended in 4 ml of 0.02 M Tris-HCl, pH 8.0, containing 0.5 % dodecyl β-D-maltoside (DDM). After incubation for 30 min on ice, this mixture was ultracentrifuged again, and the supernatant contained the solubilized membrane protein (modified after Sinegina et al., 2005).

Enrichment of NADH:quinone oxidoreductase

Both the soluble and the membrane fraction of *S. wolfei* cells from 10 l or 20 l cultures contained high activities of NADH:quinone oxidoreductase and were used for enzyme purification. Stability tests showed that the activity was stable for several hours at room temperature and under air. Therefore, all purification steps were done at room temperature under air, but all manipulations were kept as short as possible and active fractions were stored on ice under 100% N_2 gas in between the purification steps to minimize activity losses. Purification was done on an FPLC gradient system (Pharmacia, Uppsala, Sweden). Protein preparations were applied to a packed DEAE-Sepharose CL-6B column (bed volume approximately 10 ml) equilibrated with 0.02 M Tris-HCl, pH 8.0. For purification of solubilized membrane proteins, all column buffers contained 0.01 % dodecyl β-D-maltoside (DDM). Separation was performed at a flow rate of 1 ml per minute with a shallow gradient of 0.300 M to 0.360 M NaCl in 0.02 M Tris-HCl, pH 8.0, over 160 min. Fractions were tested for activity by mixing 50 µl of sample with 10 µl of 7 mg/ml iodonitrotetrazolium chloride (INT) and 10 µl of 10 mM NADH in microtiter plates. Rapid development of red coloration (within 5 min) indicated the presence of NADH:INT oxidoreductase. Further red-colored fractions appeared after longer incubation (>15 min) but were neglected as they were considered to be due to unspecific INT reduction. These fractions were also tested for butyryl-CoA dehydrogenase activity, as described below. Active fractions were pooled and concentrated with centrifugal devices (Amicon Ultra-15, 10K nominal molecular weight limit, Millipore, Bedford, Massachusetts, USA) and the presence of NADH: menadione oxidoreductase was verified as outlined in the enzyme assay section. Pooled fractions were concentrated and adjusted to 4 ml volume with 0.02 M Tris-HCl, pH 8.0, and applied to a MonoQ column (Pharmacia). Proteins were eluted in the same buffer with a gradient of 0.260 to 0.360 M NaCl over 160 min at 1 ml • min^{-1}. The combined active fractions were again concentrated and rebuffered in 0.02 M Tris-HCl, pH 7.5, using PD-10 columns (Amersham Biosciences, Freiburg, Germany). Subsequently, a second run on MonoQ was performed, but this time in 0.02 M Tris-HCl, pH 7.5, and eluted by a shallow gradient of 0.250 to 0.310 M NaCl over 160 min. The fractions which eluted at 0.28 M NaCl showed NADH:INT oxidoreductase activity were concentrated to a final volume of 1 ml and defined as the partially purified NADH:menadione oxidoreductase.

Enrichment of butyryl-CoA dehydrogenase (Bcd)

The activity of Bcd was present in a late protein peak during the first NDH-purification step on DEAE-sepharose eluting at 0.7 M NaCl at pH 8.0. Fractions of this peak were combined, concentrated and desalted as described above, and were almost pure after this step (see the results).

Electrophoresis and peptide mass fingerprinting

SDS-PAGE was done according to Laemmli (1970). Gels containing 12 % polyacrylamide in the resolving gel and 4 % polyacrylamide in the stacking gel were cast either as minigels (ProteanII, BioRad) or as large gels (Protean xi, BioRad) for the excision of bands to be analyzed by peptide mass fingerprinting. Protein samples were mixed 1:2 with loading buffer (0.125 M Tris-HCl, pH 6.8, 2% (w/v) SDS, 25% glycerol , 0.01% (w/v) bromophenolblue and 5% β-mercaptoethanol or 0.1 M DTT) and heated at 100°C for 5 min prior to loading. Where indicated, samples were prepared in the same buffer at pH 8.0, boiled for 5 min, and subsequently alkylated by adding 2 % iodacetamide and incubation for 30 min at room temperature (Westermeier, 1990). Gels were run at 15 mA for the stacking gel, and when the marker front reached the resolving gel the current was increased to 30 mA. Gels were stained with colloidal Coomassie Blue (Neuhoff et al., 1988). Stained protein bands to be identified were excised and sent to TopLab GmbH (Martinsried, Germany) for tryptic digest and peptide mass fingerprinting; the fingerprints were matched (Mascot search engine) against the amino acid sequences derived from the primary genome sequence of *Syntrophomonas wolfei subsp. wolfei* strain Goettingen (Copeland et al. 2006, complete sequence of *Syntrophomonas wolfei* subsp. *wolfei* strain Goettingen, GenBank accession no. NC_008346).

Non-denaturing (native) gels were prepared as described above, except that 8% polyacrylamide in the resolving gel and no SDS or reducing agent was used in the loading and electrode buffers. Native gels were stained either with colloidal Coomassie Blue or by activity stain. Activity staining was done by immersing the gels in 0.05 M potassium phosphate buffer, pH 7.5, containing 0.1% iodonitrotetrazolium chloride and 0.1 mM NADH (Krebs et al., 1999). Active enzymes appeared as red bands after 15 min incubation at room temperature.

Enzyme assays

All enzymes were assayed in anoxic rubber-stoppered cuvettes at 30°C in a spectrophotometer 100-40 (Hitachi, Tokyo, Japan) connected to an analogous recorder (SE 120 Metrawatt, BBC Goerz, Vienna, Austria). Substrates and inhibitors were added by syringe. All measurements were done in triplicates.

NADH:quinone oxidoreductase was measured in 950 µl anoxic 0.05 M potassium phosphate buffer, pH 7.5, containing 0.2 mM NADH if not indicated otherwise. Then 5-20 µl sample was added and NADH oxidation was followed at 340 nm (ε_{340}= 6.3 mM^{-1} cm^{-1}; Ziegenhorn et al., 1976). After 2-3 min, 0.1 mM menadione or other quinones were added, resulting in an increase of the NADH oxidation rate. Where indicated, 0.1 or 0.2 mM of TPZ was added at least 3 min before addition of quinone (modified as described in Krebs et al., 1999 and Yano et al., 2006). Electron acceptors used were menadione (2-methyl-1,4-naphthoquinone), 1,4-naphthoquinone, duroquinone, phenazine methosulfate (PMS), menaquinone-4 and ubiquinone (Q10). One unit was defined as 1 µmol NADH oxidized per min and mg protein.

NADH:acceptor oxidoreductase was measured at the wavelength specific for each acceptor tested. In all cases, 5-20 µl sample was incubated in 950 µl anoxic 0.05 M potassium phosphate buffer, pH 7.5, with the respective electron acceptor. Reactions were started by addition of 0.2 mM NADH. Electron acceptors tested were 2,3,5-triphenyltetrazolium chloride (TTC), iodonitrotetrazolium chloride (INT), nitrobluetetrazolium (NBT), benzylviologen, methylviologen, or ferredoxin from *Clostridium pasteurianum*. Concentrations, wavelengths, and extinction coefficients are indicated for the respective test. One unit was defined as 1 µmol acceptor reduced per min and mg protein (modified as described in Li et al., 2008). The activity of butyryl-CoA dehydrogenase was measured with ferricenium hexafluorophosphate as electron acceptor as described before (Li et al., 2008).

A possible electron bifurcation reaction (Bcd/EtfAB complex) was tested as oxidation of crotonyl-CoA with NADH and TTC, as described before (Li et al., 2008). The reverse reaction was tested in a reaction mixture containing 0.02 M Tris-HCl, pH 7.5, 0.375 mM NAD^+, 10 µM ferredoxin from *Clostridium pasteurianum*, and 1 mM titanium citrate to keep ferredoxin in its reduced state. Then, cell-free extract or soluble fraction was added and the increase of NADH concentration was measured at 340 nm (ε_{340}= 6.3 mM^{-1} cm^{-1}; Ziegenhorn et al., 1976). Thereafter, 50 µM of butyryl-CoA was added and the absorption increase was followed further at 340 nm (as described by Wolfgang Buckel, personal communication).

Analytical methods

Acetate was analyzed by HPLC (16) using an Aminex HPX-87H ion-exchange column (BioRad) and an LC-10AT vp pump (Shimadzu). Sodium acetate was used as standard. Protein concentrations were determined by the microprotein assay (Bradford, 1976) against bovine serum albumin as standard.

Chemicals

All chemicals were of analytical or higher grade quality and were obtained from Boehringer (Mannheim, Germany), Eastman Kodak (Rochester, NY, USA), Fluka (Neu-Ulm, Germany), Merck (Darmstadt, Germany), Pharmacia (Freiburg, Germany), Serva (Heidelberg, Germany), and Sigma (Deisenhofen, Germany). Gases were purchased from Messer-Griesheim (Darmstadt, Germany), and Sauerstoffwerke Friedrichshafen (Friedrichshafen, Germany). Trifluoperazine dihydrochloride was purchased from Sigma, and used as freshly prepared aqueous stock solutions.

Sequence analysis

Basic sequence analysis was done using the LASERGENE package version 5.5 from DNAstar (Madison, Wisconsin, USA). Database searches were done using BLAST at the NCBI website, and the general domains and motifs in protein sequences were scanned in the NCBI Conserved Domain Search database. Transmembrane helices were scanned in the programs TMHMM 2.0 and SignalP 3.0.

Results

Experiments with intact cells

In order to assign activities specifically to the syntrophically fermenting bacterium, cells of cocultures were separated by density gradient centrifugation on a Percoll gradient as described previously (Beaty et al., 1987). Butyrate oxidation by *S. wolfei* cells was measured as production of formazan and acetate from butyrate, using 2,3,5-triphenyltetrazolium chloride as electron acceptor (Fig. 1). The cell suspensions produced 0.84 mM acetate from butyrate, and 0.4 mM formazan from TTC after 180 min. Thereafter, the concentrations did not increase further (not shown). Control reactions in the absence of butyrate produced 27 μM

formazan and no detectable acetate during 180 min (Fig. 1). When TPZ (0.1 mM) was tested as a potential inhibitor of a presumed Type II NADH:menaquinone oxidoreductase in S. wolfei, the cell suspensions produced average concentrations of 0.087 mM formazan and 0.12 mM acetate during 180 min (Fig. 1). Thus, TPZ inhibited the metabolic activity of *S. wolfei* cells by 86% and 78% as measured via acetate and formazan production, respectively. In mixed cell suspensions of *S. wolfei* and *M. hungatei*, TPZ inhibited butyrate oxidation by 63% to 68% (data not shown). Thus, inhibition of butyrate oxidation by TPZ was clearly associated with *S. wolfei* cells, presumably through inhibition of an NADH:menaquinone oxidoreductase-like enzyme that is involved in butyrate oxidation.

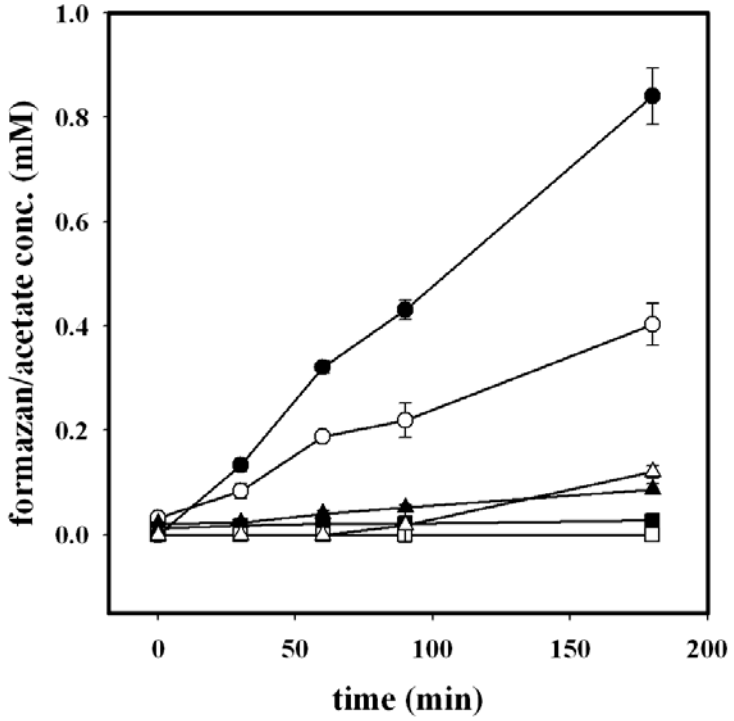

Figure 1: Oxidation of butyrate with triphenyltetrazolium chloride in cell suspensions of butyrate-grown, Percoll-separated *S. wolfei* cells. Shown are concentrations of acetate and formazan. Open symbols, formazan concentration; filled symbols, acetate concentration. Circles, no inhibitor added; triangles, cell-suspensions contained 0.1 mM TPZ; squares, negative control without butyrate; N=3, mean values +/- standard deviation.

Enrichment and characterization of NADH:quinone oxidoreductase

S. wolfei cell suspensions separated by density gradient centrifugation were opened by French press treatment, and cell extracts were assayed for NADH:quinone oxidoreductase activity. Activity was found predominantly in the soluble fraction of cell-free extracts (Table 1), but the activity was present also in the membrane fraction after one to three passages through the French press cell. After up to eight passages, almost all activity was in the soluble fraction.

This suggested that the activity was membrane-associated but could be separated from the membranes by this treatment.

Table 1: Partial purification of NADH:menadione oxidoreductase from *S. wolfei*. Mean values of activities of three independent measurements are shown.

Purification Step	Protein amount (mg)	Specific acitvity (U per mg)		Yield %	Purification factor
		NADH-oxidation [a]	NADH: menadione oxidoreductase [b]		
1st preparation run					
Cell-free extract	63.9	0.3	1.7	n.a.	n.a.
Soluble fraction	41.4	0.3	3.4	100	1
DEAE-Sepharose CL-4B pH 8.0	10.2	0.56	9.9	72	2.9
Mono Q pH 8.0	1.07	2.49	19.9	15	5.8
POROS HQ/H pH 8.0	0.6	1.65	16.5	7	4.8
Mono Q pH 7.5	0.04	2.34	59.3	1.6	17.4
2nd preparation run					
Cell-free extract	72	1.7	5.9	n.a.	n.a.
Soluble fraction	45.4	3.0	4.4	n.a	n.a.
Membrane fraction	28.8	0.3	1.55	100	1
Solubilized membrane protein	14.16	0.37	5.14	163	3.3
DEAE-Sepharose CL-6B pH 8.0	7.92	0.2	4.75	84.3	3.06
Mono Q pH 8.0	0.88	1.46	20.2	39.8	13.03
Mono Q pH 7.5	0.48	0.66	26.46	12.7	17.07

[a] unspecific oxidation of NADH before addition of menadione
[b] values corrected for unspecific NADH-oxidizing activity
n.d.= not determined , n.a.= not applicable

Enrichment of the activity was possible only by anion exchange chromatography (DEAE and MonoQ, see Material and Methods) whereas after alternative treatments (hydroxyapatite, POROS HQ/H, and gel filtration on Superdex 200) the activity was permanently lost. NADH:menadione oxidoreductase activity was enriched 17-fold from 41 mg soluble protein of *S. wolfei*, with a final specific activity of 59.3 U • mg^{-1} (Table 1). In another preparation

run, NADH:acceptor oxidoreductase was enriched from the membrane fraction to confirm whether the enzyme is membrane-associated. *S. wolfei* cells were opened by only one passage through the French Pressure cell (see above), and the washed membranes were solubilized using dodecyl β-D-maltoside (DDM) followed by purification with the same methods as described for the soluble fraction. This preparation yielded 0.49 mg of partially purified enzyme with a specific activity of 26.5 U • mg^{-1} (Table 1).

Table 2: Reactivity of partially purified NADH:quinone oxidoreductase with various electron acceptors**.**

electron acceptor	Redox potential (mV)	Extinction coefficient (mM^{-1} cm^{-1}); wavelength (nm)	TPZ concentration (mM)	Specific activity NADH: acceptor oxidoreductase (U per mg)
Duroquinone 0.2 mM	+ 35 [d]	n.a.	0	52.3
			0.1	20.1
Duroquinone 0.1 mM	+ 35 [d]	n.a.	0	15.7
			0.1	4.02
1,4-Naphthoquinone 0.1 mM	+ 64 [d]	n.a.	0	80.4
			0.1	37.4
Phenazine methosulfate 0.1 mM	+ 80 [c]	n.a.	0	189.3
			0.1	23.7
INT 0.4 mM	- 90 [a]	17.4 ; 465 [g]	0	68.9
NBT 0.4 mM	- 50 [a]	40.2 ; 605 [g]	0	0.47
TTC 0.4 mM	- 83, -240, -415 [b]	9.1 ; 546 [f]	0	41.2
Benzyl viologen 1 mM	- 360 [d]	8.65 ; 578 [d]	0	456.6
Methyl viologen 1 mM	- 440 [d]	9.7 ; 578 [d]	0	23.2

[a] Karmakar et al., 1960
[b] Rich et al., 2001
[c] Denke et al., 1998
[d] Bergmeyer, 1974 and Friedrich and Schink, 1993
[e] Li et al., 2008
[f] Altman, 1976
[g] n. a.=not applicable

The partially purified enzyme from the soluble fraction showed high NADH:menadione oxidoreductase activity but reacted also with other water-soluble quinones, as shown in Table 2. Activities were maximal with 0.2 mM NADH and 0.1 mM menadione. With 0.1 mM NADH and 0.1 mM menadione, the activity was approximately 50% of that observed with 0.2 mM NADH. All quinone-reducing activities were inhibited by TPZ. The extent of inhibition depended on the respective concentrations of NADH and quinone: with 0.2 mM TPZ, 0.2 mM NADH, and 0.1 mM menadione, the inhibition was maximal resulting in a remaining activity of 23% of the non-inhibited enzyme, whereas at equimolar concentrations of NADH and menadione almost no inhibition was observed (Table 3). A minimum concentration of 0.1 mM TPZ was needed to cause a significant inhibition at all.

Table 3: Inhibition of partially purified NADH:quinone oxidoreductase by TPZ.

TPZ concentration (mM)	NADH concentration (mM)	Menadione concentration (mM)	Specific acitvity of NADH-oxidation (U per mg)	Specific activity of NADH: menadione oxidoreductase (U per mg)	Remaining activity
0	0.2	0.1	2.34	59.3	100 %
0.1	0.2	0.1	1.61	26.2	44 %
0.2	0.2	0.1	0	14.1	23 %
0	0.1	0.1	1.0	19.8	100 %
0.1	0.1	0.1	1.31	19.1	96 %
0	0.1	0.04	1.91	32.3	100 %
0.1	0.1	0.04	1.0	18.8	58 %

No activity was observed with the commercially available menaquinone-4 or ubiquinone, and the enzyme did not react with ferredoxin of *Clostridium pasteurianum* (results not shown). The activity of NADH:acceptor oxidoreductase with TTC or ferredoxin could not be stimulated by addition of crotonyl-CoA, neither in the soluble fraction nor in the partially purified enzyme preparation. When testing the reverse reaction with butyryl-CoA and NAD^+ and with ferredoxin kept in its reduced state by titanium citrate (see Material and Methods), the enzyme reacted with NAD^+ already before addition of butyryl-CoA, thus exhibiting ferredoxin:NAD^+ oxidoreductase activity, in the range of 0.017 to 0.081 U• mg^{-1}. This activity did not increase in the presence of butyryl-CoA. The partially purified NADH:menadione oxidoreductase activity from solubilized membranes was separated on a

non-denaturing gel (Fig. 2) and appeared in a Coomassie stain two prominent bands of about 130 kDa apparent size (Fig. 2A), and both prominent bands were stained positive by NADH:iodonitrotetrazolium oxidoreductase activity staining (Fig. 2B). The same picture was obtained with NADH:menadione oxidoreductase activity purified from the soluble fraction on a non-denaturing gel (not shown). The two active bands in the non-denaturing gel (Fig. 2B) were excised, heated in SDS-buffer containing DTT, and loaded onto a denaturing SDS-gel (see Material and Methods). Both excised bands (N1 and N2 in Fig. 2B) were each resolved by SDS-PAGE into a set of four major bands (Fig. 2C), visible each at about 97 kDa, 60 kDa, 46 kDa and 15 kDa molecular size, respectively; the additional protein apparent at about 90 kDa size (from band N2) was assumed to represent partially re-folded or non-denatured 97-kDa protein (see below).

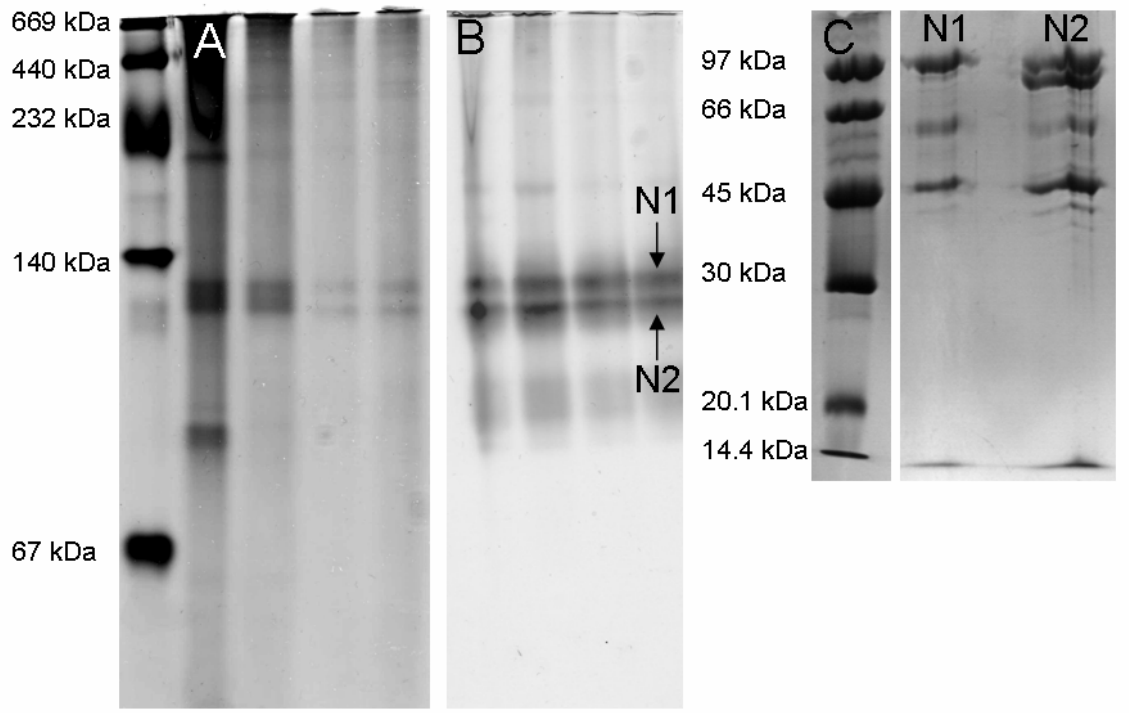

Figure 2: Partially purified NADH:quinone oxidoreductase from solubilized membranes separated on an non-denaturing gel stained with Coomassie or by activity-staining, and the two active bands further resolved on a denaturing gel. A: Separated proteins stained with Coomassie G-250. From left to right: marker, solubilized membrane protein, after DEAE CL-6B, 1st MonoQ, 2nd MonoQ. B: Activity stain with INT and NADH as outlined in the methods section. From left to right: marker, solubilized membrane protein, after DEAE CL-6B, 1st MonoQ, 2nd MonoQ. C: Further separation of the two active bands from the non-denaturing gel (N1 and N2 in Fig. 2B) after excision and transfer onto a denaturing gel.

These four prominent bands were consistently observed when the different preparations of NADH:menadione oxidoreductase obtained from the FPLC-purification steps were separated on denaturing gels (Fig. 3), no matter if purified from the membrane or from the soluble fraction (cf. Fig. 3AB), appearing as major bands at about 97 kDa, 60 kDa, 46 kDa and 15

kDa molecular size (Fig. 3C; bands A1, A2, A3 and A7, respectively). These bands were excised and submitted to peptide mass fingerprinting (see below). Other bands which were not correlated with NADH:menadione oxidoreductase activity (A4, A5, A6 in Fig. 3C), but which appeared to be enriched during the activity purifications from either the membrane fraction (cf. Fig. 3A; band A5 and A6), or from the soluble protein fraction (cf. Fig. 3B; band A4), were also excised and submitted to peptide mass fingerprinting (see below).

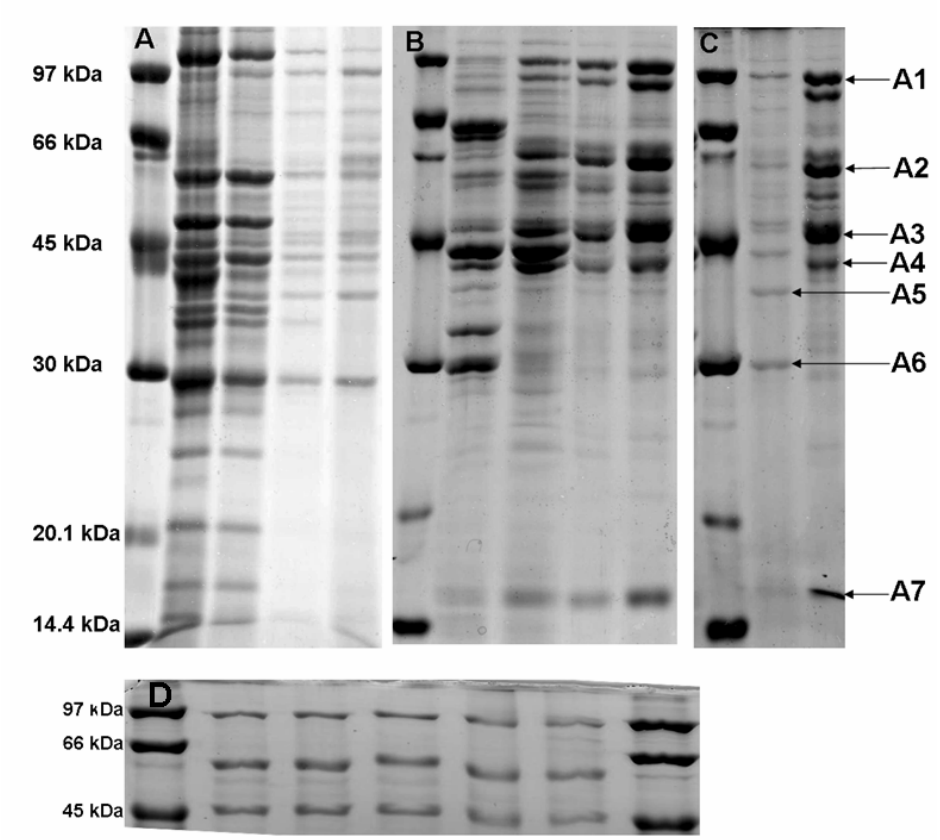

Figure 3: SDS-PAGE of the partially purified NADH:quinone oxidoreductase of *S. wolfei*. A: Purification from solubilized membrane protein. From left to right: marker, solubilized protein, after DEAE-sepharose CL-6B, after first run on MonoQ, after second run on MonoQ. B: Purification from the soluble fraction. From left to right: marker, soluble fraction, after DEAE-sepharose CL-6B, after first run on MonoQ, after second run on MonoQ. C: Comparison of membrane and soluble protein. From left to right: marker, partially purifed protein from membranes, partially purified protein from soluble fraction. Numbers A1-A7 indicate excised and identified bands. D: partially purified enzyme under different denaturing conditions. From left to right: marker, protein reduced with mercaptoethanol, protein sample with DTT, alkylated protein, no reducing agent added, sample not reduced and not boiled, marker.

Treatment of the preparations under various denaturing conditions did not produce differences in the SDS-PAGE banding pattern (Fig. 3D), which confirmed that the apparent protein complex was fully denatured when separated by SDS gel electrophoresis (for the presumably selenocysteine-linked 97-kDa protein, see below).

Peptide mass fingerprinting of proteins associated with NADH:quinone oxidoreductase activity

In total, seven different bands were excised from SDS-PAGE (see Fig. 3C), the proteins digested, and the derived peptides analyzed by mass spectrometry. The obtained peptide mass fingerprints were aligned against the *S. wolfei* genome sequence.

Table 4: Protein identification by peptide mass fingerprinting

Protein band	Estimated mass (Da, by SDS-PAGE)	Identified protein (by PMF)	Predicted mass (Da, by PMF)	Gene locus tag	Sequence coverage
A1	97000	NADH dehydrogenase I chain G	39714	Swol_0785	84 %
		Formate dehydrogenase alpha subunit	58564	Swol_0786	60 %
A2	60000	Iron hydrogenase, small subunit	64259	Swol_1017	70 %
A3	46000	NADH dehydrogenase I (quinone)	44406	Swol_1018	85 %
A4	40000	Acetate/butyrate kinase	43734	Swol_0768	93 %
A5	39000	ABC-transporter, periplasmic substrate binding protein	37964	Swol_2479	72 %
A6	30000	Extracellular solute-binding protein	28360	Swol_0316	78 %
A7	15000	NADH dehydrogenase I chain E	16563	Swol_0783	62 %
		Fe-dependent hydrogenase gamma subunit	16181	Swol_1019	67%
B1	65000	Acyl-CoA dehydrogenase	68811	Swol_1933	73 %
B2	64000	Acyl-CoA dehydrogenase	68798	Swol_2052	80 %
B3	40000	Putative iron-sulfur binding reductase (only C-terminal half)	82333	Swol_0698	46 %

A total of nine predicted genes could be attributed by peptide mass fingerprinting (Table 4): one band (A7, at 15 kDa, see below) obviously represented a mixtures of two proteins with the same apparent molecular mass on SDS-PAGE, and one band (A1, at 97 kDa) represented apparently one protein which appeared to be encoded by two predicted genes (presumably

selenocysteine-linked, see below). Furthermore, several of the identified proteins appeared to be encoded by genes that are located in clusters in the genome sequence, thus in presumed operons, as detailed in the following. The prominent band at 46 kDa (band A3 in Fig. 3C) was attributed to predicted gene Swol_1018 (derived 44.4 kDa; see Table 4), which was annotated as the NADH-binding subunit gene of a [FeFe] hydrogenase / NADH:ubiquinone oxidoreductase complex (NuoF-like; COG1894). No other identified protein (see below) could be attributed to the same enzyme function (NADH:acceptor oxidoreductase). Hence, this gene was most likely responsible for the apparent NADH:menadione reductase activity of our semi-purified enzyme. The deduced amino acid sequence showed the highest level of identity to three sequences derived from paralog genes in *S. wolfei* (Swol_1024, 1828, and 0784, with 76%, 73%, and 64% id-aa, respectively), and to a sequence derived from the genome of *Pelotomaculum thermopropionicum* (PTH_2011; 56% id-aa). Furthermore, the Swol_1018 protein sequence was closely related to those of characterized [FeFe] hydrogenase components, e.g. HydB in *Thermoanaerobacter tengcongensis* (Soboh et al., 2004) (TTE0893; 55%), HndC in *Desulfovibrio fructosovorans* (Dermoun et al., 2002) (U07229; 50%), and HydB in *Thermotoga maritima* (Schut and Adams, 2009) (TM1425; 46%). Notably, the Swol_1018 sequence lacked the N-terminal part (141 aa) of the HydB sequences of *T. tengcongensis* and *T. maritima*, which contain an additional [2Fe2S] binding site (Soboh et al., 2004), thus showing more similarity in its domain structure to HndC of *D. fructosovorans* (above) and to NuoF of NADH:ubiquinone oxidoreductase complex I in E. coli (locus tag b2284; 40% id-aa).

In the genome sequence, this attributed gene (Swol_1018) was part of an apparent three-gene operon (not shown). Peptide-mass fingerprints corresponding to the two other genes, Swol_1019 and Swol_1017, were obtained for the prominent protein bands that were excised from SDS-PAGE at about 15 kDa (band A7 in Fig. 3) and 60 kDa (band A2), respectively (see Table 4). The attributed gene Swol_1019 (derived 15.9 kDa) was predicted to encode a [2Fe2S] ferredoxin component of a [FeFe] hydrogenase complex (NuoE-like; COG1905). The deduced amino acid sequence showed the highest level of identity to sequences derived from paralog genes in *S. wolfei* (four candidates, each with 66% id-aa), and with <41% homology to ferredoxin subunits in other sequenced organisms, e.g. HydC of the characterised [FeFe] hydrogenase complex in *T. tengcongensis* (TTE0890; 33%) and *T. maritima* (TM1424; 31%). The other gene, Swol_1017 (derived 62.9 kDa), was annotated to encode a [FeFe] hydrogenase catalytic subunit (COG4624). The best BLAST hit was obtained for a paralog gene (Swol_2436; 68% id-aa), the second best for a gene predicted in

Pelotomaculum thermopropionicum (PTH_2010; 60%); furthermore, the protein sequence appeared closely related to the characterised hydrogenase component HydA of *T. tengcongensis* (TTE0894; 55%), HndD of *D. fructosovorans* (Dermoun et al., 2002) (U07229; 51%), and HydA of *T. maritima* (TM1426; 40%). Notably, the Swol_1017 protein sequence lacked the C-terminal part (89 aa) of the HydA sequences in *T. tengcongensis* and *T. maritima*, which contain an additional [2Fe2S] binding site (Soboh et al., 2004), thus showing in its domain structure more similarity to HndD of *D. fructosovorans* (above) and monomeric hydrogenase of *Clostridium pasteurianum* (P29166; 40% id-aa). Thus, the peptide mass fingerprinting and sequence analysis suggested that these three proteins are co-expressed from a presumed operon in *S. wolfei* (Swol_1017-1019) during syntrophic growth with butyrate, and constitute most likely a multimeric [FeFe] hydrogenase complex (HydABC-like). The subunit structure of the apparent NADH:quinone oxidoreductase activity (see above) confirmed that these three proteins (bands A2, A3 and A7 in Fig. 3C) form a protein complex *in vivo* which appears to be associated with the membrane.

The band which was excised at about 15 kDa (band A7) yielded also sufficiently distinctive peptide mass fingerprint signals to attribute a second NuoE-like protein to be present in our protein fraction, which was encoded by gene Swol_0783 (see Table 4). This gene was suggested to be part of an apparent four-gene operon in *S. wolfei* (not shown). Corresponding peptide mass fingerprints were obtained for two of the three other genes, Swol_0785 and Swol_0786 (Table 4). Interestingly, the fingerprint derived from the band of 97 kDa size (band A1 in Fig. 3C) matched the individual peptide masses of the genes Swol_0785 and Swol_0786, which are predicted to encode for a 39.7-kDa and a 58.6-kDa protein, respectively (see Table 4). The open reading frames (ORF) of Swol_0785 and Swol_0786 appeared to be in-frame, with an apparent non-coding spacing of 48 bp (not shown). However, when the two derived protein sequences were conjoined (predicted size: 98.1 kDa) including the non-coding spacing (16 amino acids) and aligned against the database, BLAST hits were obtained for contiguous protein sequences with either selenocysteine or cysteine at the position of the stop codon of Swol_0785 (not shown). The best BLAST hit (55% id-aa) was obtained for the selenocysteine-containing formate dehydrogenase protein of *Eubacterium acidaminophilum* (FdhA-II, CAC39239); a predicted formate dehydrogenase sequence with cysteine instead of selenocysteine was found in *Pelobacter propionicus* (YP_903170; 52% id-aa). Peptide mass fingerprinting thus suggested that a selenocysteine-containing formate dehydrogenase was expressed in *S. wolfei* cells during syntrophic growth with butyrate, which appeared to copurify with our NADH:quinone oxidoreductase activity.

The bands submitted to peptide mass fingerprinting that were not correlated to NADH:quinone oxidoreductase activity (see above, bands A4, A5 and A6 in Fig. 3C), were attributed to predicted gene Swol_0768 (band A4) annotated to code for acetate kinase (EC:2.7.2.1), and to predicted genes Swol_2479 (band A5) and Swol_0316 (band A6), which were annotated each to code for periplasmic components of ABC-type transport systems (see Table 4).

Identification of butyryl-CoA dehydrogenase activity and of a DUF224-protein in S. wolfei

The genome sequence of *S. wolfei* harbors at least nine candidate genes for butyryl-CoA dehydrogenases (bcd), one of which (Swol_0268) was co-located in a putative bcd-etfBA operon in syntheny to that in C. kluyveri, and a second one (Swol_2126) was located several genes apart from a paralog set of etfBA genes in *S. wolfei*. Other bcd candidate genes were found in presumed operons with other butyryl-metabolic genes (e.g., Swol_0788, Swol_1483, Swol_1933; not shown).

Table 5: Partial purification of butyryl-CoA dehydrogenase.

Purification Step	Protein amount (mg)	Specific acitvity (U/mg)	Yield %	Purification factor
Cell-free extract	72	n.d.	n.a.	n.a.
Soluble fraction	45.4	12.19	100	1
DEAE-Sepharose CL-6B pH 8.0	5.14	40.72	37.8	3.34
Membrane fraction	28.8	0.11	100	1
Solubilized membrane protein	14.16	0.53	236	4.81
DEAE-Sepharose CL-6B pH 8.0	0.765	14.19	342	129

The soluble protein fraction of butyrate-grown *S. wolfei* cells exhibited high activity of butyryl-CoA dehydrogenase (Bcd) (Table 5), and the activity eluted as one peak during the first FPLC purification step (DEAE), in a fraction well separated from the NADH:menadione oxidoreductase activity (data not shown).

The fraction exhibited a green-yellow colour, suggestive of a high content of flavins (not shown). SDS-PAGE (Figure 4) showed two proteins in the 66-kDa size range which were

analysed by peptide mass fingerprinting (band B1 and B2, see also Table 4). The proteins were attributed to predicted genes Swol_1933 and Swol_2052, respectively, each annotated as FAD-containing acyl-CoA dehydrogenase genes (COG1960) with high sequence identity (75% id-aa). Interestingly, the derived Bcd sequences showed much lower identity (<20% id-aa) to the sequence encoded by the bcd genes which are associated etfBA genes in the C. kluyveri genome (bcd-etfBA operon; YP_001393857), or in the *S. wolfei* genome (see above). Thus, the butyryl CoA dehydrogenase activity in *S. wolfei* cells during syntrophic growth with butyrate was represented by two similar enzymes which co-purified during FPLC, and these enzymes appeared to be different from the Bcd(s) associated with the described Buckel-Thauer reaction complex, the Bcd/EtfAB-complex.

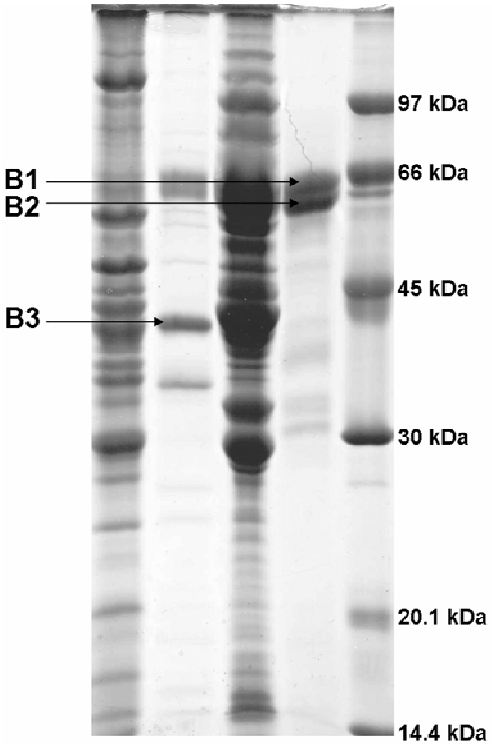

Figure 4: SDS-PAGE of partially purified butyryl-CoA dehydrogenase. From left to right: solubilized membrane protein, DEAE CL-6B, soluble fraction, soluble fraction after DEAE CL-6B, marker. Numbers B1-B3 indicate excised and identified bands.

When the butyryl CoA dehydrogenase activity was purified from the membrane fraction, an additional protein appeared on SDS-PAGE (band B3, at about 40 kDa in Fig. 4). This band was identified by peptide mass fingerprinting to represent the predicted gene Swol_0698, annotated to encode a domain-of-unknown function 224 protein (DUF224) (COG0247), which comprises a predicted transmembrane domain (*N*-terminal) and a predicted 4Fe4S-

cluster binding domain (*C*- terminal). The predicted size of the derived protein sequence (81.4 kDa) did not match the size of the protein observed on SDS-PAGE (appr. 40 kDa), and the peptide signals obtained from peptide mass fingerprinting solely matched to, and fully comprised, the C-terminal half of the predicted sequence (appr. 40 kDa) (data not shown). We conclude that *S. wolfei* expressed a DUF224-like protein during growth with butyrate, the N-terminal transmembrane domain of which was either lost during the purification procedure or absent in the protein *in vivo*. Interestingly, this protein appeared to be encoded in a presumed operon with a third paralog pair of *etfBA* genes in the *S. wolfei* genome.

Discussion

Release of electrons from butyryl-CoA oxidation to crotonyl CoA in the form of molecular hydrogen requires a reversed electron transport system to overcome the redox potential difference between the donor (E°' = -125/-10 mV; Gustafson et al., 1986, Sato et al., 1999) and the acceptor system (E°'= -414 mV; -300 mV at 10^{-4} atm H_2; Schink, 1997). An early hypothesis how such a reversed electron transport could operate in *S. wolfei* assumed the involvement of a menaquinone (Schink, 1997, Wallrabenstein and Schink, 1994). This concept seemed plausible also for glycolate-oxidizing syntrophs (Friedrich and Schink, 1993, Schink, 1997). After investigation of the genome sequence of *Syntrophus aciditrophicus*, this hypothesis was supported by a more refined model involving an NADH:quinone oxidoreductase enzyme complex. It was stated that NADH produced from menaquinone can be oxidized by proton- or Na^+-translocating Rnf-proteins reducing ferredoxin which in turn could be reoxidized by a classical ferredoxin-dependent hydrogenase (McInerney et al., 2007). However, in the genome sequence of *S. wolfei*, we found no gene cluster for Rnf proteins as in *Syntrophus acidotrophicus* (encoded by SYN_01664 - 01659; McInerney et al., 2007), especially no significant homologies for predicted integral membrane proteins RnfA, D, E, and G (McInerney et al., 2007).

After the discovery of a dismutation reaction between NADH, ferredoxin, and crotonyl CoA in *Clostridium kluyveri*, Herrmann et al. (2008) regarded a reversed electron transport via quinones unlikely because the genome of *S. aciditrophicus* lacks the complete set of enzymes for complex I. Instead, a participation of a Bcd/EtfAB complex in butyrate oxidation by syntrophic fatty acid oxidizers was postulated (Herrmann et al., 2008, Li et al., 2008; W. Buckel, pers. communication) which was supported by the fact that a gene cluster of *bcd-etfBA* genes was found in the genome of *S. wolfei*. This assumption was tested in the current

study by repeating the enzyme assays of Li et al. (2008) with cell-free extracts of *S. wolfei*. However, rapid oxidation of NADH with several electron acceptors including the artificial electron acceptor TTC never required, or showed increased oxidation rate by crotonyl-CoA, as typical of NADH oxidation by the Bcd/EtfAB complex of *C. kluyveri* (Li et al., 2008). Reduction of crotonyl-CoA with ferredoxin plus NADH could not be tested since this reaction would require hydrogenase in the assay which is not commercially available, to keep ferredoxin in the oxidized state.

We found high activity of butyryl-CoA dehydrogenase with ferricenium as electron acceptor in cell-free extracts, a reaction catalyzed by the Bcd/EtfAB complex as a side activity (Li et al., 2008). This activity could be enriched from both the soluble and the membrane fraction of *S. wolfei*, and two acyl-CoA dehydrogenases distinct from the Bcd of the Bcd/EtfAB complex were identified. This is consistent with earlier observations that up to 18% of the butyryl-CoA dehydrogenase activity in *S. wolfei* is located in the membrane fraction (Wallrabenstein and Schink, 1994), and implies that the butyryl-CoA dehydrogenases of *S. wolfei* might react with components of the membrane. Therefore, it appears unlikely that the Bcd/EtfAB complex is involved in reversed electron transport during butyrate oxidation by *S. wolfei*. Nonetheless, this complex may be expressed under different growth conditions, e.g. during growth by dismutation of crotonate to acetate and butyrate. Even if one would assume an operation of a Bcd/EtfAB complex working in reverse during butyryl-CoA oxidation with NAD^+, driven by reduced ferredoxin, there remains the problem how the reduced ferredoxin could be regenerated, since no Rnf-proteins are encoded in the genome of *S. wolfei* and there is no oxidation step involved in butyrate oxidation that could be coupled directly to ferredoxin reduction.

Several genes for butyrate metabolism are predicted to be clustered around the two identified Bcd genes (Swol_1933 and 2052) in presumed operons (not shown), i.e. enoyl-CoA hydratase (Swol_1936), 3-hydroxyacyl-CoA dehydrogenase (Swol_1935), and acetyl-CoA C-acyltransferases (Swol_1934 and 2051). We therefore suggest that these genes are likely to be co-expressed in *S. wolfei* during growth with butyrate. Furthermore, the co-purification of a DUF224 – predicted transmembrane FeS-binding reductase (Swol_0698) with the Bcd activity from the membrane fraction (Fig. 4, Table 4), and the fact that this gene is encoded in a presumed operon together with a (third) paralog set of predicted *etfBA* genes (Swol_0696 and 0697; no *bcd* candidate), makes it tempting to speculate that these genes might be co-expressed during growth with butyrate, and constitute a membrane-associated

Bcd/EtfAB/DUF224 complex which funnels electrons from the butyryl-CoA/crotonyl-CoA redox couple into the membrane.

The high NADH-oxidizing activity observed in cell-free extracts promised to be an alternative starting point to approach the proposed reversed electron transport in *S. wolfei*. For purification of the NADH-oxidizing enzyme of *S. wolfei,* the methanogenic partner had to be removed because *M. hungatei* has been reported to exhibit NADH diaphorase activity (McKellar et al., 1981). Menadione was found to be an electron acceptor of this NADH-oxidizing enzyme in *S. wolfei*, and NADH:menadione oxidoreductase activity was shown earlier to be an attribute of NADH dehydrogenases of the NDH-2-type (Yano et al., 2006) and of complex I-like enzymes (NDH-1) (Krebs et al., 1999), although menadione is an artificial, water soluble quinone lacking the alkyl side chain of natural quinones. The activity appeared to be associated with the membrane but could be resolved into the soluble protein fraction, thus showing another attribute typical of NDH-2-type and complex I-like NADH dehydrogenases which both are membrane-associated, but non-transmembral proteins (Krebs et al., 1999, Yano et al., 2006). In experiments with cell suspensions, TPZ, an antitubercular agent acting against NADH:menaquinone oxidoreductase (NDH-2) in *Mycobacterium tuberculosis* (Yano et al., 2006), was found to inhibit butyrate oxidation in *S. wolfei,* probably by blocking an NADH oxidoreductase enzyme. Accordingly, also the partially purified NADH:menadione oxidoreductase activity from butyrate-grown cells of *S. wolfei* was inhibited by TPZ. The enzyme appeared to be essential for butyrate oxidation because TPZ inhibited also butyrate oxidation and acetate production by intact *S. wolfei* cells with TTC as electron acceptor; TTC has been reported to accept electrons over a wide range of redox potentials from -83 mV to -415 mV (Rich et al., 2001, Slater et al., 1963), and was proven to be an indicator for activity of complex I in mitochondria (Rich et al., 2001). Hence, we anticipated that the NADH:menaquinone oxidoreductase activity of *S. wolfei* is represented by an enzyme similar to the membrane-associated NDH-2 or complex-I-type NADH dehydrogenases, i.e., linked to the quinone pool in the membrane, and that this enzyme is involved in the proposed reversed electron transport in *S. wolfei*.

The semi-purified NADH:menaquinone oxidoreductase activity separated by non-denaturing gels showed two prominent, active bands (Fig. 2AB) which each could be resolved into the same set of four subunits by denaturing SDS-PAGE (Fig. 2C). We conclude that the semi-purified activity was represented by a protein complex which appeared as a double band on non-denaturing gels, perhaps due to differences in charge, folding, or subunit assembly. The cumulative mass of the complex calculated from the masses of its subunits (97, 60, 46, and 15

kDa; Fig. 2C) was >210 kDa whereas the bands of the complex on native gels were found close to the 140-kDa marker (Fig. 2AB). Such a discrepancy is not uncommon because native gels do not allow reliable protein mass estimation. The four attributed subunits of the complex were consistently enriched both from the membrane and the soluble fraction, thus confirming that the NADH:menaquinone oxidoreductase activity was purified as a four-subunit protein complex.

This NADH-oxidizing protein complex contains a 46-kDa subunit (band A3 in Fig. 3) as indicated by peptide mass fingerprinting (Table 4), which was attributed as the NADH-accepting subunit of a [FeFe] hydrogenase / NADH:ubiquinone oxidoreductase complex (HydB / NuoF-like). The corresponding gene was part of an apparent three-gene operon (Swol_1017 - 1019), and the 60 kDa and 15 kDa proteins of the complex (band A2 and A7 in Fig. 3) matched the other two predicted genes: the gene for the 60-kDa subunit (Swol_1019) was indicated to encode a catalytic [FeFe] hydrogenase subunit (HydA-like), and the gene for the 15 kDa subunit a ferredoxin (HydC-like). Thus, surprisingly, the protein complex which we purified as NADH:menaquinone oxidoreductase activity was ascribed to contain the subunit homologues of a three-component hydrogenase complex, for example of *Thermotoga maritima*, which was recently described as an electron-bifurcating hydrogenase (Schut and Adams, 2009). The fourth protein that consistently was co-purified apparently as part of this protein complex, the 97-kDa protein (band A1 in Fig. 3), was attributed as a selenocysteine-containing catalytic subunit of a formate dehydrogenase complex encoded by two genes (Swol_0785 and 0786) that are translated as one protein through selenocysteine insertion (Zhang and Gladyshev, 2005, P. Worm and C. Plugge, Wageningen, pers. commun.). The homologous enzyme in *Eubacterium acidaminophilum* (FdhA-II) has been implicated to play a role also in interspecies formate transfer (Graentzdoerffer et al., 2003, Zindel et al., 1988).

The association of these attributed proteins as subunits of a membrane-associated protein complex during syntrophic growth of *S. wolfei* with butyrate appears likely based on their purification and separation properties discussed above, and the TPZ inhibition experiments indicated a crucial role for the NADH oxidoreductase component of the protein complex in butyrate oxidation. Other catalytic features attributed to the complex by sequence analysis, i.e. the predicted hydrogenase and formate dehydrogenase activities, must be confirmed in future biochemical studies. The observation that this complex could contain an electron-bifurcating hydrogenase allows to speculation whether NADH oxidation and hydrogen formation could be catalyzed in *S. wolfei* also via electron bifurcation, i.e., proton reduction with NADH plus reduced ferredoxin, as described for the *Thermotoga* enzyme system (Schut and Adams,

2009). However, for *S. wolfei* the same problem would arise as with the proposed electron-bifurcating Bcd/EtfAB complex, i.e., how ferredoxin could be reduced first to drive the bifurcation reaction (see above). Since the protein complex appears to be membrane-associated and resembles NADH:quinone oxidoreductases we assume that it could indeed be supplied with electrons from the butyryl-CoA/crotonyl-CoA redox couple, perhaps via a proton-translocating menaquinone cycle. Menaquinone-7 was previously found to be present in the membranes of *S. wolfei* (Wallrabenstein and Schink, 1994) and might likely be the physiological reaction partner of this enzyme. The necessary proton motive force could be provided by ATP hydrolysis, thus sacrificing part of the ATP produced via substrate-level phosphorylation in butyrate oxidation as proposed before (Thauer and Morris, 1984, Wallrabenstein and Schink, 1994). Shifting electrons from the level of reduced menaquinol (E_0'= -74 mV; Thauer et al., 1977) to the level of NADH (E_0'= -320 mV; Thauer at al., 1977) would require an energy expenditure of +46 kJ per mol, which can be provided by two protons pumped across the membrane. Experimental evidence for the involvement of a proton gradient in butyrate oxidation by *S. wolfei* was provided thus far only with intact cells (Wallrabenstein and Schink, 1994). To show this linkage in a cell-free system will be a matter of future investigations.

Acknowledgements

The authors acknowledge Diliana Simeonova and Karin Denger for numerous helpful suggestions concerning protein purification and identification. We also thank Petra Worm and Caroline Plugge, University of Wageningen, for help with the interpretation of sequence data. Moreover, we thank Antje Wiese for technical assistance especially for preparation of growth medium and of ferredoxin from *Clostridium pasteurianum*. The publicly available genome sequence established by DoE- JGI is highly appreciated. This project was funded by the Deutsche Forschungsgemeinschaft, Bonn-Bad Godesberg, and by research funds of the University of Konstanz.

Dedicated to Prof. Dr. Rudolph K. Thauer on the occasion of his 70th birthday.

Chapter 4: Syntrophic Oxidation of Butyrate II

Syntrophic butyrate and propionate oxidation processes: from genomes to reaction mechanisms

Nicolai Müller, Petra Worm, Bernhard Schink, Alfons J. M. Stams, and Caroline M. Plugge

Review article. Accepted for publication in Environmental Microbiology Reports (2009)

Summary

In anoxic environments such as swamps, rice fields, and sludge digestors, syntrophic microbial communities are important for decomposition of organic matter to CO_2 and CH_4. The most difficult step is the fermentative degradation of short-chain fatty acids such as propionate and butyrate. Conversion of these metabolites to acetate, CO_2, formate, and hydrogen is endergonic under standard conditions and occurs only if methanogens keep the concentrations of these intermediate products low. Butyrate and propionate degradation pathways include oxidation steps of comparably high redox potential, i. e., oxidation of butyryl-CoA to crotonyl-CoA and of succinate to fumarate, respectively, that require investment of energy to release the electrons as hydrogen or formate. Although investigated for several decades, the biochemistry of these reactions is still not completely understood. Genome analysis of the butyrate-oxidizing *Syntrophomonas wolfei* and *Syntrophus aciditrophicus* and of the propionate-oxidizing *Syntrophobacter fumaroxidans* and *Pelotomaculum thermopropionicum* reveals the presence of energy-transforming protein complexes. Recent studies indicated that *S. wolfei* uses electron-transferring flavoproteins coupled to a menaquinone loop to drive butyryl-CoA oxidation, and that *S. fumaroxidans* uses a periplasmic formate dehydrogenase, cytochrome b:quinone oxidoreductases, a menaquinone loop, and a cytoplasmic fumarate reductase to drive energy-dependent succinate oxidation. Furthermore, we propose that homologues of the *Thermotoga maritima* bifurcating [FeFe]-hydrogenase are involved in NADH oxidation by *S. wolfei* and *S. fumaroxidans* to form hydrogen.

Introduction

In anoxic environments such as swamps, rice paddy fields and intestines of higher animals, methanogenic communities are important for decomposition of organic matter to CO_2 and CH_4 (Schink and Stams, 2001, McInerney et al. 2008, Stams and Plugge, 2009). Moreover, they are the key biocatalysts in anaerobic bioreactors that are used world-wide to treat industrial wastewaters and solid wastes. Different types of anaerobes have specified metabolic functions in the degradation pathway and depend on metabolite transfer which is called syntrophy (Schink and Stams, 2001). The study of syntrophic cooperation is essential to understand methanogenic conversions in different environments (McInerney et al., 2008). The most difficult step in this degradation is the conversion of short-chain fatty acids such as propionate and butyrate. Under standard conditions (P_{H2} of 1 atm, substrate and product concentrations of 1 M, temperature 298 K), propionate and butyrate oxidation to H_2, formate and acetate are endergonic reactions (Table 1).

Table 1: Standard free reaction enthalpies of fatty acid oxidation and methane production. (values calculated from the standard free formation enthalpies of the reactants at a concentration of 1 M, pH 7.0 and T = 25°C according to (Thauer et al., 1977)

Reaction		**$\Delta G^{0'}$ (kJ/ reaction)**
$Propionate^- + 2\ H_2O \rightarrow Acetate^- + CO_2 + 3\ H_2$	eq. 1	+ 76.0
$Propionate^- + 2\ H_2O + 2\ CO_2 \rightarrow Acetate^- + 3\ HCOO^- + 3\ H^+$	eq. 1a	+ 65.3
$Butyrate^- + 2\ H_2O \rightarrow 2\ Acetate^- + H^+ + 2\ H_2$	eq. 2	+ 48.3
$Butyrate^- + 2\ H_2O + 2\ CO_2 \rightarrow 2\ Acetate^- + 2\ HCOO^- + 2\ H^+$	eq. 2a	+ 38.5
$4\ H_2 + CO_2 \rightarrow CH_4 + 2\ H_2O$	eq. 3	-131.7
$4\ HCOO^- + 4\ H^+ \rightarrow CH_4 + 3\ CO_2 + 2\ H_2O$	eq. 4	-144.5
$CH_3COO^- + H^+ \rightarrow CH_4 + CO_2$	eq. 5	- 36

In anoxic environments, methanogenic Archaea maintain low H_2, formate, and acetate concentrations which make propionate and butyrate degradation feasible (Stams and Plugge, 2009). Syntrophic propionate and butyrate oxidations involve energy-dependent reactions that are biochemically not fully understood. However, recently several novel reactions were discussed to perform energy transformation in other bacteria. These reactions will be summarized in this report with respect to their possible implications in syntrophic fatty acid oxidation. Moreover, the genomes of two propionate degraders (*Syntrophobacter fumaroxidans* and *Pelotomaculum thermopropionicum*) and two butyrate degraders (*Syntrophomonas wolfei* and *Syntrophus aciditrophicus*) have been sequenced (McInerney

et al., 2007, Kosaka et al., 2008). Based on genome analysis we propose that novel energy-transforming reactions are involved in syntrophic butyrate and propionate degradation.

Topic 1. Known energy-conserving mechanisms in syntrophic butyrate and propionate degradation

Butyrate degradation

Butyrate oxidizers known to date belong to two groups of bacteria within the family Syntrophomonadaceae and the order Syntrophobacterales. Formerly classified as Clostridia, the members of the family *Syntrophomonadaceae* have been reassigned to a new family within the order Clostridiales, based on their 16S rRNA sequence (Zhao et al., 1993). Members of this family are *Syntrophomonas wolfei*, *Syntrophomonas bryantii* (formerly *Syntrophospora bryantii* (Wu et al., 2006)), *Syntrophomonas erecta*, *Syntrophomonas curvata*, *Syntrophomonas zehnderi* and *Thermosyntropha lipolytica*.

The second group of syntrophic butyrate degraders belongs to the *Syntrophobacterales*, an order of the delta-proteobacteria subdivision. Organisms of this group are *Syntrophus aciditrophicus* and *Syntrophus buswellii*. Several other *Syntrophus* strains such as *Syntrophus gentianae* are able to oxidize benzoate or other aromatic compounds syntrophically but these processes are not considered in this article. Remarkably, all these organisms are restricted to the use of saturated or unsaturated fatty acids. Alternative substrates or alternative electron acceptors to grow these bacteria in pure culture have not been found yet for these two groups of butyrate-oxidizing bacteria.

In all known butyrate-oxidizing bacteria, the beta-oxidation pathway is used (Wofford et al., 1986, Schink, 1997, McInerney et al., 2007). First, butyrate is activated to butyryl-CoA with acetyl-CoA by a CoA transferase. Further oxidation proceeds via crotonyl-CoA and 3-hydroxybutyryl-CoA to acetoacetyl-CoA which is cleaved to two acetyl-CoA moieties. One of these is invested in butyrate activation, and the other one forms ATP via phosphotransacetylase and acetate kinase (Wofford et al., 1986). Electrons are released in the oxidation of butyryl-CoA to crotonyl-CoA and in the oxidation of 3-hydroxybutyryl-CoA to acetoacetyl-CoA at -250 mV (Gustafson et al., 1986). As the standard midpoint redox potentials of these reducing equivalents are too high for reduction of protons to form H_2 (-414 mV (Thauer et al., 1977, Schink, 1997)), it was postulated that an energy-dependent reversed electron transport is required to overcome the redox potential difference (Thauer and

Morris, 1984). The partner organism keeps the hydrogen partial pressure low, thus raising the redox potential of proton reduction to a level around -300 mV (Schink, 1997). The butyrate-oxidizing organism has to sacrifice part of the gained ATP to shift electrons to this redox potential, and the remaining ATP can be used for biosynthesis and growth. As such fractional amounts of ATP cannot be provided by substrate level phosphorylation such energy transformations have to be coupled to the cytoplasmic membrane (Thauer and Morris, 1984). Indeed, hydrogen production from butyrate has been shown to be sensitive to the protonophore CCCP and the ATPase inhibitor DCCD, thus providing evidence for participation of a transmembrane proton potential (Wallrabenstein and Schink, 1994). However, the underlying biochemical mechanisms remained enigmatic until the completion of the genome sequence of *S. aciditrophicus* (McInerney et al., 2007). It was stated that electrons released in butyryl-CoA oxidation are transferred to components of the membrane where they reduce NAD^+ to NADH in an endergonic manner, e. g., through an *rnf*-coded oxidoreductase, and the necessary energy would be supplied by a sodium ion gradient which in turn is provided by ATP-dependent proton efflux and a sodium/proton antiporter. In *S. wolfei*, however, a different reaction mechanism has to be active since the genome of this bacterium does not contain *rnf* genes which will be discussed later in this review (Müller et al., 2009).

Propionate degradation

Several bacterial strains are known to degrade propionate in syntrophic association with methanogens; *Syntrophobacter fumaroxidans, S. wolinii, S. pfennigii, S. sulfatireducens, Pelotomaculum thermopropionicum, P. schinkii, P. propionicicum, Smithella propionica and Desulfotomaculum thermobenzoicum subsp. thermosyntrophicum.* These bacteria belong to the Syntrophobacterales, an order of the delta-proteobacteria subdivision, and to the family Peptococcaceae within the order Clostridiales. *S. propionica* converts propionate through a dismutating pathway to acetate and butyrate after which butyrate is oxidized to acetate (de Bok *et al*., 2001). All other known syntrophic propionate degraders oxidize propionate to acetate plus CO_2. They use the methylmalonyl-CoA pathway which generates per molecule propionate one ATP via substrate level phosphorylation and three electron pairs by; (i) oxidation of succinate to fumarate ($E^{o'}$=+30 mV), (ii) oxidation of malate to oxaloacetate ($E^{o'}$=-176 mV), and (iii) pyruvate conversion to acetyl-CoA and CO_2 ($E^{o'}$=-470 mV) (Figure 2). The latter step can easily be coupled to proton reduction ($E^{o'}$=-414 mV) or CO_2 ($E^{o'}$=-432

mV) reduction (Thauer et al., 1977) via ferredoxin, as anaerobic bacteria generally contain pyruvate:ferredoxin oxidoreductases (Chabrière et al., 1999).

Oxidation of succinate and malate with proto ns would require hydrogen partial pressures of 10^{-15} and 10^{-8} atm, respectively (Schink, 1997). Thauer and Morris (1984) and Schink (1997) proposed a reversed electron transport mechanism. The hydrolysis of 2/3 ATP coupled with a transmembrane import of two protons would make succinate oxidation energetically possible. Later, van Kuijk et al. (1998) proposed that this reaction is analogous to that involved in fumarate respiration by *Wolinella succinogenes*. This bacterium generates a transmembrane proton gradient by periplasmic hydrogen or formate oxidation coupled to cytoplasmic fumarate reduction via cytochromes and a menaquinone loop (Kröger et al., 2002). In *S. fumaroxidans*, fumarate reductase and succinate dehydrogenase activity are membrane bound. Hydrogenase and formate dehydrogenase activity are found in the periplasmic space loosely attached to the membrane, and cells contain cytochrome *c* and *b* and menaquinone-6 and -7 as possible electron carriers (van Kuijk et al., 1998). *S. fumaroxidans* appears to gain around 2/3 ATP per mol fumarate if H_2 or formate is oxidized with fumarate. It was suggested that this mechanism in reverse could reduce periplasmic protons with the energy-dependent cytoplasmic succinate oxidation.

Malate oxidation to oxaloacetate ($E^{o'}$= -176 mV) is coupled to NAD^+ reduction ($E^{o'}$= -320 mV) (van Kuijk and Stams, 1996). Yet, the exact mechanism of NADH oxidation and terminal reduction of protons and /or CO_2 in *S. fumaroxidans* remains unclear and deserves further investigation.

Topic 2. Mechanisms for energy conservation in anaerobic microorganisms

Electron transport phosphorylation

Electron transport phosphorylation is the most important energy-conserving mechanism in organisms that reduce external electron acceptors such as oxygen, nitrate, sulfate etc., (Richardson, 2000). In most cases, the membrane-bound NADH dehydrogenase (complex I) oxidizes NADH with quinones in the membrane while translocating protons into the periplasmic space via a transmembrane proton pump (Richardson, 2000). The electrons are transferred further to the respective terminal acceptor via cytochromes.

Protons can be translocated to the periplasmic space by at least two possible mechanisms. The first one includes the translocation of protons or sodium ions through the transmembrane

proton channel of an NADH dehydrogenase (Richardson, 2000). The second mechanism involves a redox loop and is supposed to be the most common way of proton translocation in bacteria (Richardson, 2000). Here, isoprenoid quinones within the membrane are reduced by the membrane-integral domain of the electron-donating enzyme, together with protons. The reduced quinone diffuses laterally through the membrane to the membrane domain of the accepting enzyme where electrons are transferred to an electron acceptor, and the protons are released at the opposite side of the membrane. An example is the redox loop of the formate dehydrogenase FDH-N coupled to nitrate reductase in *Escherichia coli* (Jormakka et al., 2002). During anaerobic growth, formate is oxidized in the periplasm by FDH-N while protons are transferred to menaquinones, together with the electrons released in formate oxidation. Subsequently, menaquinol is oxidized at the membrane domain of the nitrate reductase, releasing protons to the periplasm while electrons are transferred to nitrate to form nitrite at the cytoplasmic side of the membrane (Jormakka et al., 2002).

The smallest quantum of energy in biology

Since only small amounts of chemical energy can be transformed in syntrophic oxidation processes (Table 1), energy has to be efficiently conserved. Thauer et al. (1977) and Schink (1997) calculated that the minimal cost of synthesis of one ATP is 60 kJ per mol. Syntrophically fermenting bacteria such as butyrate and propionate oxidizers have to invest part of their ATP to create a proton gradient. For a long time it was thought that three protons are imported for synthesis of one ATP and thus the smallest quantum of energy that can be converted into ATP is in the range of 20 kJ per mol. However, Nakanishi-Matsui and Futai (2008) documented that the number of protons translocated is determined by the number of membrane-integral c-subunits of the ATP synthase which varies between different microorganisms. ATP synthases of yeast and *Enterococcus hirae* harbor 10, while *Ilyobacter tartaricus*, *Methanopyrus kandleri* and chloroplasts harbor 11, 13 and 14 such subunits, respectively. The authors proposed that with one full rotation of the ATP synthase complex, three ATP are hydrolyzed, and each c-subunit translocates one proton. As a consequence, the number of protons translocated per ATP is between 3.3 and 4.6 and with this, the smallest quantum of biologically conservable energy may range from 13 to 18 kJ per mol reaction.

In reversed electron transport as hypothesized for syntrophic butyrate and propionate oxidation, a high number of protons transported per ATP hydrolyzed would allow ATP synthesis even at low energy gains. Hoehler et al. (2001) calculated minimal amounts of -10 to -19 kJ per translocated proton for organisms in anoxic methanogenic marine sediments.

However, the number of membrane-integral c-subunits in ATP synthases of syntrophic bacteria has not been determined yet.

Genome analysis of *S. fumaroxidans* and *S. wolfei* indicates the presence of one kind of ATP synthase in each bacterium; the cytoplasmic F1 domain is encoded by Sfum_2581-2587 and Swol_2381-2385, and the membrane-integral F_0 domain is encoded by Sfum_1604-1605 and Swol_2387-2388, respectively. The ratio of transcription of F1 domain coding genes to membrane-integral c-subunit-coding genes might give insight into the number of c-subunits per ATP synthase in *S. fumaroxidans* and *S. wolfei* in the future.

Buckel-Thauer Bcd/Etf

Most fermenting organisms have to regenerate their NAD^+ pool in the absence of external electron acceptors. It was assumed that in clostridia NADH is oxidized with ferredoxin, which in turn is oxidized with protons to form hydrogen. This reaction is endergonic and, until recently, it was not known how hydrogen-producing microorganisms could perform such a reaction while strongly accumulating hydrogen in their environment.

Clostridium kluyveri ferments ethanol plus acetate to a mix of butyrate, caproate, and hydrogen. The critical step of NADH oxidation with ferredoxin was recently found to be catalyzed by a Butyryl-CoA dehydrogenase (Bcd) / Electron-transferring Flavoprotein subunit (Etf) complex which couples this endergonic reaction to the exergonic reduction of crotonyl-CoA to butyryl-CoA with NADH (Li et al., 2008). Overall, two NADH molecules are oxidized and one molecule reduced ferredoxin (transferring two electrons) plus one molecule butyryl-CoA are formed (Li et al., 2008) which we refer to as bifurcation. For butyrate-oxidizing bacteria, a reversal of this reaction was suggested, i. e., the endergonic reduction of NAD^+ with butyryl-CoA could be driven by the exergonic reduction of another NAD^+ with reduced ferredoxin (Herrmann et al., 2008) a reaction which we refer to as confurcation. This mechanism could provide a concept for the reversed electron transport in syntrophic fatty acid degradation since homologues of this enzyme complex were found in genomes of the syntrophs *S. wolfei*, *S. fumaroxidans,* and *P. thermopropionicum*, but not in *S. aciditrophicus*.

Confurcating/bifurcating [FeFe]-hydogenases

Apart from the Buckel-Thauer Bcd/Etf-complex, another enzyme with bifurcating / confurcating activity was described recently, the [FeFe]-hydrogenase of *Thermotoga maritima* (Schut and Adams, 2009). *T. maritima* ferments glucose to acetate, CO_2 and H_2 via the Embden-Meyerhof pathway which generates two NADH and four reduced ferredoxins per

molecule of glucose. In order to re-oxidize these carriers, the proposed confurcating [FeFe]-hydrogenase uses simultaneously electrons from NADH and reduced ferredoxin in a 1:2 ratio to produce hydrogen (Schut and Adams, 2009). This hydrogenase could not use either NADH or reduced ferredoxin alone for hydrogen production. Additionally, the authors found genes with sequence similarity to this trimeric [FeFe]-hydrogenase also in other organisms such as *S. fumaroxidans, P. thermopropionicum* and *S. wolfei* (Table 2, suppl. Data figure 1). Remarkably, our gene analysis indicated that some putative [NiFe]-hydrogenases and formate dehydrogenases in *S. fumaroxidans*, *P. thermopropionicum*, *S. wolfei* and *S. aciditrophicus* contain subunits with iron-sulfur-binding motifs and subunits homologous with the NADH dehydrogenase 51 kDa subunit, which is the NADH-binding subunit of Complex I. This indicates a possible confurcating function for [NiFe]-hydrogenases and formate dehydrogenases as well.

Rnf complex

In *Rhodobacter capsulatus* nitrogen fixation (*rnf*) genes were found which code for a membrane-bound enzyme complex that is most probably involved in energy transformation (Kumagai et al., 1997). Gene analysis indicated that the encoded products RnfB and RnfC contain iron-sulfur clusters, RnfC contains potential NADH- and FMN-binding sites, and the membrane-bound RnfA, RnfD and RnfE are similar to subunits of the sodium-translocating NADH:quinone oxidoreductase (Kumagai et al., 1997). The authors proposed that this complex translocates protons or sodium ions to drive the endergonic reduction of ferredoxin by NADH oxidation. Analogous *rnf* genes were found in numerous bacteria such as *Haemophilus influenzae*, *Escherichia coli, Acetobacterium woodii,* and *Vibrio alginolyticus,* thus suggesting a general and important function for the Rnf complex in energy conservation (Müller et al., 2008, Nakayama et al., 2000, Backiel et al., 2008).

Müller et al., (2008) investigated the function of an Rnf complex in the homoacetogenic bacterium *A. woodii*. Although biochemical proof has not been obtained yet, the authors found that caffeate respiration was coupled to ATP synthesis by a chemiosmotic mechanism with sodium ions as coupling ions, and that ferredoxin:NAD^+-oxidoreductase was the only membrane-bound enzyme detected in the pathway of H_2 dependent caffeate reduction. They postulated oxidation of ferredoxin with reduction of NAD^+ and the export of Na^+.

Table 2: General and genome-based characteristics of butyrate- and propionate-degrading syntrophic bacteria

	Butyrate degraders		Propionate degraders	
Bacterial species	*Syntrophomonas wolfei* subsp. *wolfei*	*Syntrophus aciditrophicus*	*Syntrophobacter fumaroxidans*	*Pelotomaculum thermopropionicum*
Cell wall / morphology	Gram positive rod	Gram negative rod	Gram negative rod	Gram positive rod
Class	*Clostridia*	*Delta proteobacteria*	*Delta proteobacteria*	*Clostridia*
Pathway	β-oxidation	β-oxidation	Methyl malonyl CoA	Methyl malonyl CoA
Genome Genbank accession	CP000448	CP000252	CP000478	AP009389
Genes coding for confurcating FDH's and Hyd's[a)]	Swol_1829-31 [Se]-FDH (FDH IV) Swol_0783-86 [Se]-FDH (FDH II) Swol_1017-19 [FeFe]-Hyd	SYN_02138-40 [Se]-FDH SYN_00629-35 [Se]-FDH SYN_02219-22 [NiFe]-Hyd SYN_01369-70 [FeFe]-Hyd	Sfum_2703-07 [Se]-FDH (FDH1) Sfum_0844-46 [FeFe]-Hyd (Hyd1) Sfum_2713-16 [NiFe]-Hyd (Hyd4)	PTH_2645-51 [Se]-FDH PTH_1377-79 [FeFe]-Hyd PTH_2010-12 [FeFe]-Hyd
Genes coding for Tat-motif- containing FDH's and Hyd's[a,d)]	Swol_1823-26 [Se]-FDH (FDH III)	SYN_00602-05 [Se]-FDH SYN_00632-35 [Se]-FDH	Sfum_3510-11 FDH (FDH3) Sfum_0035-37 [Se]-FDH (FDH4) Sfum_1273-75 [Se]-FDH (FDH2) Sfum_2952-53 [NiFe]-Hyd (Hyd2)	PTH_1711-14 [Se]-FDH PTH_1701-04 [NiFe]-Hyd
Genes coding for other FDH's and Hyd's[a)]	Swol_0797-00 [Se]-FDH (FDH I)	Not present	Sfum_3509 FDH Sfum_0030-31 [Se]-FDH Sfum_2220-22 [NiFe]-Hyd Sfum_3535-37 [NiFeSe]-Hyd Sfum_3954-56 [NiFeSe]-Hyd	Not present
Buckel -Thauer Bcd /Etf complex[b)]	Swol_0267-68	No complete complex	Sfum_1371-73 Sfum_3929-21 Sfum_3686-88	PTH_0015-17 PTH_2000-02 PTH_2431-33
Etf AB[b)]	Swol_0696-97	SYN_02636-37	Sfum_0106-07	PTH_1552-53
Rnf cluster[c)]	Not present	Syn_01658-64	Sfum_2694-99	Not present

Gene locus tag numbers of genes in butyrate and propionate degraders, that show similarity with genes coding for energy-transforming protein complexes such as a) formate dehydrogenases (FDH), Hydrogenases (Hyd), b) Electron-transferring flavoproteins (Etf), Butyryl-CoA dehydrogenase (Bcd) and c) *Rhodobacter capsulatus* nitrogen fixation (Rnf) complexes. d) Twin arginine translocation (Tat) motives indicate that the corresponding proteins are translocated through the cell membrane.

Methods used for gene analysis

Automatic annotations of genomes from DOE-Joined Genome Institute (IMG-JGI-DOE, 2009 http://www.jgi.doe.gov/., version 2.9 August 2009) were used to indicate the presence of gene clusters coding for formate dehydrogenases, hydrogenases, Buckel-Thauer Bcd/Etf complexes and Rnf clusters in *S. wolfei*, *S. aciditrophicus*, *P. thermopropionicum* and *S. fumaroxidans*. N-terminal amino acid sequences of FDH-1 and FDH-2 identified by (de Bok et al., 2003) were used to find corresponding *fdh*-1 and *fdh*-2 nucleotide sequences in the genome of *S. fumaroxidans*. Pfam search (Sanger institute, 2009, http://pfam.sanger.ac.uk/search) was used to identify motifs in the amino acid sequences and the TMHMM Server v. 2.0 (DTU, 2009 http://www.cbs.dtu.dk/services/TMHMM/. Center for Biological sequence analysis: Technical University of Denmark) was used to identify transmembrane helices. With the TatP 1.0 Server twin-arginine translocation (Tat) motifs in the N-terminus were identified to predict protein localization in the cell (Bendtsen et al., 2005). The incorporation of selenocystein (SeCys) was examined by RNA loop predictions with Mfold version 3.2 (Mathews et al., 1999, Zuker, 2003). The RNA loop predicted in the 50-100 bp region downstream of the UGA-codon was compared with the consensus loop described by Zhang and Gladyshev (2005). Complete amino acid sequences of putative selenocystein-containing formate dehydrogenases were aligned to their homologues with ClustalX 1.81 (Kryukov and Gladyshev, 2004). SeCys incorporation was confirmed when the amino acid sequence aligned with conventional cystein in homologous proteins.

Topic 3. Hypotheses for energy conservation mechanisms in butyrate oxidizers and propionate oxidizers

Butyrate oxidation by S. wolfei

The electron transport in butyrate oxidation by *S. wolfei* was studied recently in a classical biochemical approach (Müller et al., 2009). The electron transfer from butyryl-CoA to external electron acceptors was found to be inhibited by trifluoperazine, a compound known to inhibit electron transfer to menaquinone by the respiratory complex I in *Mycobacterium tuberculosis* (Yano et al., 2006). Trifluoperazine also inhibited electron transfer from NADH to quinone analogues. An NADH-oxidizing enzyme complex was partially purified from the membrane fraction of *S. wolfei*. This activity was also found in the cytoplasmic fraction, especially after repeated treatment in the French Press cell, indicating that it is only

superficially associated with the membrane (Müller et al., 2009). The enzyme complex contained several proteins which were analyzed by peptide mass fingerprinting and were compared via the known gene sequence with redox enzymes found in other bacteria, i. e. an enzyme system similar to the confurcating hydrogenase of *T. maritima* (Schut and Adams, 2009). Moreover, this hydrogenase homologue of *S. wolfei* appeared to be associated with homologues of an NADH-dependent formate dehydrogenase of *Eubacterium acidaminophilum* (Graentzdoerffer et al., 2003), a bacterium which can also grow in syntrophic association with partner organisms (Zindel et al., 1988). This enzyme complex could either act as a confurcating hydrogenase / formate dehydrogenase or as a proton-pumping NADH dehydrogenase (NDH) (Müller et al., 2009). So far, it was not possible to show if this enzyme is directly linked to a transmembrane proton channel (Müller et al., 2009). But even if the enzyme lacks such a channel protons could be transferred via a menaquinone cycle (Figure 1) as described above for *E. coli* (Jormakka et al., 2002). Whether the hydrogenase found really acts in a bifurcating manner as observed in *T. maritima* has still to be verified. So far, there is no indication of a ferredoxin-coupled redox reaction in butyrate oxidation by this bacterium. Our results indicate that the "Buckel-Thauer" reaction, i.e., a bifurcation of electrons from NADH with crotonyl-CoA and oxidized ferredoxin by the Bcd/EtfAB complex of *C. kluyveri* (Herrmann et al., 2008, Li et al., 2008) is not involved in butyrate oxidation by this bacterium. Until now, the function of *etf* genes in syntrophic butyrate degraders remains unclear. Possibly, the Bcd/EtfAB complex is expressed when *S. wolfei* grows by dismutation of crotonate. Whether other butyrate oxidizers, e. g., *S. aciditrophicus or S. buswellii*, employ the Bcd/EtfAB complex in butyrate oxidation remains an open question at this time. Another interesting feature of the hydrogenase homologue of *S. wolfei* is its association with a formate dehydrogenase (Müller et al., 2009). This supports older speculations that electrons from NADH oxidation are released as formate rather than hydrogen. The bacterium might even be able to choose which carrier it prefers, depending on the environmental conditions (Graentzdoerffer et al., 2003), e. g., whether a partner is present which consumes hydrogen, formate or both, and this preference might even differ between different butyrate oxidizers: Coculture experiments with *S. bryantii* and different partners (Dong et al., 1994) showed highest growth and substrate conversion rates with *Methanospirillum hungatei* which uses both hydrogen and formate, whereas cocultures with the mainly formate-oxidizing *Methanobacterium formicicum* were slower, and there was no growth at all with the only hydrogen-consuming *Methanobrevibacter arboriphilus.*

Fig. 1: *S. wolfei*

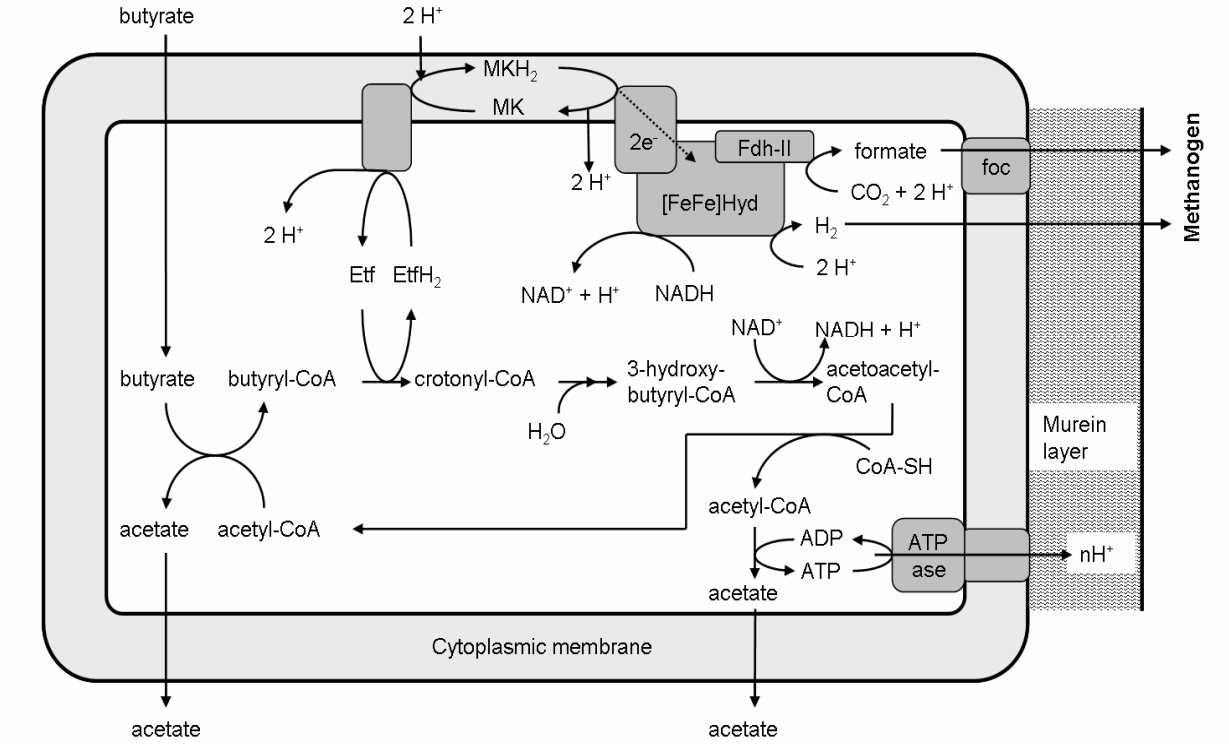

Figure 1: Hypothetical energy-transforming mechanisms in the butyrate-degrading *Syntrophomonas wolfei*. The fatty acids acetate, butyrate and formate represent $acetate^- + H^+$, $butyrate^- + H^+$ and $formate^- + H^+$, respectively. (foc) represents a formate transporter.

In contrast, it was shown earlier that *S. wolfei* grows in the presence of *M. arboriphilus*, although to a lower extent, indicating that *S. wolfei* can grow by interspecies hydrogen transfer only and formate plays only a minor role in electron transfer (McInerney et al., 1979, McInerney et al., 1981).

Therefore, the electron transport during butyrate oxidation by *S. bryantii* might be different from that described above for *S. wolfei*, although the molecular prerequisites might be similar due to the close relatedness of both organisms. The formate dehydrogenase of *S. bryantii* was found to be membrane-bound and was most likely oriented to the periplasmic space whereas the partly membrane-bound hydrogenase was found in the cytoplasm and showed also activity with NAD^+ as electron acceptor (Dong and Stams, 1995). It was assumed that hydrogen is produced inside the cell while formate is produced outside. Additionally, an NADH dehydrogenase reacting with the tetrazolium dye MTT was measured, comparable to the described NADH: quinone oxidoreductase in *S. wolfei* which also reacts with MTT (Müller et al., 2009), (Müller unpublished data). It is tempting to speculate at this point that the described NADH dehydrogenase of *S. wolfei* could also be a bifurcating hydrogenase that couples NADH-dependent proton reduction with quinone reduction by another molecule of NADH. One electron pair would then be used to reduce protons to form hydrogen and the

other one would be transferred to the external formate dehydrogenase. If hydrogenase and/or NADH dehydrogenase are coupled to the formate dehydrogenase via a quinone-mediated redox loop, two additional protons would be transferred outside the cell. Overall, proton consumption in the cytoplasmic space and proton release at the outside would result in a net proton gradient which in turn could drive menaquinol oxidation with NAD^+ or ADP phosphorylation by proton influx. This would require that formate and hydrogen both have to be kept at low concentration to allow the thermodynamically unfavourable reactions of CO_2 reduction with quinols and proton reduction with NADH. Although such a membrane-bound and quinone-oxidizing formate dehydrogenase has not yet been measured in *S. wolfei*, there are indications for such a system in its genome (Swol _0797-Swol_0799) (Table 2).

Although the formate/CO_2 couple and the hydrogen/proton couple are both at the same redox potential under physiological conditions, the question remains whether they are really equivalent inside the cell as assumed earlier (Schink, 1997). Cocultures of *Moorella* sp. strain AMP and *Desulfovibrio* sp. strain G11 with formate as substrate in coculture with hydrogen-only consuming methanogens converted formate to methane (Dolfing et al., 2008). It was assumed that formate is oxidized outside the cytoplasmic membrane, CO_2 and protons are released and electrons are shuttled to a membrane-bound hydrogenase facing the cytoplasm where protons are consumed (Dolfing et al., 2008). Thus, a net positive membrane potential could be formed without direct proton translocation but there is so far no proof that this reaction is coupled to energy conservation.

Propionate oxidation by S. fumaroxidans and P. thermopropionicum

The most difficult step in syntrophic propionate oxidation is the oxidation of succinate to fumarate. In the past, succinate dehydrogenases and fumarate reductases have been found to be similar based on their amino acid sequence (Lancaster, 2002). These authors classified fumarate reductases in five groups based on molecular composition. The fumarate reductase of *W. succinogenes* was classified within the group containing one hydrophobic subunit and two heme-groups (Kröger et al., 2002). Our present gene analyses indicate that not only hydrophobic subunits of the fumarate reductase but also those of formate dehydrogenases of *W. succinogenes* (formate dehydrogenase delta subunits: WS0027, WS0736 and WS1148) contain heme groups and are homologous to cytochrome *b*.

S. fumaroxidans genome analysis revealed the presence of periplasmic formate dehydrogenases and hydrogenases (suppl. data 2) as well as cytoplasmic fumarate reductases (Sfum_4092-4095, Sfum_1998-2000) which lack heme groups and a cytochrome *b*-like

membrane-integrated domain. As such, fumarate reductases of *S. fumaroxidans* could not be classified within the five types described by Lancaster (2002). Instead, scattered over the genome, three cytochrome *b* (cytb561; Sfum_0091, cytb5; Sfum_3227 and cytb; Sfum_2932) and three cytochrome *c* homologous genes (Sfum_0090, Sfum_4047 and Sfum_1148) were found. Moreover, three genes with homology to cytochrome *b*: quinone oxidoreductases were found (Sfum_0339, Sfum_3009 and Sfum_3051). Cytochrome *b* and cytochrome *b:*quinone oxidoreductases possibly function in a similar way as the cytochrome-containing membrane-integrated domains of fumarate reductases, hydrogenases, and formate dehydrogenases of *W. succinogenes* (Figure 2).

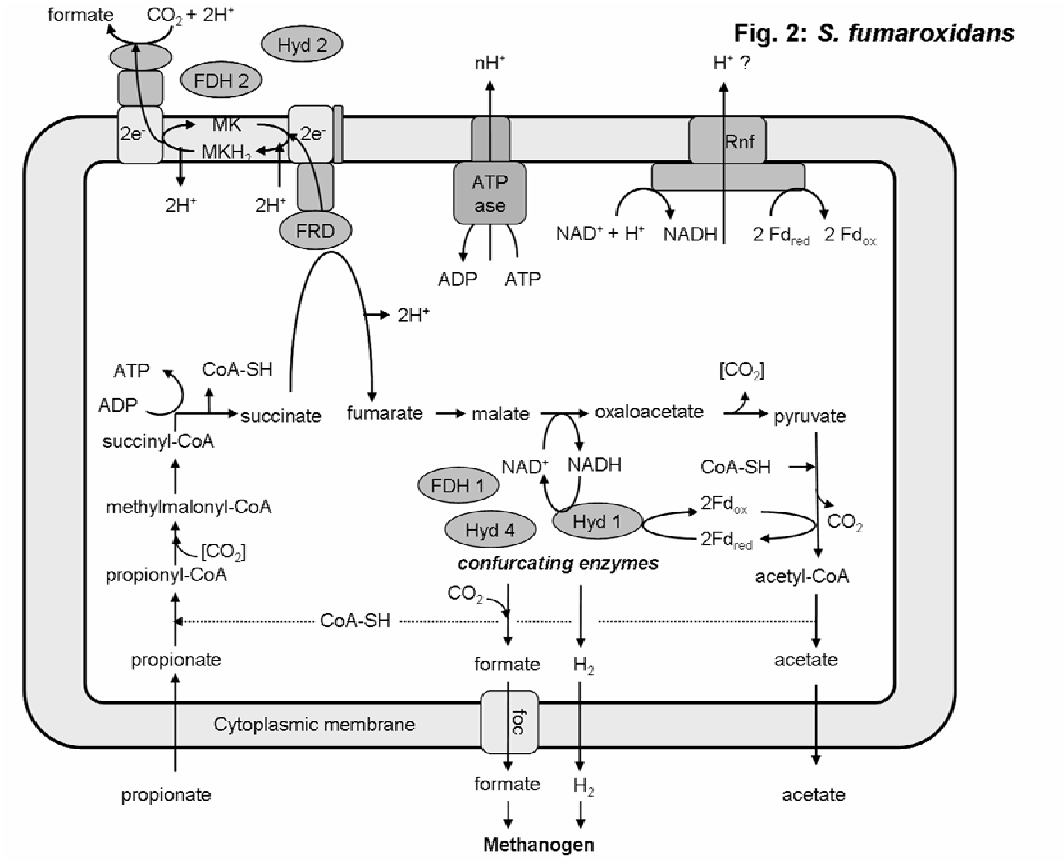

Figure 2 Hypothetical energy-transforming mechanisms in the propionate-degrading *Syntrophobacter fumaroxidans*. The fatty acids acetate, propionate and formate represent $acetate^- + H^+$, $propionate^- + H^+$ and $formate^- + H^+$, respectively. (foc) represents a formate transporter, $[CO_2]$ a biotin-bound carboxylic group.

Candidates for periplasmic formate or hydrogen oxidation are formate dehydrogenase 2, 3 and 4 and hydrogenase 2 (Figure 2, Suppl. data Figure 2). These proteins may bind periplasmic cytochrome *c* and hydrophobic cytochrome *b* for succinate oxidation or fumarate reduction. Probably they also interconvert hydrogen and formate via a cytochrome *c* network, as proposed previously for the sulfate-reducing *Desulfovibrio vulgaris* Hildenborough

(Heidelberg et al., 2004). Interconversion of hydrogen plus CO_2 and formate by *S. fumaroxidans* was observed by Dong and Stams (1995) and de Bok et al. (2002).

Formate dehydrogenase 1 of *S. fumaroxidans* was previously characterized (de Bok et al., 2003). It oxidizes formate with benzyl viologen as artificial electron acceptor, but NAD^+ did not support oxidation of formate. Based on the amino acid sequence, this selenocysteine-containing formate dehydrogenase is similar to FDHII of *S. wolfei* and to the NADH-dependent formate dehydrogenase of *Eubacterium acidaminophilum* (Graentzdoerffer et al., 2003). Whether formate dehydrogenase 1 can couple oxidation of both NADH and ferredoxin to CO_2 reduction in a manner analogous to proton reduction by the confurcating [FeFe]-hydrogenase of *T. maritima* was never tested. Based on our gene analysis, we hypothesize that hydrogenase 1, hydrogenase 4, and formate dehydrogenase 1 can couple the oxidation of NADH generated from malate oxidation with the oxidation of reduced ferredoxin generated from pyruvate oxidation to produce hydrogen or formate (Table 2, Figure 2). Especially transcription of genes coding for hydrogenase 1 (an [FeFe]-hydrogenase) appears to be up-regulated when metabolic conversions generate NADH and reduced ferredoxin (P. Worm et al. unpublished). In *S. fumaroxidans* the Rnf-complex might be used to conserve the energy of ferredoxin oxidation with NADH reduction by exporting protons, thus equilibrating the ratio of reduced ferredoxin to NADH to 1:1.

Compared to *S. fumaroxidans*, the genome of *P. thermopropionicum* contains less formate dehydrogenase- and hydrogenase-coding genes (Table 2). However, for each metabolic task, several candidates are present just as in *S. fumaroxidans*. In order to reoxidize the NADH and reduced ferredoxin that are generated during propionate degradation, *P. thermopropionicum* likely uses the confurcating formate dehydrogenase (PTH_2645-2649) and the two confurcating [FeFe]-hydrogenases (PTH_1377-1379 and PTH_2010-2012) (Kosaka et al., 2008). The produced formate would be transported through the membrane via a formate transporter (PTH_2651) of which the gene is located in the operon coding for the cytoplasmic formate dehydrogenase. The produced hydrogen diffuses through the membrane and is used by the methanogen. Also similar to *S. fumaroxidans* is the mechanism of reversed electron transfer via fumarate reductase, a menaquinone loop and a periplasmic formate dehydrogenase (PTH_1711-1714) or hydrogenase (PTH_1701-1704) (Kosaka et al., 2008). Cytoplasmic and periplasmic formate dehydrogenases and hydrogenases could be used to interconvert formate and hydrogen. *P. thermopropionicum* can grow only with a hydrogen-using methanogen as its syntrophic partner (Ishii et al., 2005), however, formate is likely to generate hydrogen.

The high number of formate dehydrogenase- and hydrogenase-encoding genes in *S. fumaroxidans* likely provides *S. fumaroxidans* with more back-up possibilities when formate and hydrogen concentrations vary according to the activity of the partner methanogen. In contrast to *S. fumaroxidans*, *P. thermopropionicum* lacks an Rnf cluster and ferredoxin-reducing hydrogenases and formate dehydrogenases. *S. furmaroxidans* might use these mechanisms as alternatives to reoxidize NADH and ferredoxin, possibly with the use of an electron potential via the Rnf-cluster, when environmental conditions change.

Concluding remarks

Recent biochemical studies and genome analyses indicated that *S. wolfei* uses electron-transferring flavoproteins coupled to a menaquinone loop to drive endergonic butyryl-CoA oxidation, and *S. fumaroxidans* uses a periplasmic formate dehydrogenase, cytochrome b:quinone oxidoreductases, a menaquione loop and a cytoplasmic fumarate reductase to drive endergonic succinate oxidation. Furthermore, we propose that confurcating [FeFe]-hydrogenases in *S. wolfei* and *S. fumaroxidans* are involved in NADH oxidation to form hydrogen. For both *S. wolfei* and *S. fumaroxidans,* a similar function is proposed for a formate dehydrogenase which would result in simultaneous hydrogen and formate transfer from the fermenting bacterium to the hydrogen- and formate-consuming syntrophic partner. *S. fumaroxidans* and *S. wolfei* are proposed to produce hydrogen and formate in the cytoplasm. *P. thermopropionicum* and *S. wolfei* are proposed to contain a mechanism to convert hydrogen into formate which would allow growth with hydrogen-only using methanogens. These proposed energy-converting mechanisms need biochemical verification. We hypothesize that they are key in syntrophic propionate- and butyrate-degrading communities, as well as in other syntrophic communities.

Acknowledgements

The authors were financially supported by the German Research Foundation (DFG) and by the Earth and Life Sciences division (ALW) and Chemical Science division (CW) of the Netherlands Organization for Scientific Research (NWO).

Chapter 5: Syntrophic Oxidation of Ethanol

Syntrophic oxidation of ethanol by *Pelobacter acetylenicus* strain WoAcy 1 and *Desulfovibrio* strain KoEME1 – a comparative biochemical study

Nicolai Müller and Bernhard Schink

Summary

Fermentative conversion of ethanol to acetate and molecular hydrogen is endergonic under standard conditions. However, some bacteria are able to oxidize this substrate in the presence of a hydrogenotrophic partner organism i.e., a sulfate reducer or a methanogen. We describe here two organisms, *Pelobacter acetylenicus* strain WoAcy1 and *Desulfovibrio* strain KoEME1, which both grow on ethanol in coculture with *Methanospirillum hungatei*. *P. acetylenicus* showed significantly higher growth yields than *Desulfovibrio* KoEME1 which was attributed to the absence of an acetylating aldehyde dehydrogenase in the latter organism. Both organisms have an NAD^+-dependent alcohol dehydrogenase and high activities of a non-acetylating aldehyde dehydrogenase, which is possibly essential for ethanol oxidation as it keeps intracellular acetaldehyde concentrations low enough to allow the endergonic oxidation of ethanol with NAD^+. Regeneration of redox carriers and release of electrons in the form of molecular hydrogen appears to be catalyzed by a comproportionating hydrogenase in both organisms, as recently described for the [FeFe]-hydrogenase in *Thermotoga maritima*. For *Desulfovibrio* strain KoEME1 we propose a hydrogen cycling model for energy conservation via cytochromes and periplasmic hydrogenase as described earlier.

Introduction

Oxidation of ethanol to acetate has to be coupled either to reduction of external electron acceptors or to syntrophic cooperation with H_2 – oxidizing partner organisms (Schink, 1997). The first ethanol-oxidizing methanogenic culture known was described already 70 years ago as *Methanobacterium omelianskii* isolated from feces of an ethanol-fed rabbit (Barker, 1940).

It turned out later that this culture consisted of two organisms, a Gram-negative rod called S-organism and a hydrogen-utilizing methanogen, strain M.o.H. (Bryant et al., 1967). The S-organism oxidized ethanol to acetaldehyde by alcohol dehydrogenase (ADH) and subsequently acetaldehyde to acetate by acetaldehyde dehydrogenase with the reducing equivalents most likely being transferred via NADH and ferredoxin to protons to form hydrogen (Reddy et al., 1972b, Reddy et al., 1972c). Attempts to classify the S-organism delineated it as a potentially new genus having characteristics of the genera *Desulfotomaculum* and *Desulfovibrio*, although lactate was not used by the S-organism and sulfate did not serve as electron acceptor (Reddy et al., 1972a). Unfortunately, the S-organism was lost later and could not be investigated further. The coculture of S-organism and M.o.H. carried out the following reaction (eq. 1, calculated after Thauer et al., 1977).

$$2CH_3CH_2OH + CO_2 \rightarrow 2CH_3COO^- + 2H^+ + CH_4 \quad \Delta G^{0'} = -112 \text{ kJ per mol} \quad \text{(eq.1)}$$

This reaction leaves roughly -60 kJ per mol of ethanol oxidized, which has to be shared amongst both partner organisms. Chemostat experiments with cocultures of *Pelobacter acetylenicus* together with several different partner organisms revealed that this energy is shared amongst both organisms, leaving approximately -40 kJ per mol for the fermenting bacterium and -20 kJ per mol for the partner organism (Seitz et al., 1990, Schink, 1997). Therefore, the reaction does not provide enough energy for the formation of one ATP, implying, that part of the gained ATP has to be reinvested into a reversed electron transport to drive the initial endergonic oxidation of ethanol to acetaldehyde with NAD^+ (eq. 2, calculated after Thauer et al., 1977, Schink, 1997).

$$CH_3CH_2OH + NAD^+ \rightarrow CH_3CHO + NADH + H^+ \quad \Delta G^{0'} = +23 \text{ kJ per mol} \quad \text{(eq. 2)}$$

Several representatives of the genus *Desulfovibrio* such as *Desulfovibrio gigas* can grow with ethanol and are also able to produce hydrogen (Kremer et al., 1988). Ethanol oxidation in these bacteria occurs by cometabolisation in which electrons are directly transferred to sulfate as the terminal electron accepting system. Therefore, these bacteria unify both the oxidative and reductive branches of ethanol oxidation in one cell which in syntrophic cocultures are provided separately in two different organisms. However, there are not many syntrophic ethanol-oxidizing cocultures of *Desulfovibrio* strains described yet, although ethanol-oxidizing and hydrogen-producing strains should theoretically also be able to cooperate with syntrophic partner organisms (Schink, 1997).

Some syntrophic sulfate reducers like *Desulfovibrio vulgaris* are able to grow syntrophically with lactate. Transcriptional studies showed that, amongst other proteins, a cytochrome and

periplasmic hydrogenases as well as ATPase were upregulated during syntrophic growth (Walker et al., 2009). Lactate is oxidized through biochemical mechanisms different from ethanol oxidation although the energetic situation is rather similar, with a free energy change of -74.2 kJ per mol lactate in methanogenic co-cultures (Walker et al., 2009). Like in ethanol oxidation, the endergonic step lies in the initial reaction, i.e. oxidation of lactate to pyruvate with NAD^+ (+25 kJ/mol, calculated after Thauer et al., 1977). Therefore, regeneration of reducing equivalents during ethanol and lactate oxidation could occur via similar mechanisms.

In the present study, we describe the biochemical properties of two ethanol-oxidizing strains that can grow in coculture with the methanogenic archaeon *Methanospirillum hungatei*. One of these organisms is a recently isolated *Desulfovibrio* strain closely related to *D. alcoholovorans* (Qatibi et al., 1991), and the other one, *Pelobacter acetylenicus,* was described earlier as an acetylene-fermenting bacterium (Schink, 1985). *Desulfovibrio alcoholovorans* was enriched previously with glycerol, 1,2-propanediol and 1,3-propanediol, but could grow with ethanol only in the presence of sulfate (Quatibi et al., 1991). *Desulfovibrio* strain KoEME1 is a sulfate-reducing bacterium that can grow on ethanol in pure culture with sulfate. It was enriched from water samples of Lake Constance originally on ethylmercaptoethanol and its ability to oxidize ethanol was discovered only later (Fahrbach and Schink, unpublished data).

Pelobacter acetylenicus strain WoAcy1 can grow on ethanol only in coculture with methanogens or sulfate reducers. This bacterium is known to ferment also several higher alcohols such as 1,3-propanediol in pure culture (Oppenberg and Schink, 1990).

Here we compare the different metabolic pathways of *Desulfovibrio* strain KoEME1 and *Pelobacter acetylenicus* strain WoAcy1 in coculture with *M. hungatei*. By comparison of the different enzyme activity patterns determined by classical enzyme assays involved in ethanol oxidation in both bacteria and comparison of growth yields, we conclude that both bacteria most likely use different metabolic pathways for degradation of this substrate. Both bacteria had dithionite-dependent hydrogenase activity which was stimulated by NADH. This NADH-stimulated hydrogenase could possibly be a comproportionating hydrogenase like the one described for *Thermotoga maritima* (Schut & Adams, 2009).

Materials and Methods

Source of organisms

All strains were from our own culture collection. *Pelobacter acetylenicus* strain WoAcy1 was isolated from creek sediment and is available at the German culture collection DSMZ (DSM 3246). *Desulfovibrio* strain KoEME1 and *Methanospirillum hungatei* strain M1h were both isolated from sediments of Lake Constance.

Cultivation techniques

Anoxic bicarbonate-buffered medium reduced with sodium sulfide was prepared as described before (Widdel et al., 1983) with the modifications specified later (Müller et al., 2008), and stored in 1l-bottles under an atmosphere of N_2/CO_2 (80%/20%). Cocultures were prepared by inoculation of anoxic medium containing 20 mM ethanol with *P. acetylenicus* plus *M. hungatei* or *Desulfovibrio* strain KoEME1 plus *M. hungatei,* and grown at a constant temperature of 28°C. Both cocultures had long lag phases (up to 5 weeks) after transfer from axenic precultures, but could be cultivated subsequently with ethanol by regular transfers after approximately one week.

Growth upon trace element limitation

Rubber-stoppered 60-ml serum bottles that were cleaned by acid and base treatment were extensively flushed with a mixture of N_2/CO_2 (80%/20%) to remove oxygen, and autoclaved at 121°C and 1 bar overpressure. Each bottle was filled by syringes with 30 ml medium prepared without tungstate and molybdate. All limitation experiments for both cocultures were done with medium from the same batch. Where indicated, the medium contained 0.1 µM tungstate or 0.15 µM molybdate or both trace elements. Precultures for those experiments were grown without tungstate or molybdate once and grew much slower than in medium containing those elements. However, this step was necessary to avoid introduction of tungstate or molybdate to limiting media by the inoculum.

Growth of the cocultures under different conditions was routinely monitored by removing 1.2 ml liquid samples at each time point indicated. Of each sample, 200 µl was used for HPLC analysis. To the remaining 1 ml, a few grains of sodium dithionite were added to keep the redox indicator resazurine in its reduced state. Then, optical densities were measured at 578 nm.

Determination of growth parameters

Both cocultures were grown in three 1.24-l bottles with rubber stoppers containing exactly 1 l medium as described above. Concentrations of acetate, ethanol and methane were measured by HPLC and GC (see below) at the beginning of the experiment and at the end of the growth phase when ethanol was completely consumed. Likewise, OD_{578} was recorded as well. Concentrations and optical densities at the end of growth were corrected for their respective initial values resulting from the inoculum for the determination of absolute amounts of substrate degraded and amounts of products and cell dry mass produced. Correlation of OD_{578} to dry mass was done essentially as described before, but using 20 mM ammonium acetate, pH 5.0, for washing and resuspending the cells (Müller et al., 2008). Cell pellets were dried in an oven at 60°C for 24 h before the mass difference of each tube was determined.

Preparation of cell-free extracts

Cells from 1-l cultures were harvested by centrifugation as described (Müller et al., 2008). Cell pellets were washed twice in anoxic 50 mM potassium phosphate buffer, pH 7.5, containing 3 mM dithiothreitol (DTT). Cell pellets were resuspended in 5 ml of the same buffer, transferred to an 8-ml serum vial sealed with a butyl rubber stopper, shock-frozen in liquid nitrogen, and stored at -20°C. All steps were performed under strictly anoxic conditions using an anoxic glove box as described before (Müller et al., 2008).

Cell suspensions thus obtained were lysed by addition of a total of 60 units mutanolysin and 0.2 mg DNaseI per ml cell suspension. Mutanolysin has proven to be a good lysing agent for syntrophic cocultures, as it leaves cell walls of archaea intact and only lyses cells of the fermenting bacteria (Wallrabenstein & Schink, 1994). The cell suspensions were then incubated at 37°C for 60 min. Non-lysed cells and debris were removed by centrifugation at 3,000 ×g for 20 min. The supernatant (cell-free extract) was stored in serum vials under N_2 on ice.

Enrichment and analysis of cytochromes

Cell extract from a 10-l culture of *Desulfovibrio* strain KoEME1 plus *M. hungatei* prepared as described above was gently stirred on ice, and pulverized $(NH_4)_2SO_4$ was added slowly to a final saturation of 60 % (390 mg per ml). After 30 min, precipitated protein was removed by centrifugation for 15 min at 16,000 × g and 4°C. The slightly red supernatant was dialyzed

overnight against 2 l of 20 mM Tris-HCl, pH 8.0, at 4°C. Absorption spectra were recorded in a double-beam photometer Uvicon 930 (Kontron, Zürich, CH) against air. Where indicated, samples were reduced prior to measurement by adding a few grains of sodium dithionite.

Enrichment and analysis of isoprenoid quinones

Isoprenoid quinones were extracted from cells by the method of Shestopalov et al. (1997). Cells from a coculture of *Pelobacter acetylenicus* strain WoAcy1 plus *M. hungatei* were harvested by centrifugation as mentioned above and washed once in 50 mM Tris-HCl, pH 7.5, with 1 mM potassium hexacyanoferrate to oxidize quinols and resuspended in 3 ml of the same buffer. Quinones were extracted by mixing the cell suspension vigorous with 2 ml n-hexane and 2 ml methanol. Two ml acetone was added and the cell suspension was mixed again. After centrifugation at 3.000 × g for 10 min, the upper, quinone-containing hexane layer was removed and the extraction procedure was repeated, but this time with mixing the cell suspension for 1 h on a shaker at 200 rpm. Again, the upper hexane layer was removed and pooled with the hexane fraction from the first extraction run.

The sample thus obtained was analyzed by thin layer chromatography (TLC) on silica gel 60 with fluorescence indicator. Menaquinone-9 (Vitamin K2, Menatetrenone) was used as standard. The mobile phase was a mixture of petrolether:ethyl acetate (2:1 vol/vol). Absorption spectra were recorded with samples in methanol in a double-beam photometer against methanol.

Enzyme assays

All assays were run anoxically in rubber-stoppered 1-ml cuvettes at 30°C as described before (Müller et al., 2008); assays were run in triplicate if not mentioned otherwise. One unit was defined as 1 μmol substrate consumed or product formed per min and mg protein at 30°C under the respective assay conditions.

Alcohol dehydrogenase (EC 1.1.1.1), oxidative. The reaction mixture contained 50 mM Tris-HCl buffer, pH 7.5 or pH 9.0, containing 3 mM dithiothreitol (DTT), 0.25 mM NAD^+, and cell extract. The reaction was started by addition of 85 mM ethanol, and the formation of NADH was followed at 340 nm (ε_{340} = 6.3 mM^{-1} cm^{-1}, Ziegenhorn & Bücher, 1976).

Alcohol dehydrogenase (EC 1.1.1.1), reductive. The reaction mixture contained 50 mM Tris-HCl, pH 7.5, with 3 mM DTT, 0.2 mM NADH, and cell extract. The reaction was initiated by addition of 1 mM acetaldehyde and NADH oxidation was followed at 340 nm.

Acetaldehyde dehydrogenase, acetylating (1.2.1.10). Assays were run in 50 mM potassium phosphate buffer, pH 7.5, with 3 mM DTT, 0.25 mM NAD^+, 0.33 mM CoASH, and cell extract. The reaction was started by adding 1 mM acetaldehyde, and the increase of absorption caused by NADH formation was followed at 340 nm. Without addition of CoASH, no activity was observed.

Non-acetylating acetaldehyde dehydrogenase (EC 1.2.1.3) was assayed as described earlier (Hensgens et al., 1995), but with 5 mM acetaldehyde. Activities of phosphotransacetylase (EC 2.3.1.8) was assayed after Bergmeyer (1974) and acetate kinase (2.7.2.1) by colorimetric determination of acetyl-phosphate consumption after Nishimura and Griffith (1981) with the modifications by Müller et al. (2008). For determination of ATPase (EC 3.6.1.3), the protocol of Hoffmann and Dimroth (1990) was modified. Each assay mixture contained 50 mM potassium phosphate buffer, pH 7.5, with 3 mM DTT, 0.2 mM NADH, 5 mM $MgCl_2$, 3 mM phosphoenolpyruvate, 20 U lactate dehydrogenase from hog muscle, 20 U pyruvate kinase from rabbit muscle, and 2.5 mM ATP. The reaction was initiated by addition of cell extract and measured as absorption decrease at 340 nm.

Hydrogenase (EC 1.18.99.1) was assayed in 50 mM potassium phosphate buffer, pH 7.5, with 3 mM DTT, 2 mM benzylviologen (ε_{578} = 8.65 mM^{-1} cm^{-1}) or methylviologen (ε_{578} = 9.7 mM^{-1} cm^{-1}) or 0.25 mM NAD^+ in cuvettes flushed with 100% H_2. Cell extract was added and the increase of absorption was followed at 578 nm or 340 nm (modified after Diekert & Thauer, 1978).

NADH:acceptor oxidoreductase was measured in 50 mM Tris-HCl, pH 7.5, with 3 mM DTT, 2 mM benzylviologen or methylviologen, and cell extract. The background activitiy of viologen reduction was followed for 3 min at 578 nm. Then, 0.2 mM NADH was added to start the reaction.

Activities of formate dehydrogenase (EC 1.2.1.2) were determined with the same reagents as for hydrogenase, but without hydrogen. The reaction was started by addition of 5 mM formate and measured at the same wavelengths as outlined for hydrogenase.

Determination of NADH-stimulated hydrogenase

Assays were performed at 25°C in 12 ml butyl rubber-stoppered glass tubes flushed with 100% N_2. The assay mixture contained 50 mM potassium phosphate buffer, pH 7.5, with 3 mM DTT, 2.5 mM NADH, 5 mM sodium dithionite, and 100 µl cell extract (approx. 0.5 mg protein) in a total assay volume of 1 ml. After 60 min, 300 µl samples were withdrawn from the headspace of the tubes with gas-tight syringes and hydrogen was quantified as described below. Controls were run in parallel without cell extract as well as controls without sodium dithionite or NADH. Activities were calculated from the amount of hydrogen produced per minute and mg protein.

Analytical methods

Concentrations of ethanol and acetate were measured by HPLC with an Aminex HPX-87H column (BioRad) as described before (Müller et al., 2008, Klebensberger et al., 2006). Methane was quantified by gas chromatography with a Carlo Erba GC 6000 (Carlo Erba, Italy) with a flame-ionization detector by injection of 100 µl sample from the headspace of cultures with gas-tight syringes. Nitrogen was used as carrier gas on a packed CarboSieve column heated to 120°C. Hydrogen was measured with a Carlo Erba GC 4300 equipped with a thermal conductivity detector operated at 180°C detector temperature and 250°C filament temperature with nitrogen as carrier gas by injection of 300 µl samples on a 5 Å molecular sieve column (60/80 mesh) heated to 120°C.

Chemicals

Chemicals were obtained from Sigma-Aldrich (Deisenhofen, Germany), Roth (Karlsruhe, Germany) or Fluka (Neu-Ulm, Germany) at analytical quality. Gases were from Messer-Griessheim (Darmstadt, Germany) and from Sauerstoffwerke Friedrichshafen (Friedrichshafen, Germany) at a purity of at least 99,999 %.

Results

Tungstate / Molybdate limitation experiments

Both cocultures, *Desulfovibrio* strain KoEME1 plus *M. hungatei* (KoEME1/M1h) and *Pelobacter acetylenicus* strain WoAcy1 plus *M. hungatei* (WoAcy1/M1h) depended on

addition of at least 0.1 µM tungstate or 0.15 µM molybdate for growth with ethanol. If none of both trace elements was added, growth was very slow, and optical densities did not increase significantly within 200 h (Fig. 1A and D).

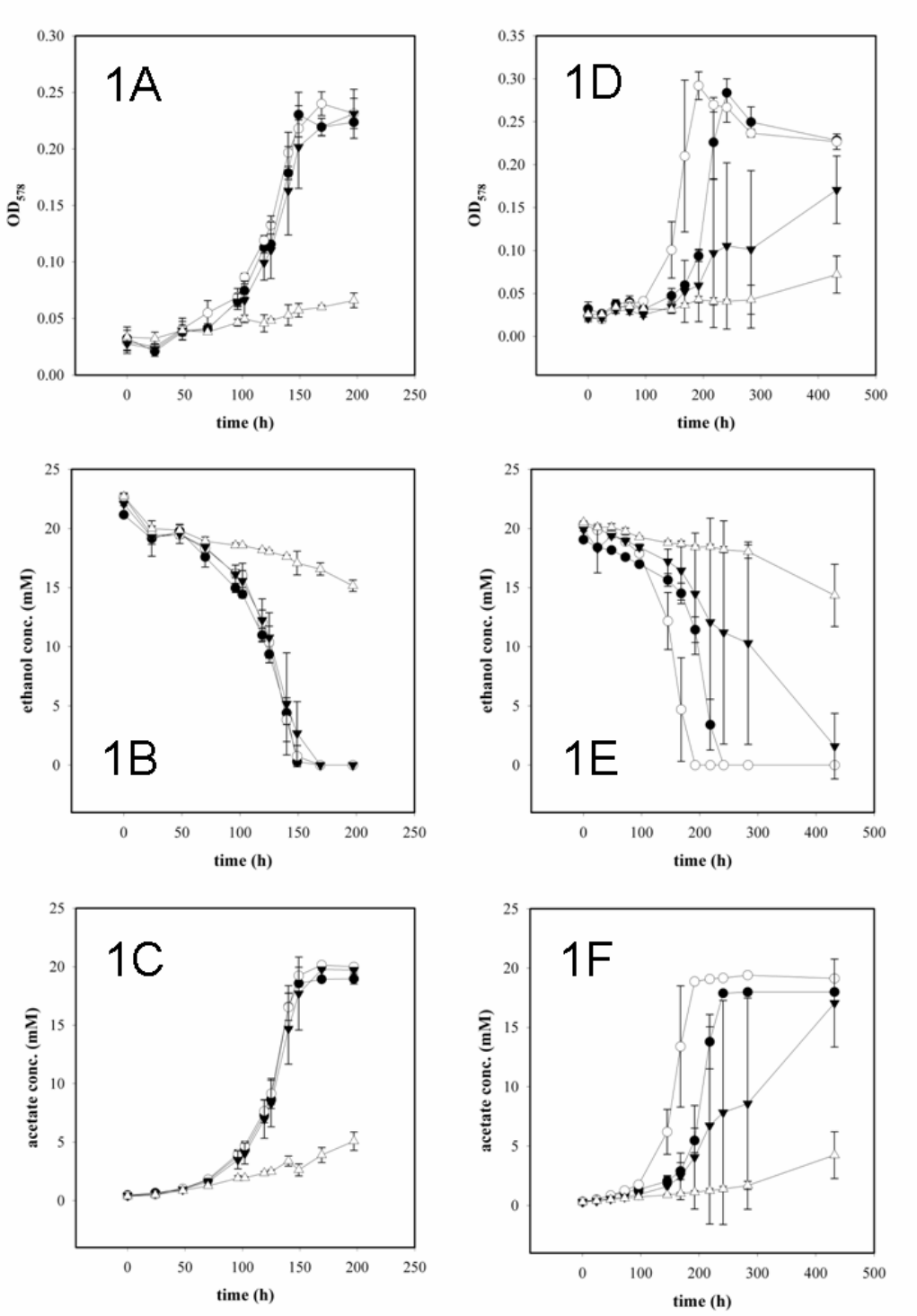

Figure 1: Tungstate / Molybdate limitation experiment. 1A-C: OD_{578}, ethanol concentration and acetate concentration during growth of *Desulfovibrio* strain KoEME1 & *M. hungatei*. 2A-C: OD_{578}, ethanol concentration and acetate concentration during growth of *Pelobacter acetylenicus* strain WoAcy1 & *M. hungatei*. Filled circles: 0.1 µM WO_4^{2-} and 0.15 µM MO_4^{2-}, open circles: 0.1 µM WO_4^{2-}, filled triangles: 0.15 µM MO_4^{2-}, open triangles: no addition of WO_4^{2-} and MO_4^{2-}. Mean values ± standard deviation of triplicates.

The coculture KoEME1/M1h had a similar time lapse of lag- and exponential growth phases in medium containing tungstate, molybdate or both trace elements together (Fig.1A). The lag-phase took on average 100 h and exponential growth became stationary after 150 h with a final optical density of 0.25 at maximum and with a doubling time of 26.5 h ($\mu = 0.026\ h^{-1}$) . During growth, ethanol was converted completely to acetate in all cultures containing tungstate and/or molybdate (Fig.1B-C). Accumulation of acetaldehyde could not be detected.

The coculture WoAcy1/M1h had a lag phase of approximately 100 h. Cultures containing tungstate but no molybdate entered the exponential growth phase earlier than cultures with molybdate (Fig. 1D). Growth without tungstate was delayed but possible. In cultures without both trace elements, growth did not enter the exponential phase and was comparably slow (Fig. 1E). Ethanol was consumed and acetate produced simultaneously with the increase of optical density (Fig. 1E-F). Small amounts of acetaldehyde were detected qualitatively by HPLC in cultures without tungstate and molybdate after 400 hours (not shown). The coculture reached a maximal optical density of 0.3 after 218 h with a doubling time of 21.5 h ($\mu = 0.032\ h^{-1}$.

Fermentation stoichiometry

The cocultures converted ethanol almost stoichiometrically to acetate and methane according to eq. 1 (Table 1).

Table 1: Stoichiometry of ethanol utilization and product formation by the syntrophic cocultures. Shown are mean values of triplicates of 1l-cultures.

Coculture with *M. hungatei*	Ethanol provided (mmol)	Ethanol assimilated (mmol)[a]	Ethanol dissimilated (mmol)	Cell dry mass formed (mg)[b]	Products formed (mmol)		Yield (g/mol)	Electron recovery
					Acetate	Methane		
Pelobacter acetylenicus strain WoAcy1	20.6	1.3	19.3	94.9	18.3	8.03	4.6 (3.2)[c]	91 %
Desulfovibrio strain KoEMEI	19.7	0.64	19.1	46.3	19.1	8.9	2.34	98 %

a: calculated from the dry mass formed and the assimilation equation for ethanol:
$34\ C_2H_6O + 7\ HCO_3^- + 7\ H^+ \rightarrow 24\ <C_4O_3H_7>$
b: calculated from the OD_{578} / dry mass correlations:
OD_{578} 0.1 = 26.6 mg dry mass *Desulfovibrio* strain KoEME1 plus *M. hungatei*
OD_{578} 0.1 = 34 mg dry mass *Pelobacter acetylenicus* strain WoAcy1 plus *M. hungatei*
c: calculated from the OD_{578} / dry mass correlation OD_{578} 0.1 = 23.8 mg dry mass Pelobacter *acetylenicus* strain WoAcy1 (axenic; Schink, 1985)

Side products could not be detected by HPLC in coculture KoEME1/M1h. The coculture WoAcy1/M1h produced traces of acetaldehyde and a further unidentified product (not shown). The OD_{578}/dry mass correlation was determined gravimetrically to OD_{578} 0.1 = 26.6 mg per l for coculture KoEME1/M1h and OD_{578} 0.1 = 34 mg per l for coculture WoAcy1/M1h (Table 1). The coculture KoEME1/M1h had a yield of 2.34 g dry mass per mol ethanol, whereas coculture WoAcy1/M1h had a yield of 4.6 g dry mass per mol ethanol (Table 1). Under the assumption of the OD_{578}/dry mass correlation of axenically grown WoAcy1 determined earlier (OD_{578} 0.1 = 23.8 mg per l; Schink, 1985) the yield would be 3.2 g dry mass per mol ethanol (Table 1).

Cytochromes

No cytochromes could be found in *Pelobacter acetylenicus* strain WoAcy1 whereas cell extracts of *Desulfovibrio* strain KoEME1 contained cytochromes. Oxidized samples of an enriched cytochrome fraction had an absorption maximum at 410 nm, which shifted to a maximum at 420 nm and two additional maxima at 520 nm and 553 nm, respectively, when samples were reduced with dithionite (Fig. 2). Those values are similar to the maxima obtained for cytochrome c_3 of *Desulfovibrio desulfuricans* Norway (Bruschi et al., 1977).

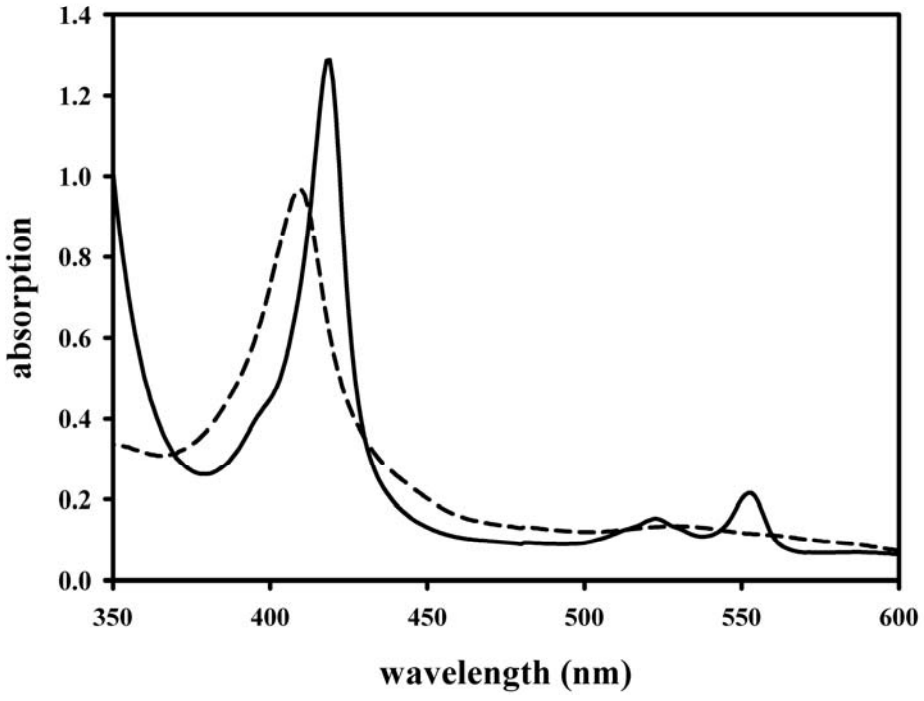

Figure 2: Absorptionspectrum of the enriched cytochrome fraction of coculture KoEME1/M1h. Dashed line: oxidized sample. Solid line: sample reduced with sodium dithionite.

Isoprenoid quinones

Isoprenoid quinones could be detected only in the coculture WoAcy1/M1h. After thin layer chromatography, two major spots were visible under UV light, one with an R_f value of 0.79 and one with an R_f value of 0.88. Menaquinone-9 had an R_f value of 0.81. The absorption spectrum recorded showed only two peaks at 230 nm and 270 nm for the extracted quinones. Menaquinone-9 had absorption maxima at 210, 250, 270 and 340 nm (Fig. 3).

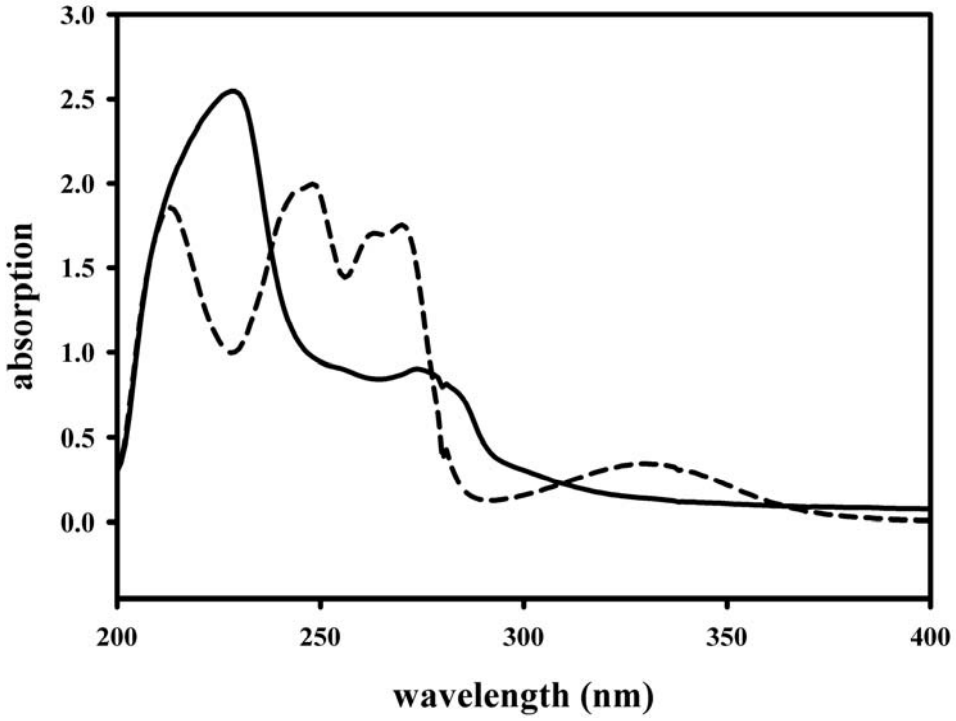

Figure 3: Absorptionspectrum of the enriched isoprenoid quinone fraction of coculture WoAcy1/M1h. Dashed line: vitamin k2 (menatetrenone). Solid line: enriched quinone fraction.

Enzyme activities

In cell extracts of selectively lysed ethanol-fermenting co-cultures, activities of NAD-dependent alcohol dehydrogenase (ADH) and a benzyl viologen-dependent acetaldehyde dehydrogenase (BV-AlDH) were found (Table 2). Accumulation of acetate was detected by HPLC in reaction mixtures for BV-AlDH (not shown). *Desulfovibrio* strain KoEME1 had ADH activity of 0.251 U per mg when assayed in the physiological, oxidative direction at pH 9.0 (Table 2).

No activities of NAD^+-dependent, acetylating acetaldehyde dehydrogenase (AlDH), phosphotransacetylase (PTA) and acetate kinase (AK) could be detected (Table 2).

Table 2: Enzyme activities of cell-free extracts of selectively lysed cocultures. One unit is defined as 1 µmol substrate degraded or product formed per minute and mg protein under the conditions described in the Methods section. Shown are mean values of triplicates.

Enzyme	Activity (U/mg)	
	Pelobacter acetylenicus strain WoAcy1	*Desulfovibrio* strain KoEME1
Alcohol dehydrogenase (EC 1.1.1.1), oxidative, pH 7.5, with NAD^+	0.115	0.061
Alcohol dehydrogenase (EC 1.1.1.1), oxidative, pH 9.0, with NAD^+	0.7	0.251
Alcohol dehydrogenase (EC 1.1.1.1), reductive, with NADH	1.12	1.66
Acetaldehyde dehydrogenase (EC 1.2.1.10), acetylating, with NAD^+ plus Coenzyme A	0.075	0
Phosphotransacetylase (EC 2.3.1.8)	18.8	0
Acetate Kinase (EC 2.7.2.1)	2.21	0
ATPase (EC 3.6.1.3)	0.875	0.511
Acetaldehyde dehydrogenase (EC 1.2.1.3) non-acetylating		
with Benzylviologen	4.86	0.23
with Methylviologen	2.33	0.1
with NAD^+	0	0
NADH:acceptor oxidoreductase		
Benzylviologen	0	2.14
Methylviologen	0	0.226
Formate dehydrogenase (EC 1.2.1.2)		
NAD^+	0.075	0.116
Benzylviologen	4.09	15.68
Methylviologen	2.17	1.03
Hydrogenase (EC 1.18.99.1)		
NAD^+	0	1
Benzylviologen	136[a]	260
Methylviologen	385[a]	71.08

[a] n = 2

In *Pelobacter acetylenicus* strain WoAcy1, ADH activity was 0.7 U per mg, and AlDH, PTA and AK activities were present (Table 2). Both strains showed ATPase activity and activities of several viologen-reducing enzymes, i.e. BV-AlDH, formate dehydrogenase, and hydrogenase (Table 2). Formate dehydrogenase catalyzed also the reduction of NAD^+ with formate in both strains, whereas hydrogenase catalyzed the reduction of NAD^+ with H_2 only in *Desulfovibrio* strain KoEME1 at low activities. Likewise, an NADH oxidizing and viologen reducing activity could be detected only in *Desulfovibrio* strain KoEME1. The hydrogenases detected had extremely high activities with viologens which is most likely due to the non-physiological assay conditions. For hydrogenase of *Desulfovibrio* strain KoEME1, benzylviologen was a better acceptor than methylviologen or NAD^+ whereas in *Pelobacter acetylenicus* strain WoAcy1, hydrogenase showed highest activities with methylviologen as electron acceptor (Table 2).

When assayed in the physiological direction, i.e. measuring hydrogen production through proton reduction by internal electron donors reduced with dithionite, NADH had a stimulatory effect on the hydrogen production rate in both organisms, with *Pelobacter acetylenicus* strain WoAcy1 having a higher activity (Table 3). The hydrogen production rate was approximately two-fold higher in assays which contained NADH, dithionite, and cell extract, compared to assays without NADH. In treatments containing only NADH but no dithionite, no hydrogen production could be observed (Table 3). Due to the high amount of protein added, the reaction mixtures were slightly yellow. After addition of dithionite, the reaction mixtures were colourless, indicating that ferredoxins were present in the cell extract.

Table 3: Activities of NADH-stimulated hydrogenase (H_2-production assay). Shown are mean values of triplicates ± standard deviation. One unit was defined as 1 µmol H_2 produced per minute and mg protein at 25°C.

	Activity (mU per mg)	
	Pelobacter acetylenicus strain WoAcy 1 plus *M .hungatei*	*Desulfovibrio* strain KoEME1 plus *M. hungatei*
cell extract	0	0
cell extract + NADH	0	0
cell extract + dithionite	13.4 ± 7.1	9.5 ± 2.4
cell extract + NADH + dithionite	35.4 ± 4.1	24 ± 1.7

The physiological substrate transformation rate was calculated from the growth rates and the growth yields of both cocultures, and the assumption that 1 mg cell dry mass corresponds to 0.5 mg protein. The coculture KoEME1/M1h had a physiological substrate transformation rate of 370 nmol min^{-1} mg $protein^{-1}$. For the coculture WoAcy1/M1h, the physiological substrate transformation rate was 231 nmol min^{-1} mg $protein^{-1}$, assuming a yield of 4.6 g dry mass per mol. When calculated with the above determined yield of 3.2 g dry mass per mol, the physiological substrate transformation rate was 333 nmol min^{-1} mg $protein^{-1}$. These substrate transformation rates are in the same range as the enzyme activities of ADH and AlDH (Table 2).

Discussion

Compared to other substrates used in syntrophic oxidation processes such as butyrate or propionate, ethanol leaves a broader range of energy exploitation (Schink, 1997). Earlier investigations showed that ethanol-oxidizing syntrophic *Pelobacter* strains had significantly different growth yields with different syntrophic partners in chemostat cultures (Seitz et al., 1990). Likewise, amongst different strains of ethanol-oxidizing sulfate reducers investigated, growth yields were different, which was attributed to the presence or absence of phosphorylating enzymes, especially acetylating acetaldehyde dehydrogenase in the respective bacteria (Hensgens et al., 1994). It was shown that bacteria having acetylating acetaldehyde dehydrogenase (AlDH) activity could grow in the absence of tungstate and molybdate whereas those trace elements were essential for all other strains having only non-acetylating acetaldehyde dehydrogenase (BV-AlDH) activity (Hensgens et al., 1994). This observation was later explained by the fact that *Desulfovibrio gigas* NCIMB 9332 has two different aldehyde dehydrogenases, BV-AlDH being a tungsten-dependent enzyme and DCPIP-AlDH which is molybdenum-dependent (Hensgens et al., 1995).

Here we present similar results showing that *Desulfovibrio* strain KoEME1 in coculture with *M. hungatei* had no acetylating acetaldehyde dehydrogenase (AlDH) and a substantially lower growth yield compared to *Pelobacter acetylenicus* strain WoAcy1, which had activity of acetylating AlDH. Moreover, both strains did not grow without tungstate and molybdate, implying that the non-acetylating acetaldehyde dehydrogenases play an essential role in syntrophic ethanol oxidation, even in bacteria having AlDH. Inhibition of the syntrophic partner *M. hungatei* by the absence of tungstate or molybdate seems unlikely, as

Methanospirillum strain SK has been shown earlier to be independent of tungstate (Widdel, 1986).

Under the assay conditions described, the activities of AlDH were low, which could be due to the high activity of ADH working in reverse, i.e., NADH-oxidizing and acetaldehyde-reducing. Both strains had also activities of BV-AlDH, but no acetylating reaction could be observed with this activity, thus these bacteria waste a remarkably high amount of energy with this reaction. Earlier work on *Pelobacter acetylenicus* strain WoAcy1 demonstrated that BV-AlDH was CoASH dependent during growth with acetylene (Schink, 1985). However, in the present study BV-AlDH activity did not require addition of CoASH, as it was also observed for *Desulfovibrio gigas* (Hensgens et al., 1995). It seems unlikely that cell extracts contained significant amounts of CoASH which could lead to a false interpretation of these results, as AlDH always required addition of CoASH in enzyme assays during this study and should have worked without addition of CoASH if cell extracts still contained this cofactor. Unfortunately, it was not possible to purify the natural electron-accepting system for BV-AlDH, and the artificial assay system with viologens possibly leads to artificially enhanced activities. Also in the case of *D. gigas*, the natural electron acceptor for this enzyme could not be identified, and it was hypothesized that flavoredoxin ($E^{0'}$=-348 mV) could be a potential electron carrier system for BV-AlDH (Hensgens et al., 1995).

The presence of an NADH-stimulated hydrogenase could be interpreted to be due to a confurcating enzyme system like the one described for *Thermotoga maritima* (Schut & Adams, 2009). This enzyme system catalyzes the endergonic oxidation of NADH with protons driven by the exergonic proton reduction with reduced ferredoxin (Schut & Adams, 2009). Although assayed in a non-physiological test with dithionite to keep ferredoxins in their reduced state, the results obtained in this study give a first hint on the presence of such an enzyme system in ethanol-oxidizing syntrophs. Future investigations have to focus on testing these activities with native redox carriers and regenerating systems, i.e., ferredoxin plus acetaldehyde dehydrogenase purified from the respective bacteria, analogous to the assay system described for *Thermotoga maritima* (Schut & Adams, 2009).

Although a comproportionating hydrogenase could be essential for syntrophic growth on ethanol, it does not fully explain the biochemical prerequisites for the respective metabolism. The major endergonic step in ethanol oxidation is the reduction of NAD^+ with ethanol by ADH; the equilibrium of the reaction lies on the side of the educts (eq. 2).

The presence of energy-dissipating BV-AlDH enzymes in both syntrophic ethanol oxidizers investigated leads to the assumption that acetaldehyde has to be kept low constantly by the bacteria to pull the oxidation of ethanol and thus waste a substantial amount of energy. In *Desulfovibrio* strain KoEMEI, ADH and BV-AlDH are most likely the only enzymes responsible for ethanol oxidation to acetate. As the organism lacks phosphorylating enzymes, the only possibility for energy conservation remains to be a membrane-associated phosphorylation by ATPase (Fig. 4).

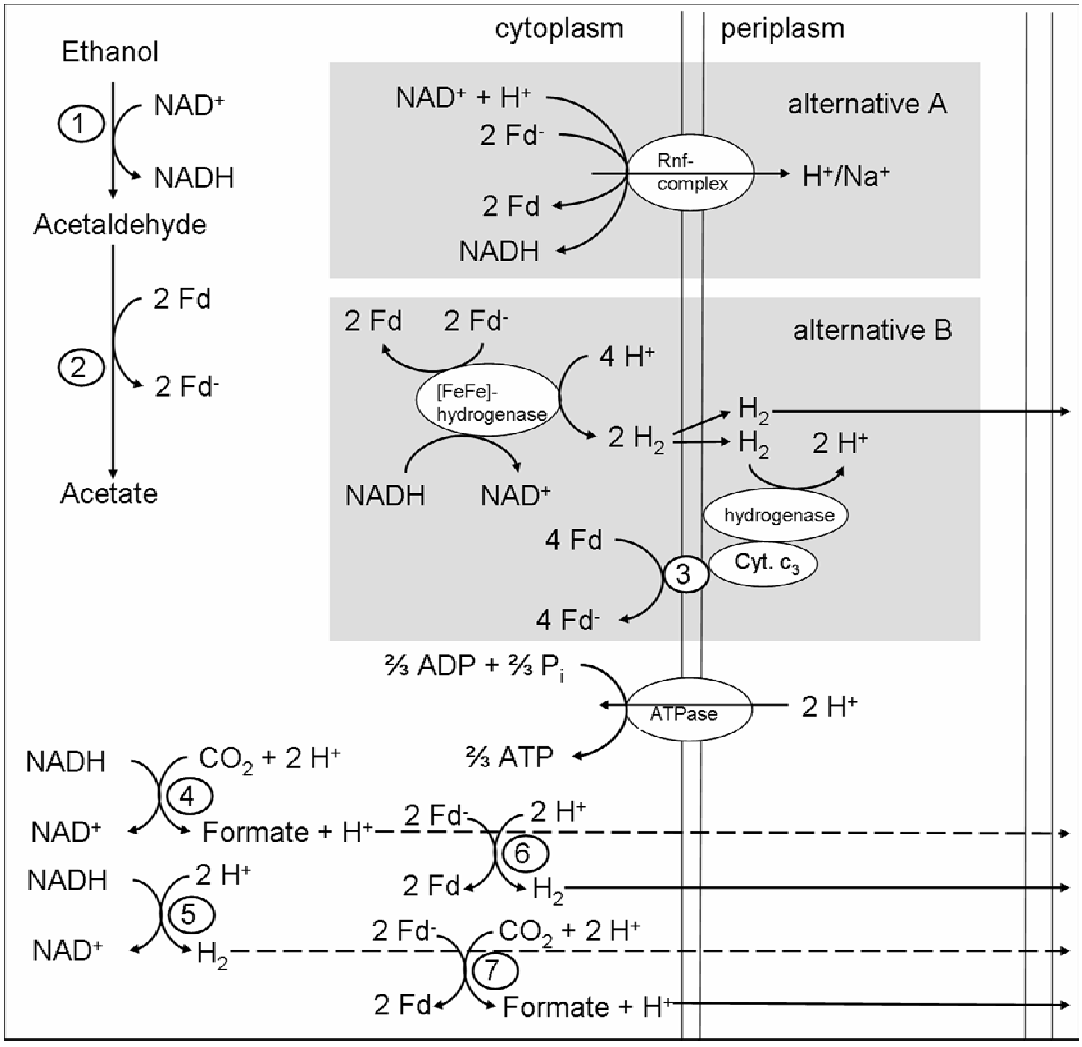

Figure 4: Possible pathway of ethanol oxidation in *Desulfovibrio* strain KoEME1. Fd: ferredoxin, 1: alcohol dehydrogenase (ADH), 2: benzylviologen-dependent acetaldehyde dehydrogenase (BV-AlDH), 3: cytochrome c_3:Fd oxidoreductase 4: NADH-dependent formate dehydrogenase, 5: NADH-dependent hydrogenase, 6: Fd-dependent hydrogenase, 7: Fd-dependent formate dehydrogenase. For explanation see the discussion.

The proton gradient could possibly be produced by an Rnf complex by oxidation of reduced ferredoxin with NAD^+ while pumping protons into the periplasm (alternative A, Fig. 4). NADH could then be oxidized by the NADH dependent hydrogenase and formate dehydrogenase present in cell-free extracts of *Desulfovibrio* strain KoEME1. Indications for

the presence of an Rnf complex could be the NADH:benzylviologen oxidoreductase activity which was described earlier as a possible reaction catalyzed by Rnf proteins (Imkamp et al., 2007). Additionally, rnf genes are likely to be present in *Desulfovibrio* strains; an example is *Desulfovibrio vulgaris* which contains several subunits for rnf genes in its genome (DVU2792-DVU2796, Heidelberg et al., 2004). However, these findings are only of preliminary nature and definite proof of Rnf complexes in this bacterium is still missing. Demonstration of membrane-association of the NADH:benzylviologen oxidoreductase activity as well as reactivity with ferricyanide or the natural electron acceptor ferredoxin could give further evidence towards Rnf complexes present in this bacterium (Imkamp et al., 2007). Without genome sequence information available for this bacterium, it will be difficult to clearly assign the observed NADH-oxidizing activity to Rnf proteins.

An alternative how protons could be translocated for the generation of a membrane potential could be the reoxidation of part of the produced hydrogen in the periplasm (alternative B, Fig. 4). Here, a comproportionating hydrogenase together with other hydrogenases could produce hydrogen, which is then oxidized by a periplasmic hydrogenase and produces a proton gradient which could then be used by ATPase for energy conservation. The electrons could then be transferred to a soluble cyctochrome c_3 in the periplasm, where they are transferred to ferredoxin by a cytochrome c_3:ferredoxin oxidoreductase in the cytoplasmic membrane (enzyme 3 in Fig. 4). Ferredoxin could then be reoxidized again by formate dehydrogenase or hydrogenase in the cytoplasm (Fig. 4). An electron transfer chain involving cytochrome c_3 during acetaldehyde oxidation has been described before for *Desulfovibrio gigas* (Barata et al., 1993). Here, electrons from acetaldehyde oxidation are transferred from flavodoxin to cytochrome c_3, which is subsequently reoxidized by hydrogenase. We now propose that this electron transfer chain reconstituted in vitro earlier by Barata et al. (1993) could work in reverse in *Desulfovibrio* strain KoEME1 and therefore allow hydrogen or formate oxidation and proton release in the periplasm (Fig. 4). These reactions would contribute to generate 0.66 mol ATP per mol ethanol oxidized (Fig. 4). Such a hydrogen cycling system has been proposed long ago for energy conservation in *Desulfovibrio* strains (Odom & Peck, 1981). However, if hydrogen and/or formate concentrations are constantly kept low, oxidation of hydrogen in the periplasm could be prevented and thus no protons are released (alternative B, figure 4). Therefore it is questionable if such hydrogen cycling reactions are possible at all under syntrophic conditions, as hydrogen most likely diffuses into the medium too fast under conditions of low hydrogen partial pressures whereas the hydrogen cycling hypothesis would require a longer retention time for hydrogen in the periplasm.

In bacteria containing a phosphorylating acetaldehyde-oxidizing system such as acetylating acetaldehyde dehydrogenase in *Pelobacter acetylenicus* strain WoAcy1, acetyl-CoA can be produced from acetaldehyde. The NADH thus produced would need to be regenerated to NAD^+ by proton reduction (Fig. 5).

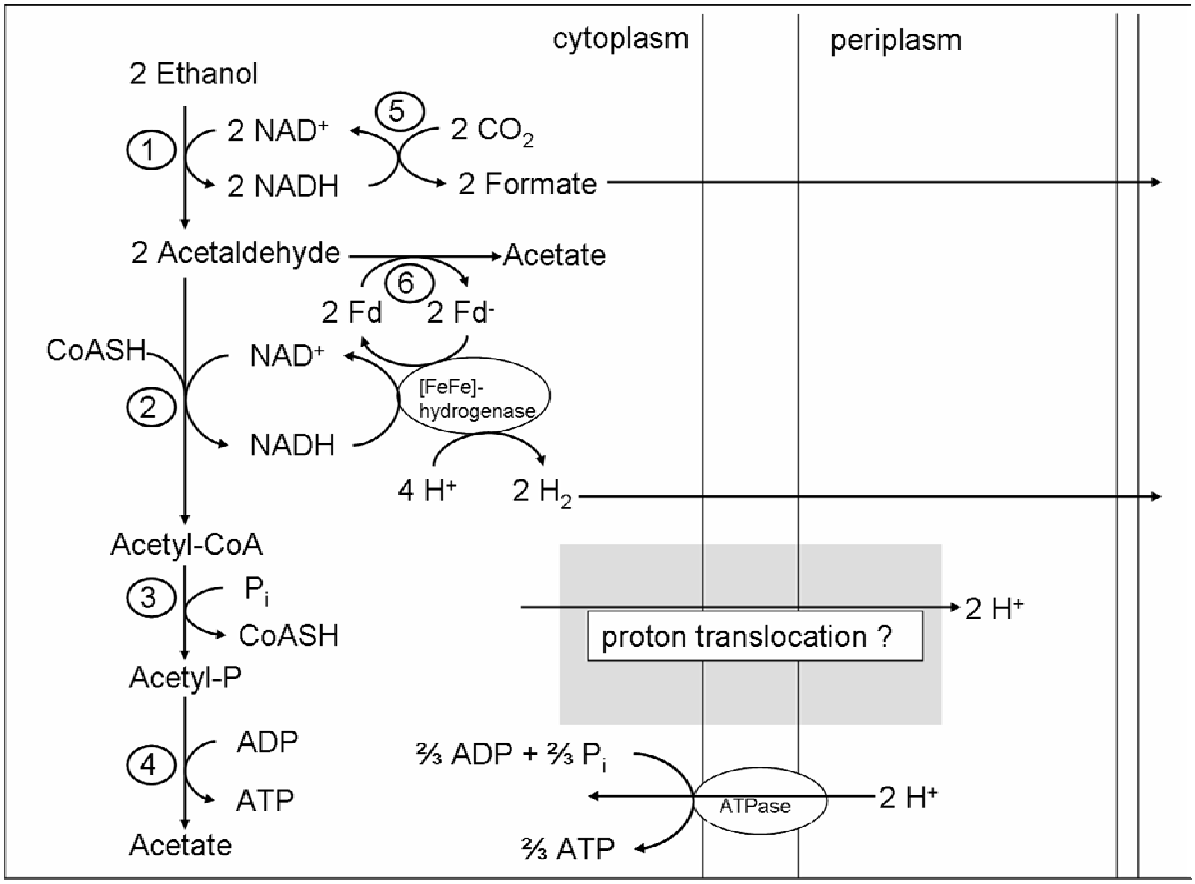

Figure 5: Possible pathway of ethanol oxidation in *Pelobacter acetylenicus* strain WoAcy1. Fd: ferredoxin, Fd^-: reduced ferredoxin, 1: alcohol dehydrogenase (ADH), 2: acetaldehyde dehydrogenase (AlDH), 3: phosphotransacetylase (PTA), 4: acetate kinase (AK), 5: formate dehydrogenase, 6: benzylviologen-dependent acetaldehyde dehydrogenase (BV-AlDH). For explanation see the discussion.

Therefore, the extent of acetylating oxidation of acetaldehyde is certainly limited as it would increase the intracellular ratio of $NADH/NAD^+$ too high for the ADH reaction to occur. NADH could be reoxidized by a comproportionating hydrogenase and a cytoplasmic, NADH-dependent formate dehydrogenase. However, the mechanism of proton transport into the periplasm is not known yet and an NADH:benzylviologen oxidoreductase suggestive of the presence of Rnf complexes like in *Desulfovibrio* strain KoEME1 could not be found (Fig. 5).

Although isoprenoid quinones have been identified in *Pelobacter acetylenicus* strain WoAcy1 which could possibly be involved in an electron transport system within the membrane, it is too early to postulate a complete electron transport pathway with the current set of data.

It seems likely that *Pelobacter acetylenicus* strain WoAcy1 can gain more ATP than *Desulfovibrio* strain KoEME1 as suggested by the higher growth yields of the former one. It can further be assumed that this is due to the presence of both substrate level phosphorylation mechanisms and membrane-bound proton translocation mechanisms in *Pelobacter acetylenicus* strain WoAcy1. Overall, *Pelobacter acetylenicus* strain WoAcy1 could gain up to 0.83 mol ATP per mol of ethanol oxidized, assuming that the ATPase activity found is involved in energy conservation, in addition to acetate kinase (Fig. 5). This fits well to the growth yields obtained for both organisms (Table 1, see below). The OD_{578} to dry mass correlation determined for the coculture WoAcy1/M1h is much higher than expected and could be due to iron sulfide precipitated with the cells which could have caused an overestimation of the cell dry mass.

The value for axenic cultures of strain WoAcy1 obtained earlier by Schink (1985) appears more reasonable and the growth yield calculated from this value is still higher than the growth yield determined for the coculture KoEME1/M1h (Table 1). Assuming a growth yield of 2.34 g per mol for the coculture KoEMEI/M1h and 3.2 g per mol for the coculture WoAcy1/M1h the growth yield of KoEME1/M1h amounts 73 % of the growth yield of WoAcy1/M1h. The ATP yields of both cocultures estimated from the reaction pathways in figures 4 and 5 have a similar percentage (80 % ATP yield of coculture KoEME1/M1h compared to WoAcy1/M1h).

Chapter 6

General Discussion and Outlook

The syntrophic consortia described in this thesis are distinct in many aspects. Hence, it was shown that there are some common attributes in the syntrophic fermenters which will be discussed here. Moreover, this chapter can be seen as an amendment to the discussions of the single chapters.

While the classical syntrophic cocultures grown with ethanol or butyrate have been described already for decades, little is known about the comparably new glucose fermenting syntrophic coculture *Bacillus* sp. BoGlc83 plus *M. hungatei*. The problem as such has been described but an explanation for the obligate dependence of the fermenter on the methanogen is still missing (Müller et al., 2008). *Bacillus* sp. BoGlc83 could not grow anaerobically to optical densities higher than 0.05 although the culture was metabolically active and produced acetate, lactate, and formate from glucose (Scherag, 2009). The accumulation of acetate stopped at a concentration of approximately 2 mM while the formate concentration exhibited the same time lapse and end concentration as acetate after 40 days of incubation, while lactate reached a concentration of 8 mM after that time (Scherag, 2009). These results could be interpreted as a lack of enzymes coupling NADH reoxidation with hydrogen or formate formation, but then there would be no explanation for the situation at a cultivation temperature of 20°C where almost no lactate is being formed (Müller et al., 2008). It seems more likely that the bacterium is forced to produce lactate at elevated temperatures when the metabolic turnover rate is higher and the intracellular $NADH/NAD^+$ ratio is higher. This together with a higher intracellular concentration of fructose-1,6-bisphosphate at higher temperatures or substrate concentrations could lead to an upregulation and allosteric activation of lactate dehydrogenase and therefore leaves the organism no other alternative than releasing reducing equivalents in the form of lactate (Scherag, 2009). This seems plausible regarding the fact that *Bacillus* sp. BoGlc83 has been isolated from sediments of Lake Constance implying that the organism is adapted to temperatures around 4-10°C and substrate concentrations in the micromolar range (Worm et al., under revision). The futile production of lactate and succinate by the organism can therefore be seen as a stress response to the suboptimal cultivation conditions at enhanced temperature in the laboratory (Worm et al., under revision).

But still this does not explain the obligately syntrophic dependence on the partner because the bacterium obviously has the necessary prerequisites for axenic growth by mixed acid fermentation with glucose. As most lactic acid bacteria depend on nutrients from their environment, one could argue that also this bacterium cannot grow without additional supplines, but the organism showed the same growth inhibited behaviour when grown with glucose and yeast extract (Müller et al., 2008). Possibly, reducing equivalents derived from pyruvate oxidation cannot be released any further during axenic growth as judged by the stable formate concentrations under these conditions, and therefore no acetyl-CoA can be formed any more which is a precursor metabolite for anabolic reactions (Scherag, 2009).

The coculture *Syntrophomonas wolfei* plus *M. hungatei* is different from the other syntrophic cocultures studied here concerning its substrate range and efficient metabolism. Until now, no other cultivation substrates other than some saturated and unsaturated fatty acids have been found nor are any alternative electron-accepting systems known for *Syntrophomonas wolfei* (Müller et al., 2009, Worm et al., under revision). All other cocultures presented in this study have numerous alternative options for growth under which they can reach higher growth yields compared to their syntrophic lifestyle. For example, *Bacillus* sp. BoGlc83 can grow aerobically with a broad range of organic substrates in the presence of thiosulfate (Scherag, 2009). The ethanol-fermenting *Pelobacter acetylenicus* can grow alternatively on acetoin, acetylene and 1,3-propanediol whereas *Desulfovibrio* sp. KoEME1 as a sulfate reducer can utilize a multitude of different organic acids and alcohols in the presence of sulfate (Schink, 1985, Rosner et al., 1997, Fahrbach and Schink, unpublished data). It seems that concerning its metabolism, *Syntrophomonas wolfei* is highly adapted to syntrophic cooperation with hydrogenotrophic organisms, which is not very surprising regarding the narrow margin of energy conservation in the fermentation of butyrate (Schink, 1997). As illustrated in Tables 1 and 2, syntrophic oxidation of butyrate necessitates a very efficient metabolism which does not allow energy loss through heat production or futile enzyme reactions. This coherence is reflected by the high thermodynamic efficiency η of butyrate oxidation in Table 2 which is close to the maximum efficiency possible at all (Thauer, 1977).

Table 1: Theoretical ATP-yields of the syntrophic cocultures.

Reaction	$n_{fermenter}$	$n_{methanogen}$[a]	n_{total}
Glucose → 2 Acetate + CO_2 + CH_4 + 2 H^+	4	0.33	4.33
2 Butyrate + CO_2 + 2 H_2O → 4 Acetate + CH_4 + 2 H^+	0.66[b]	0.33	1
2 Ethanol + CO_2 → 2 Acetate + CH_4 + 2 H^+	1.32[b]	0.33	1.65

[a]ATP yield per mol of methane formed at a hydrogen partial pressure of 10^{-5} bar (Schink, 1997)
[b]according to Schink, 1997

In the case of glucose and ethanol fermentation the thermodynamic efficiencies are much lower compared to butyrate fermentation although these values are still much higher than the average efficiencies of 25 % - 50 % for most other anaerobes (Table 2, Thauer et al., 1977). Obviously, both glucose and ethanol fermentation leave a much broader range for energy conservation (Schink, 1997). For ethanol oxidation, wasting energy by fastidious and non-energy conserving turnover of acetaldehyde has even been proposed as the only possibility known for the alcohol dehydrogenase reaction to occur (see Chapter 5). Therefore, thermodynamic efficiency of ethanol oxidation most likely can never reach values in the range of the efficiency of butyrate oxidation.

Table 2: Comparison of the thermodynamic efficiencies of syntrophic cocultures. Values calculated according to Thauer et al., 1977

Reaction	$\Delta G^{0'}$ (kJ/mol)	$\Delta G'$ (kJ/mol)[b]	η[a]
Glucose → 2 Acetate + CO_2 + CH_4 + 2 H^+	-338	-415	52 %
2 Butyrate + CO_2 + 2 H_2O → 4 Acetate + CH_4 + 2 H^+	-42	-62	80 %
2 Ethanol + CO_2 → 2 Acetate + CH_4 + 2 H^+	-112	-132	62.5 %

[a]calculated assuming 50 kJ per mol ATP of chemically available energy form ATP-hydrolysis (Schink, 1997)
[b]at a substrate concentration of 20 mM

Despite of minimizing energy loss by enzyme reactions of the energy metabolism, another option for optimization of energy yields could be to reduce the expenditures. In the case of *Syntrophomonas wolfei*, this could possibly be accomplished by the maintenance of a comparably small genome of a size of only 2642 genes (Copeland et al. 2006, complete sequence of *Syntrophomonas wolfei* subsp. *wolfei* strain Goettingen, GenBank accession no. NC_008346). This is not without disadvantage for the organism. *Syntrophomonas wolfei* depends on vitamins and could never be grown without at least 0.02 % yeast extract in the medium (Wallrabenstein and Schink, 1994). Therefore the organism most likely lacks some important genes for the synthesis of building blocks. *Syntrophomonas wolfei* has been isolated from digestor sludge where a high concentration of nutrients should always be present to overcome this problem (McInerney et al., 1979).

Biochemical prerequisites for syntrophic cooperation

It was demonstrated in the previous chapters that all syntrophic fermenters described here need at least an enzyme system which oxidizes NADH and produces hydrogen or formate. Such an enzyme system could be an iron-hydrogenase like the one described for *Thermotoga*

maritima (Schut and Adams, 2009). Additionally, the NADH-dependent formate dehydrogenase of *Eubacterium acidaminophilum* could be a candidate for a reversed electron transport system (Graentzdoerffer et al., 2003). Enzymes oxidizing NADH have been found in cell-free extracts of syntrophic cultures fermenting butyrate and ethanol but not in glucose-fermenting cocultures. Nonetheless, such enzymes must be present in *Bacillus* sp. BoGlc83 as glycolysis inevitably yields NADH. Future investigations should focus on finding these enzymes in *Bacillus* sp. BoGlc83.

One of the central elements in the theory that tries to explain syntrophy is that syntrophic fermenters have to invest part of their energy in a reversed electron transport by proton influx into the cell that is fuelled by the proton gradient obtained through ATP hydrolysis (Schink, 1997). Alternative hypotheses were presented in Chapter 5. Moreover, ATP investment seems not essential for syntrophic glucose oxidation, as this reaction is endergonic enough to run without energy input under methanogenic conditions. It is therefore questionable if this general hypothesis is restricted only to the cases of energetically difficult substrates like butyrate and propionate. And even in those cases, the system has to be very simple, i.e. without biochemically expensive proton channels and only few enzymes involved.

It was shown that protein identification *via* genome sequence information provides a powerful tool also for the investigation of syntrophic bacteria. In the case of *S. wolfei*, future comparative transcriptional studies could show, which enzymes are upregulated during growth with butyrate. Moreover, the participation of menaquinone in the reversed electron transport could be tested in enzyme assays with chemically reduced quinones.

For syntrophic oxidation of ethanol, classical enzyme assays revealed the central metabolic routes but the reversed electron transport in syntrophic ethanol fermenters still remains obscure. Again, genome sequence information together with comparative transcriptional studies could help to understand the composition of the enzyme pool upon growth with ethanol. Further studies should mainly focus on the isolation of the electron carriers involved in acetaldehyde oxidation and hydrogen production and testing them in enzyme assays under physiological conditions without artificial electron acceptors. It is still unclear if the investigated syntrophic ethanol-fermenting bacteria have enzymes similar to the one enriched from cell-free extracts of *S. wolfei*. Purification of the revealed NADH-oxidizing activities will hopefully answer this question.

Chapter 7

Summary

The anaerobic bacteria investigated in this thesis can gain energy from metabolization of their respective substrates only by close cooperation with methanogenic archaea. By fermentation of the substrate through the fermenting bacterium hydrogen is being formed, which is used by the hydrogen-scavenging partner bacterium for the production of methane. Thus a low hydrogen partial pressure is being maintained which allows the oxidation of the thermodynamically unfavourable substrate. This exceptional case of a symbiotic relationship is defined as syntrophy. In some cases, the fermenting bacterium has to invest energy in addition to shift electrons derived from oxidation processes to the redox potential of proton reduction to hydrogen, which is called reversed electron transport.

The aim of this study was the biochemical characterization of the components of the reversed electron transport in the fermenting bacteria of syntrophic cocultures growing on glucose, butyrate, or ethanol. For the glucose-utilizing bacterium *Bacillus* sp. BoGlc83 it was shown that, besides acetate, lactate and traces of succinate could be formed during syntrophic growth. Interspecies electron transfer occurs most likely through formate. The bacterium has all glycolytic enzymes as well as all enzymes necessary for the formation of acetate and lactate from pyruvate. Therefore, a fermentation of glucose should be possible without syntrophic partner. However, the bacterium strictly depends on the presence of a methanogenic partner organism. This phenomenon could not be explained sufficiently during this study.

For syntrophic oxidation of butyrate by *Syntrophomonas wolfei*, a novel enzyme system has been described which catalyzes the oxidation of NADH with several different electron acceptors. By inhibition of this enzyme system with trifluoperazine *in vivo,* it was shown that this enzyme system is essential for butyrate oxidation and regeneration of redox carriers. More detailed characterization on the basis of sequence information from the genome of *S. wolfei* revealed a homology of this enzyme system with the confurcating enzyme system from *Thermotoga maritima*, which catalyzes the concomitant oxidation of NADH and reduced ferredoxin with protons to form hydrogen. Yet, this reaction could not be shown for *S. wolfei*. Instead, an enzyme reaction with quinones located in the cytoplasmic membrane was postulated. This process could be driven by proton influx into the cell.

In the case of syntrophic oxidation of ethanol, enzyme activities and growth yields of two different cocultures were compared. The coculture *Desulfovibrio* strain KoEME1 plus *Methanospirillum hungatei* had significantly lower growth yields compared to the coculture *Pelobacter acetylenicus* plus *M. hungatei*. This was explained by the absence of an acetylating acetaldehyde dehydrogenase in *Desulfovibrio* strain KoEME1. Both *Desulfovibrio* strain KoEME1 and *Pelobacter acetylenicus* showed activities of a non-acetylating und therefore non-energy conserving acetaldehyde dehydrogenase which most likely facilitates the endergonic oxidation of ethanol by lowering the intracellular concentration of acetaldehyde.

Chapter 8

Zusammenfassung

Die in dieser Arbeit untersuchten anaeroben Bakterien können Energie aus dem Abbau der jeweils beschriebenen Substrate nur gewinnen, indem sie eng mit methanogenen Archaeen kooperieren. Durch die Vergärung des Substrats durch das gärende Bakterium wird Wasserstoff gebildet, welcher vom wasserstoffzehrenden Partnerbakterium zur Bildung von Methan verwendet wird. Somit wird ein niedriger Wasserstoffpartialdruck aufrechterhalten, wodurch die Oxidation des thermodynamisch ungünstigen Substrats überhaupt erst ermöglicht wird. Dieser Sonderfall einer Symbiose wird als Syntrophie bezeichnet. In einigen Fällen muß der Gärer zudem Energie aufwenden, um die bei der Oxidation freiwerdenden Elektronen auf das Redoxpotential der Protonenreduktion zu Wasserstoff anzuheben, was als revertierter Elektronentransport bezeichnet wird.

Ziel der vorliegenden Arbeit war die biochemische Charakterisierung der Komponenten des revertierten Elektronentransports in den gärenden Bakterien der syntrophen Kokulturen, die auf Glucose, Butyrat oder Ethanol wuchsen. Im Fall des Glucose-verwertenden Bakteriums *Bacillus* sp. BoGlc83 wurde gezeigt, dass während des Wachstums neben Acetat mit steigender Kultivierungstemperatur auch Lactat und Spuren von Succinat gebildet wurden. Der Transfer von Reduktionsäquivalenten zum methanogenen Partner findet vermutlich über Formiat statt. Das Bakterium besitzt alle Glykolyseenzyme sowie alle Enzyme, die zur Bildung von Acetat und Lactat aus Pyruvat nötig sind. Somit sollte die Vergärung von Glucose problemlos ohne Partnerorganismus möglich sein. Dennoch ist das Bakterium obligat auf die Anwesenheit eines methanogenen Partnerorganismus angewiesen. Dieses Phänomen konnte im Zuge dieser Arbeit noch nicht hinreichend geklärt werden.

Für die syntrophe Oxidation von Butyrat durch *Syntrophomonas wolfei* wurde in dieser Arbeit ein neuartiges Enzymsystem beschrieben, das die Oxidation von NADH mit verschiedenen Elektronenakzeptoren katalysiert. Durch Hemmung dieses Enzymsystems durch Trifluoperazin *in vivo* wurde gezeigt, dass letzteres für die Oxidation von Butyrat und die Regeneration von Redoxcarriern essentiell ist. Eine genauere Charakterisierung anhand von Sequenzinformationen des Genoms von *Syntrophomonas wolfei* zeigte eine Ähnlichkeit des Enzymsystems zu einem comproportionierenden Enzymsystem aus *Thermotoga maritima*, welches unter gleichzeitiger Oxidation von NADH und reduziertem Ferredoxin Protonen zu

Wasserstoff reduziert. Diese Reaktion konnte jedoch für *S. wolfei* noch nicht nachgewiesen werden. Stattdessen wurde eine Enzymreaktion mit Chinonen in der cytoplasmatischen Membran vorgeschlagen. Die Energetisierung dieses Prozesses könnte durch Protoneneinstrom in die Zelle erfolgen.

Im Fall der syntrophen Oxidation von Ethanol wurden jeweils bei zwei verschiedenen Kokulturen die beteiligten Enzymaktivitäten in Zellextrakten und die Wachstumserträge miteinander verglichen. Die Kokultur *Desulfovibrio* sp. KoEME1 plus *Methanospirillum hungatei* hatte deutlich niedrigere Wachstumserträge im Vergleich zur Kokultur *Pelobacter acetylenicus* plus *M. hungatei*. Dies wurde durch die Abwesenheit einer acetylierenden Acetaldehyddehydrogenase in *Desulfovibrio* sp. KoEME1 erklärt. Sowohl *Desulfovibrio* sp. KoEME1 als auch *Pelobacter acetylenicus* zeigten Aktivitäten einer nicht-acetylierenden und somit nicht-energiekonservierenden Acetaldehyddehydrogenase, welche vermutlich durch Niedrighalten der intrazellulären Acetaldehydkonzentration die endergone Oxidation von Ethanol möglich macht.

Record of Achievement

Unless stated otherwise all experiments in this work were performed and analyzed by myself. Cultivation media were prepared mainly by Antje Wiese. All experiments were developed and planned by myself and my supervisor Prof. Dr. Bernhard Schink. Drafts for the respective manuscripts were written by me and corrected by Prof. Dr. Bernhard Schink and the coauthors of the respective publications.

Sequencing of the 16S-rDNA, taxonomic classification and compilation of the phylogenetic tree of *Bacillus* sp. BoGlc83 in chapter 2 was done by Ulrich Stingl. Enrichment and isolation of *Bacillus* sp. BoGlc83 as well as MPN-determinations and preliminary enzyme assays were done by Benjamin Griffin and Bernhard Schink already before the beginning of my doctoral studies.

The nucleotide sequences of the identified proteins in chapter 3 were annotated by David Schleheck. After the first revision of the manuscript in chapter 3, this work had to be improved significantly and completed by additional experiments. Textual changes as well as ideas and proposals for these additional experiments were also contributed by David Schleheck.

For the review article in chapter 4 we cooperated with the group of Prof. Dr. Alfons Stams, Wageningen, Netherlands. The contributions to syntrophic oxidation of propionate were from Petra Worm whereas contributions to the syntrophic oxidation of butyrate were written by me. The general parts of the text were written by both of us in equal contribution. Revisions and corrections were done by our respective supervisors.

Abgrenzung der Eigenleistung

Falls nicht anders angegeben wurden alle Experimente zu dieser Arbeit von mir selbst durchgeführt und ausgewertet. Nährmedien zur Anzucht von Bakterien wurden zum Großteil von Antje Wiese hergestellt. Die Experimente wurden von meinem Betreuer Prof. Dr. Bernhard Schink oder mir selbst konzeptioniert und geplant. Die Entwürfe für die jeweiligen Manuskripte wurden von mir geschrieben und von Prof. Dr. Bernhard Schink sowie den jeweiligen Koautoren der einzelnen Arbeiten gegengelesen und korrigiert.

Die Sequenzierung der 16S-rDNA von *Bacillus* sp. BoGlc83 in Kapitel 2 sowie die taxonomische Einordnung und die Erstellung des Stammbaumes wurde von Ulrich Stingl durchgeführt. Die Anreicherung und Isolierung von *Bacillus* sp. BoGlc83 sowie die MPN-Bestimmungen und Vorversuche zu den Enzymtests wurden von Benjamin Griffin und Bernhard Schink schon vor Beginn meiner Doktorandenzeit durchgeführt.

Die Annotationsarbeit zu den Nukleotidsequenzen der identifizierten Proteine in Kapitel 3 wurde von David Schleheck beigetragen. Die in diesem Kapitel beschriebene Arbeit musste nach der ersten Einreichung gravierend überarbeitet und mit zusätzlichen Experimenten ergänzt werden. Textänderungen hierzu sowie Ideen und Vorschläge zu den zusätzlichen Experimenten wurden ebenfalls von David Schleheck beigetragen.

Für den Übersichtsartikel in Kapitel 4 haben wir mit der Arbeitsgruppe von Prof. Dr. Alfons Stams, Wageningen, Niederlande kooperiert. Die Beiträge zur syntrophen Propionatoxidation stammen hauptsächlich von Petra Worm während der Beitrag zur Butyratoxidation zum Großteil von mir geschrieben wurde. Die allgemeinen Teile des Texts wurden von uns beiden zu gleichen Anteilen beigetragen. Die Überarbeitung und Korrektur des Manuskripts wurde von unseren jeweiligen Betreuern übernommen.

References

Altman, F. P. (1976) Tetrazolium salts and formazans. Prog. Histochem. Cytoc. 9:1-51.

Altschul, S. F., Gish, W., Miller, W., Myers, E. W., and Lipman, D. J. (1990) Basic local alignment search tool. J. Mol. Biol. 215:403-410.

Amann, R. I., Ludwig, W., and Schleifer, K. H. (1995) Phylogenetic identification and *in situ* detection of individual microbial cells without cultivation. Microbiol. Rev. 59:143-169.

Amann, R., Fuchs, B. M., and Behrens, S. (2001) The identification of microorganisms by fluorescence *in situ* hybridisation. Curr. Opin. Biotechnol. 12:231-236.

Backiel, J., Juárez, O., Zagorevski, D. V., Wang, Z., Nilges, M.J., and Barquera, B. (2008) Covalent binding of flavins to RnfG and RnfD in the Rnf complex from *Vibrio cholera*. Biochemistry 47:11273-11284.

Barata, B. A. S., Le Gall, J., and Moura, J. J. G. (1993) Aldehyde oxidoreductase activity in *Desulfovibrio gigas*: *In vitro* reconstitution of an electron-transfer chain from aldehydes to the production of molecular hydrogen. Biochemistry 32:11559-11568.

Barker, H. A. (1940) Studies upon the methane fermentation. IV. The isolation and culture of *Methanobacterium omelianskii*. Antonie van Leeuwenhoek, 6:201-220.

Beaty, P. S., Wofford, N. Q., and McInerney, M. J. (1987) Separation of *Syntrophomonas wolfei* from *Methanospirillum hungatei* in syntrophic cocultures by using percoll gradients. Appl. Environ. Microbiol. 53:1183-1185.

Beaty, P. S., and McInerney, M. J. (1990) Nutritional features of *Syntrophomonas wolfei*. Appl. Environ. Microbiol. 56:3223-3224.

Bendtsen, J. D., Nielsen, H., Widdick, D., Palmer, T., and Brunak, S. (2005) Prediction of twin-arginine signal peptides. BMC Bioinformatics 6:167.

Bergmeyer, H. U. (1974) Methoden der enzymatischen Analyse., 3rd edition. Verlag Chemie, Weinheim.

Bradford, M. M. (1976) A rapid and sensitive method for the quantification of microgram quantities of protein utilizing the principle of protein-dye binding. Anal. Biochem. 72:248-254.

Brune, A., and Schink, B. (1990) Pyrogallol-to-phloroglucinol conversion and other hydroxyl-transfer reactions catalyzed by cell extracts of *Pelobacter acidigallici*. J. Bacteriol. 172:1070-1076.

Bruns, A., Cypionka, H., and Overmann, J. (2002) Cyclic AMP and acyl homoserine lactones increase the cultivation efficiency of heterotrophic bacteria from the central Baltic Sea. Appl. Environ. Microbiol. 68:3978-3987.

Bruschi, M., Hatchikian, C. E., Gololeva, L. A., and LeGall, J. (1977) Purification and characterization of cytochrome c_3, ferredoxin, and rubredoxin isolated from *Desulfovibrio desulfuricans* Norway. J. Bacteriol. 129:30-38.

Bryant, M. P., Wolin, E. A., Wolin, M. J. and Wolfe, R. S. (1967) *Methanobacillus omelianskii*, a symbiotic association of two species of bacteria. Arch. Microbiol. 59:20-31.

Bussmann, I., Philipp, B., and Schink, B. (2001) Factors influencing the cultivability of lake water bacteria. J. Microbiol. Meth. 47:41-50.

Chabrière, E., Charon, M. H., Volbeda, A., Pieulle, L., Hatchikian, C. E., and Fontecilla-Camps, J. C. (1999) Crystal structures of the key anaerobic enzyme pyruvate : ferredoxin oxidoreductase, free and in complex with pyruvate. Nat. Struct. Biol. 6:182-190.

Chin, K. J., Hahn, D., Hengstmann, U., Liesack, W., and Janssen, P. H. (1999) Characterization and identification of numerically abundant culturable bacteria from the anoxic bulk soil of rice paddy microcosms. Appl. Environ. Microbiol. 65:5042-5049.

de Bok, F. A. M., Stams, A. J. M., Dijkema, C., and Boone, D. R. (2001) Pathway of propionate oxidation by a syntrophic culture of *Smithella propionica* and *Methanospirillum hungatei*. Appl. Environ. Microbiol. 67:1800-1804.

de Bok, F. A. M., Luijten, M. L. G. C., and Stams, A. J. M. (2002) Biochemical evidence for formate transfer in syntrophic propionate-oxidizing cocultures of *Syntrophobacter fumaroxidans* and *Methanospirillum hungatei*. Appl. Environ. Microbiol. 68:4247-4252.

de Bok, F. A. M., Hagedoorn, P. L., Silva, P. J., Hagen, W. R., Schiltz, E., Fritsche, K., and Stams, A. J. M. (2003) Two W-containing formate dehydrogenases (CO_2-reductases) involved in syntrophic propionate oxidation by *Syntrophobacter fumaroxidans*. Eur. J. Biochem. 270:2476-2485.

Denke, E., Merbitz-Zahradnik, T., Hatzfeld, O. M., Snyder, C. H., Link, T. A., and Trumpower, B. L. (1998) Alteration of the midpoint redox potential and catalytic activity of the Rieske iron-sulfur protein by changes of amino acids forming hydrogen bonds to the iron-sulfur cluster. J. Biol. Chem. 273:9085-9093.

Dermoun, Z., De Luca, G., Asso, M., Bertrand, P., Guerlesquin, F., and Guigliarelli, B. (2002) The NADP-reducing hydrogenase from *Desulfovibrio fructosovorans*: functional interaction between the C-terminal region of HndA and the N-terminal region of HndD subunits. Biochim. Biophys. Acta 1556:217-225.

Diekert, G. B., and Thauer, R. K. (1978) Carbon monoxide oxidation by *Clostridium thermoaceticum* and *Clostridium formicoaceticum*. J. Bacteriol. 136:597-606.

Dolfing, J., Jiang, B., Henstra, A. M., Stams, A. J. M., and Plugge, C. M. (2008) Syntrophic growth on formate: a new microbial niche in anoxic environments. Appl. Environ. Microbiol. 74:6126-6131.

Dong, X. Z., Cheng, G., and Stams, A. J. M. (1994) Butyrate oxidation by *Syntrophospora bryantii* in coculture with different methanogens and in pure culture with pentenoate as electron-acceptor. Appl. Microbiol. Biotechnol. 42:647-652.

Dong, X. Z., and Stams, A. J. M. (1995) Evidence for H_2 and formate formation during syntrophic butyrate and propionate degradation. Anaerobe 1:35-39.

Doré, J., and Bryant, M. P. (1990) Metabolism of one-carbon compounds by the ruminal acetogen *Syntrophococcus sucromutans*. Appl. Environ. Microbiol. 56:984-989.

Edwards, U., Rogall, T., Blöcker, H., Emde, M., and Böttger, E. C. (1989) Isolation and direct complete nucleotide determination of entire genes. Characterization of a gene coding for 16S ribosomal RNA. Nucleic Acids Res. 17:7843-7853.

Felsenstein, J. (1989) PHYLIP, phylogeny inference package version 3.57c. Cladistics 5:164-166.

Friedrich, M. W., and Schink, B. (1993) Hydrogen formation from glycolate driven by reversed electron transport in membrane vesicles of a syntrophic glycolate-oxidizing bacterium. Eur. J. Biochem. 217:233-240.

Fry, J. (2000) Bacterial diversity and 'unculturables'. Microbiol. Today 27:186-188.

Giovannoni, S. J., Britschgi, T. B., Moyer, C. L., and Field, K. G. (1990) Genetic diversity in Sargasso Sea bacterioplankton. Nature 345:60-63.

Graentzdoerffer, A., Rauh, D., Pich, A., and Andreesen, J. R. (2003) Molecular and biochemical characterization of two tungsten- and selenium-containing formate dehydrogenases from *Eubacterium acidaminophilum* that are associated with components of an iron-only hydrogenase. Arch. Microbiol. 179:116-130.

Gustafson, W. G., Feinberg, B. A., and McFarland, J. T. (1986) Energetics of β-oxidation. Reduction potentials of general fatty acyl-CoA dehydrogenase, electron transfer flavoprotein and fatty acyl-CoA substrates. J. Biol. Chem. 261:7733-7741.

Gunsalus, R. P., Romesser, J. A., and Wolfe, R. S. (1978) Preparation of coenzyme M analogues and their activity in the methyl coenzyme M reductase system of *Methanobacterium thermoautotrophicum*. Biochemistry 17:2374-2377.

Hägerhäll, C. (1997) Succinate:quinone oxidoreductases variations on a conserved theme. Biochim. Biophys. Acta 1320:107-141.

Hauck, S., Benz, M., Brune, A., and Schink, B. (2001) Ferrous iron oxidation by denitrifying bacteria in profundal sediments of a deep lake (Lake Constance). FEMS Microbiol. Ecol. 37:127-134.

Heidelberg, J. F., Seshadri, R., Haveman, S. A., Hemme, C. L., Paulsen, I. T., Kolonay, J. F., Eisen, J. A., Ward, N., Methe, B., Brinkac, L. M., Daugherty, S. C., Deboy, R. T., Dodson, R. J., Durkin, A. S., Madupu,R., Nelson, W. C., Sullivan, S. A., Fouts, D., Haft, D. H., Selengut, J., Peterson, J. D., Davidsen, T. M., Zafar, N., Zhou, L., Radune, D., Dimitrov, G., Hance, M., Tran, K., Khouri, H., Gill, J., Utterback, T. R., Feldblyum, T. V., Wall, J. D., Voordouw, G., and Fraser, C. M. (2004) The genome sequence of the anaerobic, sulfate-reducing bacterium *Desulfovibrio vulgaris* Hildenborough. Nat. Biotechnol. 22:554-559.

Henckel, T., Friedrich, M., and Conrad, R. (1999) Molecular analyses of the methane-oxidizing microbial community in rice field soil by targeting the genes of the 16S-rRNA, particulate methane monooxygenase and methanol dehydrogenase. Appl. Environ. Microbiol. 65:1980-1990.

Hensgens, C. M. H., Nienhuis-Kuiper, M. E. and Hansen, T. A. (1994) Effects of tungstate on the growth of *Desulfovibrio gigas* NCIMB 9332 and other sulfate-reducing bacteria with ethanol as substrate. Arch. Microbiol. 162:143-147.

Hensgens, C. M. H., Hagen, R. H. and Hansen, T. A. (1995) Purification and characterization of a benzylviologen-linked, tungsten-containing aldehyde oxidoreductase from *Desulfovibrio gigas*. J. Bacteriol. 177:6195-6200.

Herrmann, G., Jayamani, E., Mai, G., and Buckel, W. (2008) Energy conservation via electron-transferring flavoprotein in anaerobic bacteria. J. Bacteriol. 190:784-791.

Hoehler, T. M., Alperin, M. J., Albert D. B., and Martens C. S. (2001) Apparent minimum free energy requirements for methanogenic archaea and sulfate-reducing bacteria in an anoxic marine sediment. FEMS Microbiol. Ecol. 38:33-41.

Hoffman, A., and Dimroth, P. (1990) The ATPase of *Bacillus alcalophilus*. Purification and properties of the enzyme. Eur. J. Biochem., 194:423-430.

Ianotti, E. L., Kafkewitz, D., Wolin, M. J. and Bryant, M. P. (1973) Glucose fermentation products of *Ruminococcus albus* grown in continuous culture with *Vibrio succinogenes*: changes caused by interspecies transfer of H_2. J. Bacteriol. 114:1231-1240.

Imachi, H., Sekiguchi, Y., Kamagata, Y., Hanada, S., Ohashi, A., and Harada, H. (2002) *Pelotomaculum thermopropionicum* gen. nov., sp. nov., an anaerobic, thermophilic syntrophic propionate-oxidizing bacterium. Int. J. Syst. Evol. Microbiol. 52:1729-1735.

Imkamp, F., Biegel, E., Jayamani, E., Buckel, W., and Müller V. (2007) Dissection of the caffeate respiratory chain in the acetogen *Acetobacterium woodii*: Identification of an Rnf-type NADH dehydrogenase as a potential coupling site. J. Bacteriol. 189:8145-8153.

Ishii, S., Kosaka, T., Hori, K., Hotta, Y., and Watanabe, K. (2005) Coaggregation facilitates interspecies hydrogen transfer between *Pelotomaculum thermopropionicum* and *Methanothermobacter thermoautotrophicus*. Appl. Environ. Microbiol. 71:7838-7845.

Jormakka, M., Törnroth, S., Byrne, B., and Iwata, S. (2002) Molecular basis of proton motive force generation: Structure of formate dehydrogenase-N. Science 295:1863-1868.

Karmakar, S. S., Pearse, A. G. E., and Seligman, A. M. (1960) Preparation of nitrotetrazolium salts containing benzothiazole. J. Org. Chem. 25:575-578.

Kemerer, V. F., Griffin, C. C., and Brand, L. (1975) Phosphofructokinase from *Escherichia coli*. *In:* Methods in Enzymology, Colowick, S. P., and Kaplan, N. O. (eds.), 42:91-98. Academic Press, New York.

Klebensberger, J., Rui, O., Fritz, E., Schink, B. and Philipp, B. (2006) Cell aggregation of *Pseudomonas aeruginosa* strain PAO1 as an energy-dependent stress response during growth with sodium dodecyl sulfate. Arch. Microbiol. 185:417-427.

Kremer, D.R., Nienhuis-Kuiper, H. E., and Hansen, T. A. (1988) Ethanol dissimilation in *Desulfovibrio*. Arch. Microbiol. 150:552-557.

Kosaka, T., Kato, S., Shimoyama, T., Ishii, S., Abe, T., and Watanabe, K. (2008) The genome of *Pelotomaculum thermopropionicum* reveals niche-associated evolution in anaerobic microbiota. Genome Res. 18:442-448.

Krebs, W., Steuber, J., Gemperli, A. C., and Dimroth, P. (1999) Na^+ translocation by the NADH:ubiquinone oxidoreductase (complex I) from *Klebsiella pneumoniae*. Mol. Microbiol. 33:590-598.

Kröger, A., Biel, S., Simon, J., Gross, R., Unden, G., and Lancaster, C. R. D. (2002) Fumarate respiration of *Wolinella succinogenes*: enzymology, energetics and coupling mechanism. Biochim. Biophys. Acta Bioenergetics 1553:23-38.

Krumholz, L. R., and Bryant, M. P. (1986) *Syntrophococcus sucromutans* sp. nov. gen. nov. uses carbohydrates as electron donors and formate, methoxybenzenoids or *Methanobrevibacter* as electron acceptor systems. Arch. Microbiol. 143:313-318.

Kryukov, G. V., and Gladyshev, V. N. (2004) The prokaryotic selenoproteome. EMBO Rep. 5:538-543.

Kumagai, H., Fujiwara, T., Matsubara, H., and Saeki, K. (1997) Membrane localization, topology, and mutual stabilization of the *rnfABC* gene products in *Rhodobacter capsulatus* and implications for a new family of energy-coupling NADH oxidoreductases. Biochemistry 36:5509-5521.

Laemmli, U. K. (1970) Cleavage of structural proteins during the assembly of the head of bacteriophage T4. Nature 227:680-685.

Lancaster, C. R. D. (2002) Succinate:quinone oxidoreductases: an overview. Biochim. Biophys. Acta Bioenergetics 1553:1-6.

Li, F., Hinderberger, J., Seedorf, H., Zhang, J., Buckel, W., and Thauer, R. K. (2008) Coupled ferredoxin and crotonyl coenzyme A (CoA) reduction with NADH catalyzed by the butyryl-CoA dehydrogenase/Etf complex from *Clostridium kluyveri* J. Bacteriol. 190:843-850.

Ludwig, W., Bauer, S. H., Bauer, M., Held, I., Kirchhof, G., Schulze, R., Huber, I., Spring, S., Hartmann, A., and Schleifer, K. H. (1997) Detection and *in situ* identification of representatives of a widely distributed new bacterial phylum. FEMS Microbiol. Lett. 153:181-190.

Mathews, D. H., Sabina, J., Zuker, M., and Turner, D. H. (1999) Expanded sequence dependence of thermodynamic parameters improves prediction of RNA secondary structure. J. Mol. Biol. 288:911-940.

McInerney, M. J., Bryant, M. P., and Pfennig, N. (1979) Anaerobic bacterium that degrades fatty acids in syntrophic association with methanogens. Arch. Microbiol. 122:129-135.

McInerney, M. J., Bryant, M. P., Hespell, R. B., and Costerton, J. W. (1981) *Syntrophomonas wolfei* gen. nov. sp. nov., an anaerobic, syntrophic, fatty acid-oxidizing bacterium. Appl. Environ. Microbiol. 41:1029-1039.

McInerney, M. J. (1986) Transient and persistent associations among prokaryotes. *In:* Bacteria in nature, Vol. 2., Poindexter, J. S., and Leadbetter, E. R. (eds.), Pp. 293-338. Plenum Press, New York.

McInerney, M. J. (1988) Anaerobic degradation of proteins and lipids. *In:* Biology of anaerobic microorganisms, Zehnder, A. J. B. (ed.), Pp. 373-415. John Wiley and Sons, New York.

McInerney, M. J., Rohlin, L., Mouttaki, H., Kim, U., Krupp, R. S., Rios-Hernandes, L., Sieber, J., Struchtemeyer, C. G., Battacharyya, A., Campbell, J. W., and Gunsalus, R. P. (2007) The genome of *Syntrophus aciditrophicus*: Life at the thermodynamic limit of microbial growth. PNAS 104:7600-7605.

McInerney, M. J., Struchtemeyer, C. G., Sieber, J., Mouttaki, H., Stams, A. J. M., Schink, B., Rohlin, L., and Gunsalus, R. P. (2008) Physiology, ecology, phylogeny, and genomics of microorganisms capable of syntrophic metabolism. Ann. N. Y. Acad. Sci. 1125:58-72.

McKellar, R. C., Shaw, K. M., and Sprott, G. D. (1981) Isolation and characterization of a FAD-dependent NADH diaphorase from *Methanospirillum hungatei* strain GP1. Can. J. Biochem. 59:83-91.

Mitchell, P. (1966) Chemiosmotic coupling in chemotrophic and photosynthetic phosphorylation. Biol. Rev. Cambridge Philos. Soc. 41:445-502.

Müller, N., Griffin, B. M., Stingl, U., and Schink, B. (2008) Dominant sugar utilizers in sediment of Lake Constance depend on syntrophic cooperation with methanogenic partner organisms. Environ. Microbiol. 10:1501-1511.

Müller, N., Schleheck, D., and Schink, B. (2009) Involvement of NADH: acceptor oxidoreductase and butyryl-CoA dehydrogenase in reversed electron transport during syntrophic butyrate oxidation by *Syntrophomonas wolfei*. J. Bacteriol. 191:6167-6177.

Müller, N., Worm, P., Schink, B., Stams, A. J. M., and Plugge, C. M. (2009) Syntrophic butyrate and propionate oxidation processes: from genomes to reaction mechanisms. Review article. Environ Microbiol Rep, accepted for publication.

Müller, V., Imkamp, F., Biegel, E., Schmidt, S., and Dilling, S. (2008) Discovery of a ferredoxin:NAD^+-oxidoreductase (Rnf) in *Acetobacterium woodii*: a novel potential coupling site in acetogens. Ann. N. Y. Acad. Sci. 1125:137-146.

Nakanishi-Matsui, M., and Futai, M. (2008) Stochastic rotational catalysis of proton pumping F-ATPase. Philos. T. Roy. Soc. B. 363:2135-2142.

Nakayama, Y., Yasui, M., Sugahara, K., Hayashi, M., and Unemoto, T. (2000) Covalently bound flavin in the NqrB and NqrC subunits of Na^+-translocating NADH-quinone reductase from *Vibrio alginolyticus*. FEBS Lett. 474:165-168.

Neuhoff, V., Arold, N., Taube, D., and Erhardt, W. (1988) Improved staining of proteins in polyacrylamide gels including isoelectric focusing gels with clear background at nanogram sensitivity using Coomassie Brilliant Blue G-250 and R-250. Electrophoresis 9:255-262.

Nishimura, J.S., and Griffith, M.J. (1981) Acetate kinase from *Veillonella alcalescens*. *In:* Methods in Enzymology, Lowenstein, J. M. (ed.), 71:311-316. Academic Press, New York.

Odom, J. M., and Peck Jr., H. D. (1981) Hydrogen cycling as a general mechanism for energy coupling in the sulfate-reducing bacteria, *Desulfovibrio* sp. FEMS Microbiol. Lett. 12:47-50.

Olsen, G. J., Matsuda, H., Hagstrom, R., and Overbeek, R. (1994) fastDNAmL: a tool for construction of phylogenetic trees of DNA sequences using maximum likelihood. Comput. Appl. Biosci. 10:41-48.

Oppenberg, B., and Schink, B. (1990) Anaerobic degradation of 1,3-propanediol by sulfate-reducing and by fermenting bacteria. Antonie van Leuwenhoek 57:205-213.

Platen, H., and Schink, B. (1987) Methanogenic degradation of acetone by an enrichment culture. Arch. Microbiol. 149:136-141.

Plugge C. M., Balk, M., Zoetendal, E. G., Stams, A. J. M. (2002) *Gelria glutamica* gen. nov., sp. nov., a thermophilic, obligately syntrophic, glutamate-degrading anaerobe. Int. J. Syst. Evol. Microbiol. 52:401-407.

Qatibi, A. I., Nivière, V. and Garcia, J. L. (1991) *Desulfovibrio alcoholovorans* sp. nov., a sulfate-reducing bacterium able to grow on glycerol, 1,2- and 1,3-propanediol. Arch. Microbiol. 155:143-148.

Rainey, A., Janssen, P. H., Wild, D. J. C., and Morgan, H. W. (1991) Isolation and characterisation of an obligately anaerobic, polysaccharolytic, extremely thermophilic member of the genus Spriochaeta. Arch. Microbiol. 155:396-401.

Ramakrishnan, B., Lueders, T., Dunfield, P. F., Conrad, R., and Friedrich, M. W. (2001) Effect of soil aggregate size on methanogenesis and archaeal community structure in anoxic rice field soil. FEMS Microbiol. Ecol. 37:175-186.

Reddy, C. A., Bryant, M. P., and Wolin, M. J. (1972a) Characteristics of S organism isolated from *Methanobacillus omelianskii*. J. Bacteriol. 109:539-545.

Reddy, C. A., Bryant, M. P., and Wolin, M. J. (1972b) Ferredoxin- and nicotinamide adenine dinucleotide-dependent H_2 production from ethanol and formate in extracts of S-organism isolated from *Methanobacillus omelianskii*. J. Bacteriol. 110:126-132.

Reddy, C. A., Bryant, M. P., and Wolin, M. J. (1972c) Ferredoxin-dependent conversion of acetaldehyde to acetate and H_2 in extracts of S organism. J. Bacteriol. 110:133-138.

Rich, P. R., Mischis, L. A., Purton, S., and Wiskich, J. T. (2001) The sites of interaction of triphenyltetrazolium chloride with mitochondrial respiratory chains. FEMS Microbiol. Lett. 202:181-187.

Richardson, D. J. (2000) Bacterial respiration: a flexible process for a changing environment. Microbiology 146:551-571.

Rosner, B., Rainey, F. A., Kroppenstedt, R. M., and Schink, B. (1997) Acetylene degradation by new isolates of aerobic bacteria and comparison of acetylene hydratase enzymes. FEMS Microbiol. Lett. 148:175-180.

Sambrook, J., Fritsch, E. F. and Maniatis, T. (eds.) (1989) Molecular cloning, Vol. 3 appendix, 2nd edition, Cold spring harbour laboratory press, New York.

Sato, K., Nishina, Y., Setoyama, C., Miura, R., and Shiga, K. (1999) Unusually high standard redox potential of acrylyl-CoA/propionyl-CoA couple among enoyl-CoA/acyl-CoA couples: A reason for the distinct metabolic pathway of propionyl-CoA from longer acyl-CoAs. J. Biochem. 126:668-675.

Scherag, F. 2009. Aerober und anaerober Stoffwechsel von *Bacillus sp.* BoGlc83. Diploma thesis. Universität Konstanz, Konstanz, Germany

Schink, B., and Zeikus, J. G. (1982) Microbial ecology of pectin decomposition in anoxic lake sediments. J. Gen. Microbiol. 128:393-404.

Schink, B. (1985) Fermentation of acetylene by an obligate anaerobe, *Pelobacter acetylenicus* sp. nov. Arch. Microbiol. 142:295-301.

Schink, B. (1990) Conservation of small amounts of energy in fermenting bacteria, Pp. 63-89. *In*: R. K. Finn and P. Präve (eds.), Biotechnology, focus 2. Hanser Publishers, Munich, Germany.

Schink, B. (1997) Energetics of syntrophic cooperation in methanogenic degradation. Microbiol. Mol. Biol. Rev. 61:262-280.

Schink, B., and Stams, A. J. M. (2001) Syntrophism among prokaryotes. *In:* The Prokaryotes: An evolving electronic resource for the microbiological community, 3rd edition, Dworkin, M., Falkow, S., Rosenberg, E., Schleifer, K.-H., and Stackebrandt, E. (eds.), p. 25. Springer-Verlag, New York, USA.

Schut, F., de Vries, E. J., Gottschal, J. C., Robertson, B. R., Harder, W., Prins, R. A., and Button D. K. (1993) Isolation of typical marine bacteria by dilution culture: growth, maintenance, and characteristics of isolates under laboratory conditions. Appl. Environ. Microbiol. 59:2150-2160.

Schut, G. J., and Adams, M. W. W. (2009) The iron-hydrogenase of *Thermotoga maritima* utilizes ferredoxin and NADH synergistically: a new perspective on anaerobic hydrogen production. J. Bacteriol. 191:4451-4457.

Seitz, H.-J., Schink, B., Pfennig, N. and Conrad, R. (1990) Energetics of syntrophic ethanol oxidation in defined chemostat cultures. 2. Energy sharing in biomass production. Arch. Microbiol. 155:89-93.

Shestopalov, A. I., Bogachev, A. V., Murtazina, R. A., Viryasov, M. B. and Skulachev, V. P. (1997) Aeration-dependent changes in composition of the quinone pool in *Escherichia coli*. FEBS Lett. 404:272-274.

Sinegina, L., Wikstrm, M., Verkhovsky, M. I. and Verkhovskaya, M. L. (2005) Activation of isolated NADH:ubiquinone reductase I (complex I) from *Escherichia coli* by detergent and phospholipids. Recovery of ubiquinone reductase activity and changes in EPR signals of iron-sulfur clusters. Biochemistry 44:8500-8506.

Slater, T. F., Sawyer, B., and Sträuli, U. (1963) Studies on succinate-tetrazolium reductase systems. III. Points of coupling of four different tetrazolium salts. Biochim. Biophys. Acta 77:383-393.

Sneath, P. H. A. (1986) Endospore-forming Gram-positive rods and cocci. *In:* Bergey's manual of systematic bacteriology, Vol. 2, Sneath, P. H. A., Mair, N. S., Sharpe, M. E., and Holt, J. G. (eds.), Williams and Wilkins, Baltimore, USA.

Soboh, B., Linder, D., and Hedderich, R. (2004) A multisubunit membrane-bound [NiFe] hydrogenase and an NADH-dependent Fe-only hydrogenase in the fermenting bacterium *Thermoanaerobacter tencongensis*. Microbiology 150:2451-2463.

Soutschek, E., Winter, J., Schindler, F., and Kandler, O. (1984) *Acetomicrobium flavidum*, gen. nov. sp. nov., a thermophilic anaerobic bacterium from sewage sludge, forming acetate, CO_2 and H_2 from glucose. System. Appl. Microbiol. 5:377-390.

Staley, J. T., and Konopka, A. (1985) Measurement of *in situ* activities of non-photosynthetic microorganisms in aquatic and terrestrial habitats. Annu. Rev. Microbiol. 39:321-346.

Stams, A. J. M., and Plugge, C. M. (2009) Electron transfer in syntrophic communities of anaerobic bacteria and archaea. Nat. Rev. Microbiol. 7:568-577.

Stingl, U., Maass, A., Radek, R., and Brune, A. (2004) Symbionts of the gut flagellate *Staurojoenina* sp. from *Neotermes cubanus* represent a novel, termite-associated lineage of *Bacteroidales*: Description of '*Candidatus* Vestibaculum illigatum'. Microbiology 150:2229-2235.

Takahashi, N., Kalfas, S., and Yamada, T. (1995) Phosphorylating enzymes involved in glucose fermentation by *Actinomyces naeslundii*. J. Bacteriol. 177:5806-5811.

Tewes, F. J. and Thauer, R. K. (1980) Regulation of ATP synthesis in glucose fermenting bacteria involved in interspecies hydrogen transfer. *In:* Anaerobes and anaerobic infections, Gottschalk, G., Pfennig, N., and Werner, H. (eds.), Pp. 97-104. G. Fischer, Stuttgart, New York.

Thauer, R. K., and Morris, J. G. (1984) Metabolism of chemotrophic anaerobes: old views and new aspects. *In:* The microbe 1984, part II. Prokaryotes and eukaryotes, Kelly, D. P., and Carr, N. G. (eds.), Pp. 123-168. Cambridge University Press, Cambridge.

Thauer, R. K., Jungermann, K., and Decker, K. (1977) Energy conservation in chemotrophic anaerobic bacteria. Bacteriol. Rev. 41:100-180.

Uyeda, K., and Rabinowitz, J. C. (1971). Pyruvate-ferredoxin oxidoreductase III. Purification and properties of the enzyme. J. Biol. Chem. 246:3111-3119.

van Kuijk, B. L. M., and Stams, A. J. M. (1996) Purification and characterization of malate dehydrogenase from the syntrophic propionate-oxidizing bacterium strain MPOB. FEMS Microbiol. Lett. 144:141-144.

van Kuijk, B. L. M., Schlösser, E., and Stams, A. J. M. (1998) Investigation of the fumarate metabolism of the syntrophic propionate-oxidizing bacterium strain MPOB. Arch. Microbiol. 169:346-352.

Wagner, M., Loy, A., Nogueira, R., Purkhold, U., Lee, N., and Daims, H. (2002) Microbial community composition and function in wastewater treatment plants. Antonie van Leeuwenhoek 81:665-680.

Walker, C. B., He, Z., Yang, Z. K., Ringbauer Jr., J. A., He, Q., Zhou, J., Voordouw, G., Wall, J. D., Arkin, A. P., Hazen, T. C., Stoylar, S., and Stahl, D. (2009) The electron transfer system of syntrophically grown *Desulfovibrio vulgaris*. J. Bacteriol. 191:5793-5801.

Wallrabenstein, C., and B. Schink. (1994) Evidence of reversed electron transport in syntrophic butyrate or benzoate oxidation by *Syntrophomonas wolfei* and *Syntrophus buswellii*. Arch. Microbiol. 162:136-142.

Weisburg, W. G., Barns, S. M., Pelletier, D. A., and Lane, D. J. (1991) 16S ribosomal DNA amplification for phylogenetic study. J. Bacteriol. 173:697-703.

Westermeier, R. (1990) Elektrophorese Praktikum. Verlag Chemie, Weinheim.

Widdel, F., Kohring, G. W., and Mayer, F. (1983) Studies on dissimilatory sulfate-reducing bacteria that decompose fatty acids. III. Characterization of the filamentous gliding *Desulfonema limicola* gen. nov. sp. nov., and *Desulfonema magnum* sp. nov. Arch. Microbiol. 134:286-294.

Widdel, F. (1986) Growth of methanogenic bacteria in pure culture with 2-propanol and other alcohols as hydrogen donors. Appl. Environ. Microbiol. 51:1056-1062.

Widdel, F., and Bak, F. (1992) Gram-negative mesophilic sulfate-reducing bacteria. *In:* The Prokaryotes, 2nd edition, Balows, A., Trüper, H. G., Dworkin, M., Harder, W., and Schleifer, K. H. (eds.), Pp. 3352-3378. Springer Verlag, Berlin.

Williams, K., Lowett, P. N., and Leadlay, P. F. (1987) Purification and characterization of pyruvate:ferredoxin oxidoreductase from the anaerobic protozoon *Trichomonas vaginalis*. Biochem. J. 246:529-536.

Winogradsky, S. N. (1949) Microbiologie du sol. Problèmes et méthodes, p. 473. Masson et Cie., Paris.

Wofford, N. Q., Beaty, P. S., and McInerney, M. J. (1986) Preparation of cell-free-extracts and the enzymes involved in fatty-acid metabolism in *Syntrophomonas wolfei*. J. Bacteriol. 167:179-185.

Wood, W. A. (1971) Assay of enzymes representative of metabolic pathways. *In:* Methods in Microbiology, Norris, J. R., and Ribbons, D. W. (eds.), 6A:411-424. Academic Press, New York.

Wu, C. G., Liu, X. L., and Dong, X. Z. (2006) *Syntrophomonas cellicola* sp. nov., a spore-forming syntrophic bacterium isolated from a distilled-spirit-fermenting cellar, and assignment of *Syntrophospora bryantii* to *Syntrophomonas bryantii* comb. nov. Int. J. Syst. Evol. Microbiol. 56:2331-2335.

Yano, T., Lin-Sheng, L., Weinstein, E., Teh, J. S., and Rubin, H. (2006) Steady-state kinetics and inhibitory action of antitubercular phenothiazines on *Mycobacterium tuberculosis* type-II NADH-menaquinone oxidoreductase (NDH-2). J. Biol. Chem. 281:11456-11463.

Yoon, J. H., Kang, S. S., Lee, K. C., Kho, Y. H., Choi, S. H., Kang, K. H., and Park, Y. H. (2001) *Bacillus jeotgali* sp. nov., isolated from jeotgal, Korean traditional fermented seafood. Int. J. Syst. Evol. Microbiol. 51:1087-1092.

Zeikus, J. G. (1977) The biology of methanogenic bacteria. Bacteriol. Rev. 41:514-541.

Zeikus, J. G. (1983) Metabolic communication between biodegradative populations in nature. *In:* Microbes in their natural environments, Slater, J. H., Whittenbury, R., Wimpenny, J. W. T. (eds.), 34, Pp. 423-462. Soc. Gen. Microbiol. Symp. Cambridge University press, Cambridge, UK.

Zhang, Y., and Gladyshev, V. N. (2005) An algorithm for identification of bacterial selenocysteine insertion sequence elements and selenoprotein genes. Bioinformatics 21:2580-2589.

Zhao, H. X., Yang, D. C., Woese, C. R., and Bryant, M. P. (1993) Assignment of fatty acid-beta-oxidizing syntrophic bacteria to *Syntrophomonadaceae* fam. nov. on the basis of 16S rRNA sequence analyses. Int. J. Syst. Bacteriol. 43:630-630.

Ziegenhorn, J., Senn, M. and Bücher, T. (1976) Molar Absorptivities of β-NADH and β-NADPH. Clin. Chem. 22:151-160.

Zindel, U., Freudenberg, W., Rieth, M., Andreesen, J. R., Schnell, J., and Widdel, F. (1988) *Eubacterium acidaminophilum* sp. nov., a versatile amino acid-degrading anaerobe producing or utilizing H_2 or formate. Description and enzymatic studies. Arch. Microbiol. 150:254-266.

Zuker, M. (2003) Mfold web server for nucleic acid folding and hybridization prediction. Nucleic Acids Res. 31:3406-3415.

List of publications

Published:

Müller, N., Hempel, M., Philipp, B., and Gross, E. M. (2007) Degradation of gallic acid and hydrolysable polyphenols is constitutively activated in the freshwater plant-associated bacterium *Matsuebacter* sp. FB25. Aquat. Microb. Ecol. 47:83-90.

Müller, N., Griffin, B. M., Stingl, U., and Schink, B. (2008) Dominant sugar utilizers in sediment of Lake Constance depend on syntrophic cooperation with methanogenic partner organisms. Environ. Microbiol. 10:1501-1511.

Müller, N., Schleheck, C., and Schink, B. (2009) Involvement of NADH:acceptor oxidoreductase and butyryl-CoA dehydrogenase in reversed electron transport during syntrophic butyrate oxidation by *Syntrophomonas wolfei*. J. Bacteriol. 191:6167-6177.

Accepted for publication:

Müller, N., Worm, P., Schink, B., Stams, A. J. M., and Plugge, C. M. (2009) Syntrophic butyrate and propionate oxidation processes: from genomes to reaction mechanisms. Review article. Environ. Microbiol. Rep. accepted.

Under revision:

Worm, P., Müller, N., Plugge, C. M., Stams, A. J. M., and Schink, B. (2009) Syntrophy in methanogenic degradation. Book chapter in “Microbiology Monographs”, Hackstein, J., ed.